CONNEXINS IN THE ZEBRAFISH (*DANIO RERIO*) VISUAL AND CARDIOVASCULAR SYSTEMS

By

SHAOHONG CHENG

A Thesis Submitted to the Faculty of Graduate Studies
In Partial Fulfillment of the Requirements for the
Degree of

DOCTOR OF PHILOSOPHY

Department of Zoology

University of Manitoba

2004

THE UNIVERSITY OF MANITOBA

FACULTY OF GRADUATE STUDIES
*****
COPYRIGHT PERMISSION

CONNEXINS IN THE ZEBRAFISH (*DANIO RERIO*) VISUAL AND CARDIOVASCULAR SYSTEM

BY

SHAOHONG CHENG

A Thesis/Practicum submitted to the Faculty of Graduate Studies of The University of Manitoba in partial fulfillment of the requirement of the degree

Of

DOCTOR OF PHILOSOPHY

ABSTRACT

In this study, I used the zebrafish model system to investigate the functional role of gap junction proteins, connexins (Cx), in the development of the visual and cardiovascular systems. Firstly, I cloned the zebrafish Cx48.5 gene by screening a PAC zebrafish genomic library with a rat Cx46 probe. Cx48.5 shares 61% amino acid identity with mouse Cx46, and grouped with the Cx46 subfamily in sequence similarity analysis. Reverse transcriptase-Polymerase Chain Reaction (RT-PCR) detected Cx48.5 expression in both adult and embryonic lens and heart, as well as the adult testis. Whole mount *in situ* hybridization (WMISH) detected Cx48.5 expression in the otic vesicles at 1 days post fertilization (dpf), and in the lens throughout all developmental stages starting from 1.5 dpf. RT-PCR also showed that Cx44.1, Cx43, and Cx48.5 are the only three connexins expressed in the adult zebrafish lens, as is the case in mammals and chicken. The expression profiles of all three zebrafish lens connexins were also compared with the WMISH technique. Cx43 transcription is restricted to the lateral epithelium and the early stage differentiating fibers. In contrast, Cx48.5 and Cx44.1 are abundantly expressed in the differentiating lens fibers with distinct temporal regulation: Cx44.1 transcription begins during the lens placode stage at 21 hours post fertilization (hpf), while Cx48.5 expression was not detected until 1.5 dpf.

Secondly, the *in vivo* function of Cx48.5 was analyzed using the morpholino knockdown technique. The embryos microinjected with Cx48.5 antisense morpholinos (Cx48.5 morphants) developed small lenses and eyes. Histological analysis revealed disrupted lens fiber differentiation in 3 dpf morphants, and cataract formation by 5.5 –7.5

dpf. The Cx48.5 morphants also exhibited severe abnormalities in cardiac function, which resulted in blood circulation failure. Finally, an antisense morpholino targeting Cx44.1, and potentially also Cx48.5 was microinjected into zebrafish embryos. These embryos also developed smaller lenses and eyes, and cataracts that were trigged by apoptosis, a strikingly different mechanism than the non-apoptotic cataract formation in the Cx48.5 morphants. This phenotypic difference indicates non-redundant functions of connexins in the lens.

I conclude that Cx48.5 is the orthologue of mammalian Cx46, and is essential for lens growth and homeostasis, as well as cardiovascular function in zebrafish. Cx44.1 is co-expressed with Cx48.5 in the differentiating lens fibers with a distinct temporal pattern. Connexin48.5 and Cx44.1 likely have distinct functions in the zebrafish lens.

ACKNOWLEDGEMENTS

This thesis would not exist without the mentorship of my supervisor, Dr. Gunnar Valdimarsson. The journey of my Ph. D. training has seemed like a miracle, starting from the day that I was admitted into the Master's program as a foreign student. This opportunity became a turning point in my career and life. Within the many qualities he has, I particularly appreciate his unusual patience with the research activities and my personality, the space of freedom that he allowed me in my research, and his continuous support of my career pursuits. Dr. Valdimarsson has certainly created a rich environment for graduate students to grow in. I also cannot thank Lorna Jakobson enough. She has helped me in many ways, directly and indirectly.

I am also grateful for an excellent thesis advisory committee. I would like to thank Dr. Huebner for the many things that he has done as the departmental head, and a member of my thesis committee. Dr. Huebner has influenced my training here in a profound way. I still remember how he urged me forward after the failure of my first fellowship application. I also thank Dr. Ross McGowan, who helped me in many ways, from assisting me through his very rough course, to showing me his "scientific" approach by kicking the autoclave machine, and many other inspiring things. I thank Dr. Deborah Court for her support over the past five years. I still remember how Dr. Court encouraged me by commenting on the exam papers when I was taking my very first course in Canada, and how that influenced my early adjustment to Canada in a very positive way. I also owe Dr. Jeffrey Wigle, who became my committee member in 2002. His expertise has been invaluable for my thesis. I thank him for the many instances of kind help that he

offered to me, and I feel very lucky to know somebody that I can always search out for help. In addition to my thesis committee members, I also thank my candidacy exam committee, including Dr. Wiens, Dr. Diehl-Jones, and Dr. Eales.

I am thankful to the students that have been or, are currently in Gunnar's lab. I thank them for their friendship and numerous times of help. They are Liz, Tara, Karen, Monica, Carolyn, Liang, Jackie, Rryan, and David. I am also grateful to many people in the Department of Zoology for sharing their research instruments, giving statistical suggestions, personal connections, or simply offering smiles.

Finally I would like to express my deep appreciation to my family, my husband and my son. I owe them so many lonely nights. Their genuine nature is the sunshine of my life and their love is my vital resource. I am also in debt to my parents and in-laws, for their continuous trust, love, and support.

TABLE OF CONTENTS

LIST OF FIGURES

LIST OF TABLES

LIST OF MOVIE LEGENDS

LIST OF ABBREVIATIONS

CK ---------- casein kinase

Cx ---------- connexin

CMTX ---------- X-linked dominant Charcot-Marie-Tooth disease

dpc ---------- days post coitum

dpf ---------- days post fertilization

eF1α ---------- elongation factor 1α

EGF ---------- epidermal growth factor

ER ---------- endoplasmic reticulum

ERK ---------- extracellular signal-regulated kinase

FGF ---------- fibroblast growth factors

GFP ---------- green fluorescent protein

hpf ---------- hours post fertilization

IGF-I ---------- insulin-like growth factor-I

IP_3 ---------- inositol 1,4,5-trisphosphate

MAPK ---------- mitogen-activated protein kinase

PDGF ---------- platelet-derived growth factor

PKA ---------- cAMP-dependent protein kinase

PKC ---------- protein kinase C

RT-PCR ---------- Reverse transcriptase-Polymerase Chain Reaction

TPA ---------- 12-*O*-tetradecanoylphorbol-13-acetate

TUNEL ---------- terminal deoxytransferase (TdT) mediated dUTP-biotin nick end

labeling

UTR ---------- untranslated region

WMISH ---------- Whole mount *in situ* hybridization

WMI ---------- Whole mount immunohistochemistry

CHAPTER I

GENERAL INTRODUCTION

1.1 Gap Junctions and Connexins

Gap junctions are cellular structures that provide a direct pathway between adjacent cells. In transmission electron micrographs, gap junctions appear as tight seams joining the neighboring cells, between which only a small gap of 2 to 3 nm exists (Benedetti and Emmelot, 1965), whereas freeze-fracture electron micrographs reveal gap junctions as plaques of hexagonal particles, about 8 to 9 nm in diameter (Chalcroft and Bullivant, 1970; Goodenough and Gilula, 1974). The hexagonal particles represent individual gap junction intercellular channels, and each plaque contains up to a few thousand particles.

A gap junction channel is composed of two half channels termed connexons, or gap junction hemichannels, each contributed by one of the two neighboring cells (Fig. 1.1). Each connexon is constructed by protein subunits called connexins. Six connexins form a cylinder with an aqueous pore in the center (Makowski *et al.*, 1977). Advances in the structural analysis of gap junctions have recently been achieved by cryo-microscopy and image analysis techniques. In the three-dimensional density map of channels formed by a recombinant truncated connexin43 (Cx43), 24 closely packed rods of density are coincident with the four alpha-helical transmembrane structures of the six connexins. A continuous wall of protein seals the extracellular part of the channel (Unger *et al.*,

1999a). The aqueous pore of gap junction channels selectively allows ions, nutrients, second messengers, and electrical signals to traverse between the connected cells. The intercellular communication mediated by gap junctions play important roles in tissue homeostasis, proliferation, differentiation, and response to environmental changes (White *et al.,* 1995).

The connexins belong to a multi-gene family. To date, 20 or more connexins have been identified in the mammalian genome (Table 1.1, Sohl and Willecke, 2003). The nomenclature of connexins is based on the molecular mass predicted from the polypeptide sequence (Beyer *et al.*, 1987). For example, connexin43, is named by the abbreviation Cx, followed by the suffix 43 indicating a molecular mass of 43 KDa. To distinguish connexin orthologues from different organisms, a suitable prefix can be appended. For example, in the case of zfCx44.1, zf represents zebrafish. An alternative nomenclature system has also been used (but less widely), in which the connexin family is classified into three subgroups according to the level of amino acid sequence homology and the length of the cytoplasmic tail: α, β, and γ (O'Brien *et al.*, 1998).

A connexin protein is constructed of four transmembrane segments, two extracellular loops, one N-terminus, one central loop, and one C-terminus (Fig. 1.2). The highly conserved amino acid residues of the four transmembrane regions adapt an alpha-helical conformation and are embedded in the plasma membrane. The amino acids of the two extracellular loops are also conserved between connexin members and are involved in docking with its counterpart connexin from the connected cell. Each extracellular loop has three highly conserved cysteine residues, participating in the formation of disulfide bonds within and between the loops. Such a conformation appears to be crucial because

the three cysteine residues are conserved throughout all known connexin isoforms (John and Revel, 1991). The N-terminus, C-terminus, and the central loop face the cytoplasm. The amino acid sequences of the C-terminus and the central loop are less conserved than other parts of the connexin protein, and give uniqueness to each connexin. Gap junction channels formed from different connexin subunits have different physiological properties, such as sensitivity to voltage and cytoplasmic pH, selectivity to small molecules, etc., that presumably allow them to uniquely fit the needs of various tissues and developmental processes (Bruzzone *et al.*, 1996).

Most connexin genes have a similar structure consisting of two exons. The first exon includes only 5'-untranslated (UTR) sequences, while the second exon contains the entire coding region, the remainder of the 5'-UTR and 3'UTR sequences. The length of the intron between the two exons varies. However, there are exceptions to this standard gene structure. The mouse Cx45 gene possesses three exons. Both exon 1 and exon 2 contain only 5'-UTR, while exon 3 contains the complete coding region and 3'-UTR (Jacob and Beyer, 2001). The two exons of Cx35/36 both contain a portion of the coding region, as well as untranslated sequences (O'Brien *et al.*, 1996; Condorelli *et al.*, 1998). In addition to Cx36, it was recently reported that mouse Cx39 (Cx40.1 in the human) contains a coding region interrupted by an intron (Willecke *et al.*, 2002).

Studies of the transcriptional regulation of the connexin genes have focused on mammalian Cx43, Cx26, and Cx32. The mouse Cx43 promoter contains a number of putative transcription factor binding sites including a TATA box, AP-1, AP-2, Sp1, CRE sites, and estrogen response elements (Chen *et al.*, 1995). Mutations in the AP-1 sites result in the loss of c-Fos and c-Jun mediated protein kinase C (PKC) regulation of Cx43

(Geimonen *et al.,* 1996). Human Cx26 has a basal promoter without a TATA box (Kiang *et al.,* 1997), instead the promoter region between –140 to –113 contains Sp1 and AP-2 binding sites that are responsible for Cx26 up-regulation in the myometrum and the mammary gland (Tu *et al.*, 2001). Human Cx32 uses two tissue specific promoters (P1 and P2) in liver and pancreas, and in nerve cells, respectively. The P1 promoter is located 8 kb upstream of the translational start codon, while the P2 promoter is located 497 bp unpstream from the translational start codon (Neuhaus *et al.*, 1995).

Following translation, several steps must occur before functional gap junction channels are formed. First, connexins are oligomerized into connexons. This process usually occurs in the *trans*-region of the Golgi apparatus, not in the endoplasmic reticulum where multimeric protein assembly typically takes place (Bruzzone *et al.,* 1996). A possible explanation for this exception is that if hexamers of connexins were already assembled in the ER, which has multiple membrane layers, there is a high probability the connexons might dock together to form complete channels, which could lead to leakage between cytosolic and lumenal compartments (Bruzzone *et al.,* 1996). However, alternative routes for connexin oligomerization and transportation also exist, for example, Cx26 is integrated directly into the plasma membrane rather than via the secretory pathways (Ahmad and Evans, 2002). After connexons are transported from the *trans*-Golgi network to the plasma membrane, the two connexons from adjacent cells need to recognize each other and seal together to make a complete channel.

Connexons can be oligomerized from either the same or different types of connexins. A homomeric connexon is composed of a single kind of connexin, while a heteromeric connexon consists of different types of connexins. Two identical connexons

dock together to form homotypic channels, while different types of connexons dock to form heterotypic channels. Homomeric connexons and homotypic channels exist in a variety of tissues. On the other hand, although extensive studies have shown that many connexins can form heteromeric connexons and heterotypic channels, most of these studies were carried out in cell lines [e.g., (He *et al.*, 1999; Beyer *et al.*, 2001)]. *In vivo* evidence for the existence of heteromeric connexons and heterotypic channels is rare but does exist. Chemical cross-linking treatment and immunoprecipitation with antibodies to Cx26 and Cx32 revealed that guinea-pig liver gap junctions are constructed of heteromeric Cx26 and Cx32 connexons (Diez *et al.*, 1999). The existence of heteromeric connexons *in vivo* is not a surprise, because it is commonly observed that several different connexins are expressed in one cell. This provides an opportunity for them to oligomerize and form channels composed of different combinations of connexins. On the other hand, heterotypic channels likely form between two different types of cells that express different types of connexins. Asymmetric voltage gating of gap junction channels found in cochlear supporting cells and chicken embryo cardiac cells suggest the existence of heterotypic channels (Chen and DeHaan, 1996; Zhao and Santos-Sacchi, 2000). Unidirectional coupling by gap junctions was also found between neuroglia in the retina. Lucifer Yellow and biocytin were transferred efficiently from astrocytes to adjacent astrocytes, oligodendrocytes, and Muller cells, but rarely from oligodendrocytes and Muller cells to astrocytes (Robinson *et al.*, 1993). In the mouse retina, Cx36 is expressed in AII amacrine cells, but not in cone bipolar cells. However, the Cx36 immunoreactivity was localized on the dentritic arborizations of AII amacrines ,

indicating that the Cx36 (from AII amacrine cells) forms heterotypic channels with another connexin expressed in the cone bipolar cells (Feigenspan *et al.*, 2001).

Most connexins are phosphorylated as the primary form of post-translational modification. This modification has been implicated in the regulation of many aspects of connexin function such as trafficking, assembly, membrane insertion, degradation, channel conductance, channel permeability, and channel gating. Multiple serine and tyrosine phosphorylation sites are clustered within the C-terminal region, and occasionally in the central loop. The majority of the most extensively studied connexins (Cx43, Cx32, Cx40, Cx45, Cx37, Cx31, Cx46, Cx50) are phosphoproteins, except Cx26 (Lampe and Lau, 2000). Many studies have shown that activation of PKC by 12-*O*-tetradecanoylphorbol-13-acetate (TPA) reduces dye propagation through gap junctions [e.g., (Reynhout *et al.*, 1992; Tenbroek *et al.*, 1997)]. Regulation of rat Cx43 involves Cx43 phosphorylation on Ser368 by PKC. Mutation of Cx43 at Ser368 abolished the negative regulation of gap junction communication by TPA, and accelerated the degradation of Cx43 (Lampe *et al.*, 2000). Other kinases phosphorylating connexins include cAMP-dependent protein kinase (PKA), mitogen-activated protein kinase (MAPK), EGF/PDGF activated receptor tyrosine kinases, and non-receptor tyrosine protein kinase. (Lampe and Lau, 2000). Another extreme modification of connexins is the cleavage of the C-terminus. This will be discussed in more detail in a later section.

Gap junction channels composed of single connexins have unique electrophysiological properties suggesting a unique biological function for each connexin. The electrophysiological properties of gap junction channels are assessed in the paired *Xenopus* oocytes expression system, or in communication-deficient cell lines

transfected with specific connexins. Channel conductance and voltage gating behaviour are quantitatively measured with a double voltage clamp. Channel permeability can be assessed by the efficiency of transfer of dyes such as Lucifer Yellow, DAPI, and neurobiotin (White *et al.,* 1995). The opening and closing of gap junction channels (gating) can be controlled by multiple mechanisms, such as pH, calcium, membrane potential, and biochemical modifications such as phosphorylation. In an extreme example of calcium gating, when a cell is damaged, gap junction channels will close immediately with the influx of the calcium. The consequence of this quick response is crucial to protect adjacent cells from further damage (White *et al.,* 1995).

Previously, gap junction channels were regarded as non-selective. This opinion has been refuted by the accumulating evidence from both *in vitro* and *in vivo* studies showing that intercellular channels exert selectivity based on the size and charge of the traversing molecules (Nicholson *et al.*, 2000). In Hela cells transfected with Cx26, Cx32, and Cx43, the Cx32 transfectants showed more efficient permeation of inositol 1,4,5-trisphosphate (IP_3) than the Cx26 and Cx43 transfectants (Niessen *et al.*, 2000). Bevans and colleagues have shown that gap junction channels can even distinguish different second messenger molecules. Heteromeric channels formed by Cx32 and Cx26 were significantly more permeable to cGMP than to cAMP (Bevans *et al.,* 1998).

In vertebrates, almost all cell types express connexins, except a few fully differentiated ones, such as red blood cells, and spermatozoa. Connexins exhibit a complex spatial epression pattern. For example, Cx43 is expressed in a variety of tissues while other connexins are found predominantly in specific tissues, with a certain overlap. Cx45 and Cx40 are primarily expressed in the heart, the Cx36 subgroup is highly

expressed in brain and retina, while Cx46 and Cx50 are primarily expressed in the lens (Saez *et al.*, 2003). Table 1.1 summarizes the expression pattern of each characterized connexin. The expression of many connexins is also temporally regulated. For example, the expression of Cx26 and Cx32 in mouse mammary gland during pregnancy and lactation showed a dynamically regulated pattern. Cx26 protein was not detected in the mammary gland of the virgin mouse. Its expression began during pregnancy and reached maximum during lactation, but sharply diminished during involution. On the other hand, Cx32 was only expressed during lactation (Monaghan *et al.*, 1994).

The importance of gap junctions has been shown by studies of human diseases and mouse knockout experiments. For example, Cx43 is highly expressed in cardiomyocytes and Cx43-knockout mice died of heart defects after birth (Reaume *et al.*, 1995). Cx32 forms channels that transfer ions and metabolites in the myelinating Schwanns cells in the peripheral nervous system. Many mutations have been identified in human Cx32 that are related to X-linked dominant Charcot-Marie-Tooth disease, a common inherited neurological disorder (Abrams *et al.*, 2000). Mutations in Cx26 have been detected in patients with hereditary hearing loss (McGuirt *et al.*, 1999). Mutations of Cx46 and Cx50 have been found in patients with congenital cataracts (Berry *et al.*, 1999; Mackay *et al.*, 1999; Pal *et al.*, 1999; Rees *et al.*, 2000). The phenotypes of connexin knockout mice and connexin associated human diseases are listed in Table 1.1.

1.2 Lens Development

In mammals and birds, lens morphogenesis is initiated during late gastrulation (Fig. 1.3). The surface ectoderm forms the lens placode after interacting with the optic vesicle, which will eventually develop into retina. The lens placode invaginates and forms a hollow single layered epithelial lens vesicle, which then separates from the surface ectoderm (Fig. 1.3A). Subsequently, the posterior epithelial cells of the lens vesicle begin to elongate and reach the anterior part to form the primary lens fibers (Fig. 1.3B & C). The anterior epithelial cells proliferate, and the cells close to the equatorial region move towards the posterior. After passing through the equatorial region, they also begin to elongate, and finally form concentric layers, called secondary lens fibers, around the primary lens fibers (Fig. 1.3D &E; Fini *et al.,* 1997). Differentiated lens fiber cells are devoid of most of the intracellular organelles and are instead filled with large amounts of crystallin proteins (Wride, 1996; McAvoy *et al.*, 1999).

Insight into the genetic control of lens fiber differentiation is just beginning to emerge. The lens differentiation process appears to involve two major steps. In the first step, the mitotic epithelial cells at the border of the equatorial region exit the cell cycle, and initiate fiber cell differentiation. This cell fate transition is influenced by a number of factors including fibroblast growth factors (FGF), insulin-like growth factor-I (IGF-I), alpha 6 integrin, as well as transcription factors such as Prox1, C-Maf, and Sox1 (Lang, 1999; Wigle *et al.*, 1999; Menko, 2002). The cell cycle withdrawal is dependent on the expression of cyclin-dependent kinase inhibitors p27 and p57, inhibition of Src kinase

activity, and up-regulation of the extracellular signal-regulated kinase (ERK) signaling pathway (Menko, 2002).

Once differentiation is initiated, the lens cells undergo dramatic morphological changes including cell elongation, degradation of the cellular organelles, and synthesis of crystallins. Interestingly, the mechanism of fiber cell denucleation has many of the hallmarks of apoptosis, such as chromatin condensation, DNA fragmentation, and the involvement of bcl-2 family and caspases (Counis *et al.*, 1998; Wride and Sanders, 1998; Wride, 2000). However, there are also important difference between lens fiber formation and apoptosis. Lens fibers retain their cytoskeleton and the loss of asymmetrical distribution of plasma membrane phosphatidylserine is not detected in lens fibers. Non-caspase proteases have an important role in fiber denucleation. Results from TUNEL assay are conflicting; both positive and negative results have been reported. Nevertheless, lens fiber cells provide a unique model for studies of a naturally occurring "apoptotic" process (Wride, 2000).

1.3 Connexins In the Lens

The avascular lens is an excellent model for studying connexin function, as it is composed of only two types of cells, and expresses only three types of connexins. Gap junctions play crucial roles in lens development and homeostasis by providing a pathway for the movement of nutrients and metabolites between the fiber cells and the aqueous and vitreous humors (Mathias *et al.*, 1997; White and Paul, 1999)

Three connexins have been identified in the mammalian lens: Cx43, Cx46, and Cx50. Cx43 is also expressed in many other tissue and organ systems. In the lens, Cx43 is strongly expressed in the epithelial cells (Musil *et al.*, 1990; Yancey *et al.*, 1992). During lens cell differentiation, Cx43 expression is down regulated, whereas Cx46 and Cx50 expression is up regulated (Paul *et al.*, 1991; White *et al.*, 1992; Rup *et al.*, 1993; Jiang *et al.*, 1994). Cx46 and Cx50 are most abundantly expressed in the lens fibers and therefore traditionally regarded as lens specific. Cx50 and Cx46 also co-localize to the same gap junction plaques between lens fibers (Paul *et al.*, 1991; Lo *et al.*, 1996). The chicken orthologues of mammalian Cx46 and Cx50, Cx56 and Cx45.6 respectively, coimmunoprecipitate indicating the existence of heteromeric connexons with a mixture of Cx56 and Cx45.6 isoforms (Jiang and Goodenough, 1996).

Lens connexins are subjected to post-translational modifications such as phosphorylation and peptide cleavage. Chicken Cx45.6 is phosphorylated *in vivo* (Jiang *et al.*, 1994), most likely by casein kinase (CK) II at Ser363 site. Mutation of Ser363 to Ala resulted in a longer Cx45.6 half-life, indicating that phosphorylation regulates Cx45.6 degradation (Yin *et al.*, 2000). Other kinases that appear to phosphorylate lens connexins include casein kinase I and protein kinase C (Cheng and Louis, 1999; Saleh *et al.*, 2001; Wagner *et al.*, 2002). In mature lens fibers, Cx46 and Cx50 are cleaved at their carboxy-terminals (Kistler *et al.*, 1990; Jacobs *et al.*, 2004). This process may be a part of the fiber terminal differentiation process. The proteases responsible for the cleavages of lens connexins include the calcium-dependent protease calpain and caspase-3 (Lin *et al.*, 1997; Yin *et al.*, 2001). The consequence of Cx46 and Cx50 cleavage seems to be a low

resistant transportation pathway in the mature lens, which may be required for maintaining the homeostasis of the dense, avascular lens (Lin *et al.*, 1998).

Although Cx46 and Cx50 have a similar expression pattern in the lens, they have distinct functions in lens development and homeostasis, as revealed by genetic manipulation in mouse embryos. Cx46 knockout mice developed cataracts, beginning at 2-3 weeks of age that became increasingly severe with age (Gong *et al.*, 1997). In contrast to the Cx46 knockouts, Cx50 knockout mice developed mild cataracts, but also a significant reduction in the size of the lens that was not seen in the Cx46 knockouts (White *et al.*, 1998; Rong *et al.*, 2002). This phenotypic difference strongly suggests that Cx46 and Cx50 play different roles during lens development. This notion was confirmed by the genetic replacement of Cx50 with Cx46. The expression of Cx46 under the control of the Cx50 promoter corrected the cataract, but not the ocular growth phenotype of Cx50 deficient mice (White, 2002). How Cx50 participates in controlling lens growth is not clear, although it appeared to be involved in lens fiber maturation (Rong *et al.*, 2002). The role of Cx43 in lens development and function is also not clear. Cx43 knockout mice died at birth with normal sized lens. However, histological analysis of those newborns revealed some lens cell abnormalities. The fiber cells were separated from the apical surfaces of the epithelial cells, with large vacuolar spaces in between (Gao and Spray, 1998). Cx43 and Cx50 double knockout mice have also been generated, and the double knockout lenses developed normally up to E18.5, suggesting that connexins are more important for post-natal, rather than pre-natal lens function (White *et al.*, 2001). In addition to retarded lens growth, Cx50 knockouts also had smaller eyes. Eye growth is known to be influenced by lens growth (Coulombre and Coulombre, 1964). Whether the

smaller eye in the Cx50 knockouts resulted from the undergrowth of the lens, or if Cx50 has a direct role in eye growth is not clear.

Mutations of human Cx46 and Cx50 have been identified in families with congenital cataracts (Shiels *et al.*, 1998; Berry *et al.*, 1999; Mackay *et al.*, 1999). This evidence strongly supports the notion that gap junctions play important roles in lens development, as well as in the maintenance of lens transparency.

1.4 Connexins In the Heart

The electrical coupling responsible for the rhythmic contractions of the myocardium is exclusively fulfilled by gap junctions located at the intercalated disk of the cardiomyocytes. Four connexins are abundantly expressed in the mammalian heart: Cx43, Cx40, Cx45 and Cx37. Cx45 transcripts were detected by *in situ* hybridization at 8.5 days post coitum (dpc) in all compartments of the developing mouse heart, a time when the first rhythmic contractions appear (Alcolea *et al.*, 1999). By 9.5 dpc, Cx43 and Cx40 transcripts became detectable in whole-mount *in situ* hybridized embryos in both the atiral and ventricular primordials (Delorme *et al.*, 1995; Delorme *et al.*, 1997). This expression pattern undergoes dynamic changes as development progresses. In the adult rodent heart, Cx43 is exclusively expressed in the atrial and ventricular working myocardium, Cx40 is found in the atrial working myocardium, and the conducting bundle branches and Purkinje fibres, while Cx45 is restricted to the atrioventricular conduction system (Van Kempen *et al.*, 1991; Gourdie *et al.*, 1993; Coppen *et al.*, 1999). Cx37 is expressed in the cardiac endothelial cells (Reed *et al.*, 1993). In addition to Cx43, Cx40,

Cx45, and Cx37, Cx46 and Cx50 have also been reported to be expressed in the heart, though their function in the cardiovascular system is not clear (Paul *et al.*, 1991; Gourdie *et al.*, 1992; Davis *et al.*, 1995; Verheule *et al.*, 2001).

Mouse knockout experiments have demonstrated that Cx43, Cx40, and Cx45 are all essential for cardiac function. For instance, connexin43 knockout mice died neonatally from pulmonary outflow tract obstruction (Reaume *et al.*, 1995). Connexin40-deficient mice on the other hand exhibited slowed cardiac conduction and a partial atrioventricular block (Kirchhoff *et al.*, 1998; Simon *et al.*, 1998). Lastly, Cx45 knockout mice died by embryonic day 10 displaying the effects of a conduction block, endocardial cushion defects and abnormalities of vascular development (Kruger *et al.*, 2000; Kumai *et al.*, 2000). The Cx37 knockout mice had no apparent cardiovascular abnormalities (Simon *et al.*, 1997).

1.5 The Zebrafish Model System

The zebrafish is a powerful model system for the investigation of vertebrate development. It is a lower vertebrate species with relatively simple mechanisms of development and is therefore easier to study than higher vertebrates such as the mouse. Although the fine details of developmental processes in zebrafish are different than in humans in many aspects, and our knowledge of zebrafish anatomy and physiology still needs to be extended considerably, the zebrafish has remarkable genetic and anatomic similarities with both mouse and human, and hence can serve as a valuable model to study mechanisms of development, as well as a model for human diseases.

The zebrafish has several unique advantages that are attractive to developmental biologists. It is small (3-4 cm for adult) and is easy and inexpensive to care for. It has short generation time (3 months) and each clutch has a large number of eggs. The zebrafish egg is relatively large and develops externally, which allows extensive observations and embryonic manipulations. The transparency throughout embryogenesis greatly facilitates direct monitoring of developmental events. The above advantages permit the use of large scale mutagenesis screens to quickly identify many genes that are crucial for vertebrate development. A number of large scale mutagenesis screens have been carried out since Christian Nusslein-Volhard began the pioneering work in 1994, using chemical mutagens as well as retrovirus-mediated insertional mutagenesis (Mullins and Nusslein-Volhard, 1993; Fishman and Stainier, 1994; Mullins *et al.*, 1994; Driever *et al.*, 1996; Amsterdam *et al.*, 1999). In the last few years, smaller scale screens have also been carried out in many labs focusing on specific developmental processes or organs. The genomic sequencing project, expected to be completed in 2004, will significantly expedite the cloning of the mutated genes.

Complementary to mutagenesis, morpholino mediated gene knockdown methodology has been used as a powerful tool to assign functions to cloned genes *in vivo*. Morpholinos are low toxicity chemical analogs of oligonucleotides, constructed from four morpholino subunits, each containing one of the four bases (Pyrimidines and Purines) and a morpholine ring. The morpholino subunits are oligomerized by phosphorodiamidate linkages to give the morpholino oligos. The morpholinos bind complementary RNA strands, but are resistant to nuclease degradation (Summerton, 1999). Specific targeting of the regions around the mRNA translation start codon or

splice sites usually generates a gene specific phenotype during the first two days of embryonic development at least (Ekker, 2000; Nasevicius and Ekker, 2000; Ekker and Larson, 2001; Heasman, 2002). Morpholinos can also be used to target two genes simultaneously, which is particularly useful to analyze genes with redundant functions (Henry *et al.*, 2002). Two major potential problems with the morpholino knockdown method are non-specific toxic side effects and mistargetting. These problems can be addressed by gene rescue experiments or by using two independent morpholinos. Another limitation of the morpholino method is that the level of gene knockdown can usually only be detected by protein analysis, since, unless the morpholino sequence crosses splice sites, the mRNA usually remains intact (Nasevicius and Ekker, 2000; Ekker and Larson, 2001).

Zebrafish have unique advantages for studies of the visual and cardiovascular systems. The zebrafish eye is relatively large and develops quickly. In zebrafish, the lens placode forms at about 19 hours post fertilization (hpf) (Schmitt and Dowling, 1994; Kimmel *et al.*, 1995; Li *et al.*, 2000), a process quite similar to the formation of the lens placode in birds and mammals. The presumptive lens cells then separate from the ectoderm as a solid ball of cells at approximately 24 hpf (Schmitt and Dowling, 1994; Easter and Nicola, 1996; Li *et al.*, 2000), never forming a hollow lens vesicle as is the case in birds and mammals. The cells in the detached lens then differentiate into two distinct cell populations: the lateral cuboidal epithelium (equivalent to the anterior epithelium in the mammalian lens) and the primary lens fiber cells. Subsequently, lateral epithelial cells in the equatorial region differentiate into secondary lens fibers. Functional vision has developed by 3 days post fertilization (dpf) (Easter and Nicola, 1996).

The zebrafish cardiovascular system becomes functional by 24 hpf, but it is not required for the embryo to develop and survive for the first few days (Pelster and Burggren, 1996; Warren and Fishman, 1998; Lohr and Yost, 2000), which allows abnormalities of cardiac morphology and function to be investigated in live embryos. The zebrafish has a prototypical vertebrate heart composed of four continuous structures (sinus venosus, atrium, ventricle, and bulbus arteriosus), and shares many developmental and physiological similarities to the mammalian heart (Chen and Fishman, 2000; Hu *et al.*, 2000; Hu *et al.*, 2001).

1.6 Objectives of Thesis

The main focus of this thesis is to characterize the functions of zebrafish Cx48.5 and Cx44.1 (zebrafish orthologues of mouse Cx46 and Cx50 respectively). Cx46 and Cx50 have been regarded as lens specific, as they are predominantly expressed in the lens. Mouse knockout experiments and human disease studies have also revealed that both are crucial for the lens integrity. However, several fundamental biological question about the roles of Cx46 and Cx50 remain unclear.

Recall how Cx46 and Cx50 have distinct, yet overlapping functions in the lens: Cx46 solely functions in the maintenance of lens transparency (or homeostasis), while Cx50 participates in both lens growth and homeostasis (Gong *et al.*, 1997; White *et al.*, 1998; Rong *et al.*, 2002; White, 2002). One important question to be answered is: What is the molecular mechanism by which Cx50 controls lens epithelial cell proliferation and differentiation, especially how the proliferation or differentiation signals are influenced

by the expression of Cx50. Another important question is whether or not Cx46 and Cx50 have a role in organs other than lens? Studies have shown that Cx46 is also expressed in other organs including heart, kidney, alveolar epithelial cells, osteoblastic cells, and degenerating Schwann cells (Paul *et al.*, 1991, Davis *et al.*, 1995, Koval *et al.*, 1997, Abraham *et al.*, 2001, Verheule *et al.*, 2001, Silverstein *et al.*, 2003). The expression of Cx46 in the heart has been reported in a few studies, while its function in the cardiovascular system is entirely unknown.

To answer these intriguing questions, I carried out extensive studies on zebrafish Cx48.5 and Cx44.1, including the molecular cloning and sequence analysis of Cx48.5, expression analysis of Cx48.5 and Cx44.1 (as well as Cx43) with a variety of techniques, and functional studies with the morpholino knockdown technology. These comprehensive studies have laid a solid basis for future study. More importantly, key novel insights have been gained from these studies: 1) Cx44.1 is expressed well in advance of Cx48.5 during lens development, which may partially explain why they have different roles in the lens. 2) Cx48.5 is crucial for cardiovascular function in zebrafish. 3) Cx48.5 also contributes to lens growth, as well as eye growth in zebrafish. 4) Microinjection of a morpholino potentially targeting both Cx48.5 and Cx44.1 induced cataractogenesis, mediated by an apoptosis like process that is distinct from the non-apoptotic cataract formation in the Cx48.5 knockdown embryos.

Table 1.1. Summary of Mouse and Human Connexin Genes: Expression and Phenotypes

Mouse connexin	Major expression	Phenotypes of Cx-deficient mice	Human hereditary disease(s)	Human connexin
mCx23	n.a.	n.a.	n.a.	hCx23
	n.a.	n.a.	n.a.	hCx25
mCx26	Breast, skin, cochlea, liver, placenta	Lethal on ED 11 *OTOcre*[1]: hearing loss	Sensorineural hearing loss, palmoplantar hyperkeratosis	hCx26
mCx29	Schwann cells, oligodendrocytes	n. a.	n. a.	hCx30.2 (hCx31.3)
mCx30	Skin, brain, cochlea	Hearing loss	Nonsyndromic hearing loss, hydrotic ectodermal dysplasia	hCx30
mCx30.2	Vascular smooth muscle cells	n.a.	n.a.	hCx31.9
mCx30.3	Skin	n. a.	Erythrokeratodermia variabilis (EKV)	hCx30.3
mCx31	Skin, cochlea, placenta, uterus	Placental dysfunction	Hearing impairment, erythrokeratodermia variabilis (EKV)	hCx31
mCx31.1	Skin	n. a.	n. a.	hCx31.1
mCx32	Liver, Schwann cells	Decreased glycogen mobilization, increased liver carcinogenesis, CMTX	CMTX, (hereditary peripheral neurophathy)	hCx32
mCx33	Testis	n. a.		
mCx36	(Inter)-neurons	Visual transmission defects	n. a.	hCx36
mCx37	Endothelium	Female sterility	Association with atherosclerosis	hCx37
mCx39	n. a.	n. a.	n. a.	hCx40.1
mCx40	Heart, endothelium	Atrial arrhythmias	n. a.	hCx40

(continued on next page)

Table 1.1. Summary of Mouse and Human Connexin Genes: Expression and Phenotypes (continued)

Mouse connexin	Major expression	Phenotypes of Cx-deficient mice	Human hereditary disease(s)	Human connexin
mCx43	Many cell types	Lethal on P0 heart malformations, *MHCcre*[2]: arrhythmias, *GFAPcre*[3]: dysregulation of spreading depresion	Visceroatrial heterotaxia, oculodentodigital dysplasia syndrome (ODDD), syndactyly type III	hCx43
mCx45	Heart, smooth muscle, neurons	Lethal on ED 10.5	n. a.	hCx45
mCx46	Lens fiber cells	Zonular nuclear cataract	Congenital cataract	hCx46
mCx47	Oligodendrocytes	Myelin deformation	n. a.	hCx47
mCx50	Lens fiber cells	Microphthalmia, zonular pulverulent congenital cataract	Zonular pulverulent cataract	hCx50
	n. a.	n. a.	n. a.	hCx59
mCx57	Retinal horizontal cells	n. a.	n. a.	hCx62

(Reproduced from Sohl and Willecke, 2003).

[1]*OTOcre*: Otogelin-cre mediated excision of Cx26 in the mouse cochlea.

[2]*MHCcre*: myosin heavy chain-cre mediated excisionof Cx43 in mouse cardiomyocytes.

[3]*GFAPcre*: glial fibrillary acidic protein-cre mediated excision of Cx43 in mouse astrocytes.

Figure 1.1

Gap junctions are collections of intercellular channels that link the adjacent cells into a cytoplasmic syncytium. A gap junction channel is constructed of two half-channels termed connexons, each contributed by one of the two neighboring cells. A connexon is composed of six subunits termed connexins, which polymerize to form a hemi-channel. The aqueous pore of the channel selectively allows ions, nutrients, second messengers, and electrical signals to traverse between the connected cells. (Adapted from White *et al.*, 1995).

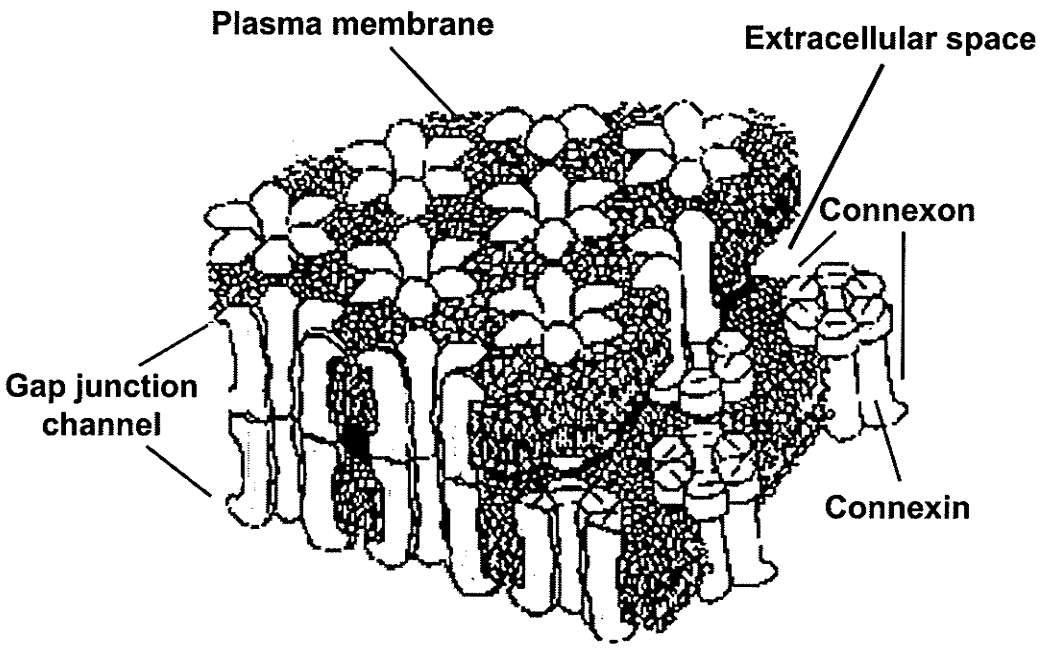
Plasma membrane
Extracellular space
Connexon
Gap junction channel
Connexin

Figure 1.2

A connexin protein has four highly conserved alpha-helical transmembrane segments (M1, M2, M3, and M4) embedded in the plasma membrane and two extracellular loops (E1 and E2) involved in docking with the counterpart from the connected cell. The N-terminus (NT), C-terminus (CT), and a central loop (CL) face the cytoplasm. (Adapted from Zimmer *et al.*, 1987).

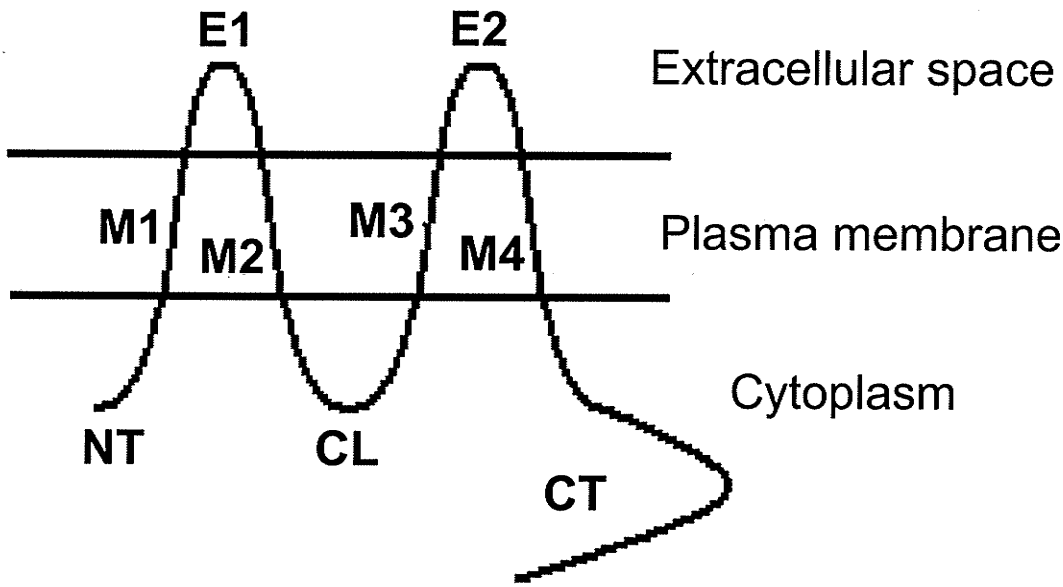
E1
E2
Extracellular space
M1
M2
M3
M4
Plasma membrane
Cytoplasm
NT
CL
CT

Figure 1.3

Lens cell differentiation starts after the formation of the lens vesicle (A). The posterior epithelial cells of the lens vesicle begin to elongate (B) and reach the anterior part to form the primary lens fibers, which are anucleate and filled with crystallins (C). The anterior epithelial cells keep dividing throughout life. The daughter cells from this region move toward the equator of the vesicle. After passing through the equator region, they also begin to elongate (D), and finally form concentric layers, called secondary lens fibers, around the primary lens fibers (E). The mature lens is composed of the anterior mitotic epithelial cells, the central primary lens fibers, and the cortical secondary lens fibers (F). (Figure adapted from Kral, 1998, website: http://aussie-health.westga.edu/research/cataracts/development.html)

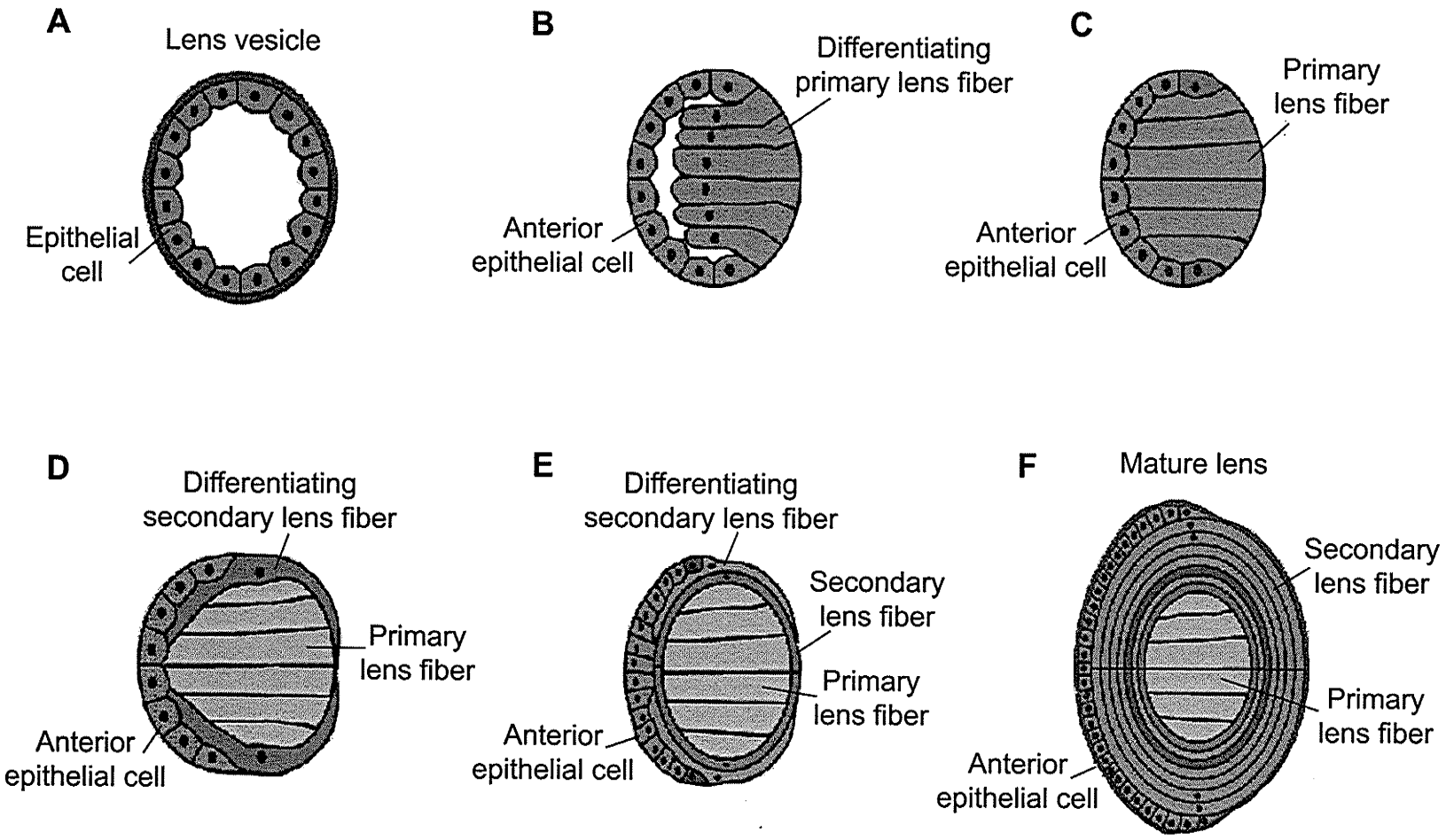
A
Lens vesicle
Epithelial cell
B
Differentiating primary lens fiber
Anterior epithelial cell
C
Primary lens fiber
Anterior epithelial cell
D
Differentiating secondary lens fiber
Primary lens fiber
Anterior epithelial cell
E
Differentiating secondary lens fiber
Secondary lens fiber
Primary lens fiber
Anterior epithelial cell
F
Mature lens
Secondary lens fiber
Primary lens fiber
Anterior epithelial cell

CHAPTER II

EXPRESSION OF CONNEXIN48.5, CONNEXIN44.1, AND CONNEXIN43 DURING ZEBRAFISH (*DANIO RERIO*) LENS DEVELOPMENT

2.1 Rationale

Previous studies in the mouse have shown that each of the three lens connexins, Cx43, Cx46, and Cx50, have a specific expression pattern and function in the lens. However, the relationships between the timing and location of expression of all these three connexins during lens development have not been directly compared in a single study previously. Comparison of the expression patterns of the lens connexins in zebrafish with the expression patterns in other species will allow us to determine which aspects are conserved and which may be species specific. Ultimately, this comparative information will be essential for establishing whether the zebrafish is a useful model for the study of the role of connexins in human lens growth and homeostasis. Here we report whole mount *in situ* hybridization data on the expression patterns of zebrafish Cx43, Cx48.5, and Cx44.1 (the orthologues of mammalian Cx43, Cx46, and Cx50 respectively) from 1 dpf to 4 dpf. Our analysis showed that the spatial expression patterns of the three connexins in the zebrafish lens are similar to their orthologues in birds and mammals. In addition, we found that both Cx44.1 and Cx43 transcripts began to accumulate during the

lens placode stage, whereas the initiation of Cx48.5 expression appeared to be delayed relative to the other two connexins.

2.2 Materials and Methods

2.2.1 Zebrafish care

Adult zebrafish were purchased from a local pet shop and maintained at 28.5°C on a 10 hr light/14 hr dark light cycle according to standard procedures (Westerfield, 1995). Embryos were raised in egg water at 28.5°C and staged using the time elapsed since fertilization. Embryos used for WMISH were treated with 0.003% 1-phenyl-2-thiourea (Sigma, Oakville, Ontario) after 24 hpf to prevent pigment formation.

2.2.2 Sequence analysis

To construct the phylogeny tree of the connexin genes expressed in the lens, mouse Cx43, Cx46, and Cx50, chicken Cx43, Cx56, and Cx45.6 sequences were retrieved from GenBank. The amino acid sequences encoded by these genes, together with the zebrafish Cx43, Cx48.5, and Cx44.1 amino acid sequences (all available in GenBank), were aligned using ClustalX (Thompson *et al.*, 1997), and the phylogenetic tree was displayed with the TREEVIEW program (Page, 1996). Zebrafish Cx35 was used as an outlier.

2.2.3 RT-PCR

Total RNA was isolated from adult tissues using TRIzol Reagent (Invitrogen, Burlington, ON). Total RNA (2 μg) from adult lens and liver was reverse transcribed using SuperScript II reverse transcriptase (Invitrogen Life Technologies, Burlington, Ontario) according to the manufacturer's suggestions. PCR was performed in a 20 μl reaction volume using 4% of the volume of the reverse transcription reactions as template, and 5 μl of the PCR products were loaded onto an agarose gel for analysis. The sequences of all primers used are shown in Table 2.2. The eF1α primers anneal to exon sequences flanking an intron in the zfeF1alpha gene. The expected size of the elongation factor amplicon is 569 bp from cDNA and 733 bp from genomic DNA.

2.2.4 Whole mount *in situ* hybridization

Probes for WMISH were as follows: the Cx48.5 probe was 775 bp long extending from 612 nucleotides downstream of the start codon to 81 nucleotides after the stop codon; the Cx44.1 probe was 840 bp long extending from 348 nucleotides upstream of the stop codon to 492 nucleotides downstream of the stop codon; the Cx43 probe was 1085 bp long extending from 156 nucleotides downstream of the start codon to 98 nucleotides downstream of the stop codon. DIG labeled antisense RNA probes were synthesized according to standard protocols (Jowett, 1999). Sense control RNA probes were synthesized in the opposite direction using the same templates. The WMISH protocol was essentially according to Thiesse *et al.* (Thisse *et al.*, 1993), with the following modifications: alkaline hydrolysis of the probe was omitted; embryos from 1 to 4 dpf were fixed in 4% paraformaldehyde in 1x PBS overnight; the hybridization buffer contained 50% deionized formamide, 5x SSC, 1 mg/ml *Torula* RNA, 100 μg/ml heparin,

1x Denhart's solution, 0.1% Tween 20, 0.1% CHAPS, and 5 mM EDTA; prehybridization was carried out for 4-6 hours, and hybridization for 14-18 hours, at 60°C; *Torula* RNA and heparin were not added to the wash solutions. The alkaline phosphatase reaction was allowed to proceed for 4-24 hours. After the color reached the appropriate intensity, the embryos were fixed with 4% paraformaldehyde in 1x PBS from overnight to 3 days, then washed 2x10 minutes with 1x PBS, and cleared in glycerol. To obtain plastic sections, WMISH embryos were dehydrated with 70%, 80%, 90%, and absolute ethanol, then infiltrated and embedded in JB-4 resin (Polysciences, Inc., Warrington, PA). Sections were cut at 3-4 μm thickness.

2.3 Results and Discussion

2.3.1 Sequence similarities between zebrafish Cx48.5, Cx44.1, Cx43 and their orthologues in mouse and chicken

Sequence similarity analysis at the amino acid level showed that zebrafish Cx48.5, mouse Cx46, and chicken Cx56 belong to one subfamily, zebrafish Cx44.1, mouse Cx50, and chicken Cx45.6 belong to a second subfamily, and all three Cx43 members are in a third subfamily (Fig. 2.1). Zebrafish Cx48.5, Cx44.1, and Cx43 share 61%, 62%, and 80% amino acid identity with their mouse orthologues respectively. Previously, we have shown that Cx44.1 is the zebrafish orthologue of mammalian Cx50 and chicken Cx45.6 (Cason *et al.*, 2001), and the analysis presented here shows that zebrafish Cx48.5 is orthologous to mouse Cx46 and chicken Cx56, and that zebrafish

Cx43 is orthologous to mammalian and chicken Cx43. The Cx43 subfamily is clearly much more conserved than the other two subfamilies.

2.3.2 Cx48.5, Cx44.1, and Cx43 are all expressed in the adult zebrafish Lens

RT-PCR analysis was performed with adult lens and liver RNA (Fig. 2.2). RT-PCR products of the appropriate size for all three connexins were amplified from the lens RNA, but only Cx43 was amplified from the liver RNA. This result is consistent with previous observations from mammals and birds that the Cx46 and Cx50 subfamilies are predominantly expressed in the lens (Paul *et al.*, 1991; White *et al.*, 1992; Rup *et al.*, 1993; Jiang *et al.*, 1994), while Cx43 is expressed in a variety of tissues including the vascular system (White *et al.*, 1995). RT-PCR analysis of adult lens RNA with primers specific for the following zebrafish connexins, Cx43.4 (Essner *et al.*, 1996), Cx35 (McLachlan *et al.*, 2003) and Cx45.6 (Christie *et al.*, 2004) failed to detect expression (data not shown). Furthermore, it has previously been shown that Cx27.5 and Cx55.5 are not expressed in the lens (Dermietzel *et al.*, 2000). Zebrafish elongation factor 1α primers that span an intron were used to compare the amount of cDNA included in each reaction and to confirm the absence of genomic DNA contamination. A band of appropriate size for cDNA was amplified from both the lens and liver samples, and no bands indicating genomic DNA contamination were observed. Thus, Cx48.5, Cx44.1, and Cx43 are all expressed in the adult lens, whereas Cx43.4, Cx35, Cx45.6, Cx27.5 and Cx55.5 are not.

2.3.3 Differential expression of Cx48.5, Cx44.1, and Cx43 during zebrafish lens development

Whole mount *in situ* hybridization (WMISH) was performed with Cx48.5, Cx44.1, and Cx43 DIG labeled antisense RNA probes. Following the WMISH procedure the embryos were embedded in plastic and sectioned. The lenticular expression patterns of the three connexins are shown in Fig. 2.3. We previously reported that Cx44.1 is exclusively expressed in the lens (Cason *et al.*, 2001). No signal was detected with the RNA sense control probes in any of the stages we investigated (Fig. 2.3A-E). The results of the *in situ* hybridization analyses are summarized in Table 2.1.

Cx48.5 transcripts were not detected in the lens at 24 hpf (Fig. 2.3F), but a strong signal was detected throughout most of the lens at 36 hpf (Fig. 2.3G). The lateral epithelial cells did not contain Cx48.5 transcripts, whereas the differentiating epithelial cells in the equatorial region did. The bulk of the lens was composed of differentiating primary fiber cells that expressed Cx48.5 strongly as well. Cx48.5 signals were also detected in the ganglion cell layer of the retina, adjacent to the equatorial and medial portions of the lens. Similar retinal staining pattern was also seen in embryos probed with Cx44.1 at 36 hpf (Fig. 2.3L), and in embryos probed for the lens markers mafB/valentino and Prox 1 (data not shown). Prox 1 is expressed in amacrine and horizontal cells in the inner nuclear layer of the retina during development (Tomarev *et al.*, 1996; Belecky-Adams *et al.*, 1997; Jeffery *et al.*, 2000; Vihtelic *et al.*, 2001), whereas MafB/valentino is not expressed in the retina (Kajihara *et al.*, 2001). The staining we observed in the retina adjacent to the lens therefore might represents diffusion of the alkaline phosphatase reaction product away from the lens. The expression pattern of Cx48.5 at 2 dpf (Fig.

2.3H) was similar to that seen at 36 hpf. At 3 and 4 dpf, the core region of the lens contained enucleated mature fiber cells that were devoid of Cx48.5 transcripts (Fig. 2.3I, J). Instead the Cx48.5 signal was restricted to the differentiating secondary fiber cells at the equatorial and medial poles of the lens. These data clearly show that Cx48.5 is expressed in differentiating lens fiber cells and not in mature fibers. Connexin48.5 expression appears to be most widespread from 36 hpf to 2 dpf, a period during which the core primary lens fibers differentiate. We cannot completely rule out the possibility that the lack of a Cx48.5 signal in the lens at 24 hpf is due to the lack of sensitivity of our WMISH technique. However, the Cx48.5 antisense probe never produced a signal above the control probe at this stage, even when the colour reaction was allowed to proceed for 12 hours longer than for the Cx44.1 and Cx43 probes. Therefore, if Cx48.5 is expressed at all at this stage, it is at a much lower level than Cx44.1 and Cx43.

These results confirm and extend the results from previous studies on Cx56 and Cx46, the chicken and mouse orthologues of Cx48.5. Connexin56 transcripts were present in primary lens fibers in lens vesicles at day 3.5 (Mu *et al.*, 2003). Immunofluorescence studies using Cx56 specific antisera have also demonstrated Cx56 protein expression in early primary lens fibers (Berthoud *et al.*, 1994; Jiang *et al.*, 1995). Analysis of *lacZ* expression in Cx46 knockout mice showed expression in primary lens fibers at 11 dpc and in the differentiating secondary lens fibers in the equatorial region throughout life (Gong *et al.*, 1997). Our data showing the absence of Cx48.5 expression in the earliest stages of lens formation therefore differs from the chick data, but studies from mice have not reported the absence of Cx46 expression in the earliest stages of lens

formation. Whether this reflects a species difference, or that the earlier stages of lens development in the mouse were not investigated for expression is unclear.

Previously, we detected Cx44.1 transcripts in the lens by WMISH at 24 and 36 hpf, but not at later stages (Cason *et al.*, 2001). We have re-examined Cx44.1 mRNA expression during lens development in the present study using a more sensitive WMISH protocol. Using this improved protocol Cx44.1 expression was detected at 24hpf and later stages (Fig. 2.3K-O), and the pattern was very similar to that detected for Cx48.5. However, in agreement with our previous results, but in contrast to the Cx48.5 expression reported here, strong Cx44.1 expression was also detected in most of the developing lens except the lateral portion at 24 hpf (Fig. 2.3K). These lateral lens cells at 24 hpf are probably the precursors of the lateral cuboidal epithelium. We also detected Cx44.1 expression in lens placode at 21 hpf (data not shown). Expression of the chicken orthologue Cx45.6 has been demonstrated by immunofluorescence in primary lens fibers while the lens vesicle is still attached to the ectoderm (Jiang *et al.*, 1995). The expression of chicken Cx45.6 and zebrafish Cx44.1 therefore appear to be initiated at similar stages of lens development. Evidence from the mouse is conflicting, however. Evans and colleagues (Evans *et al.*, 1993) showed, using immunohistochemistry, the absence of Cx50 expression in the early mouse lens vesicle (11 dpc) but as soon as 12 dpc expression was detected in differentiating primary fibers. At 13 dpc, when the lens vesicle lumen has closed, expression remained in the fibers but was absent from the epithelium. However, analysis of *lacZ* expression in Cx50 knockout mice indicates extensive expression throughout the epithelium, but when expression is initiated was not reported (Rong *et al.*, 2002).

The timing difference between the initiation of Cx48.5 and Cx44.1 expression, suggests that they might have different roles in zebrafish lens development. In the mouse, it has been previously suggested that Cx46 and Cx50 have distinct functions in lens development, although it is not clear whether or not the timing of their initiation of expression are different. Both Cx46 and Cx50 knockout mice developed cataracts, but the timing of the appearance of the cataracts differed (Gong *et al.*, 1997; White *et al.*, 1998; Rong *et al.*, 2002). Furthermore, only the Cx50 knockout mice developed microphakia and microphthalmia. Also, in mice in which the Cx50 coding sequence was replaced with the Cx46 coding sequence by gene targeting, small but transparent lenses developed (White, 2002). In the mouse it seems Cx50 is required for lens growth, while Cx46 is more involved in fiber homeostatic maintenance. On the other hand the timing difference between the initiation of Cx48.5 and Cx44.1 expression we detected has not been previously reported in the chick or mouse, and may indicate more diverse roles for these two connexins in early zebrafish lens development and homeostatic maintenance.

Cx43 expression was detected throughout the lens at 24 hpf (Fig. 2.3P). The widespread expression of Cx43 during early lens development has also been observed in mouse and chicken (Yancey *et al.*, 1992; Wiens *et al.*, 1995). By 36 hpf, Cx43 staining was less intense in the core region, compared to the lateral epithelium and the equatorial differentiating cells (Fig. 2.3Q). By 2 dpf, Cx43 expression had declined further in the maturing fiber cells (Fig. 2.3R). At 3 and 4 dpf stages, Cx43 transcripts were only detected in the lateral epithelium and the differentiating cells in the equatorial region (Fig. 2.3S, T).

2.4 Summary

Cx48.5, and Cx44.1, and Cx43 are the zebrafish orthologues of mammalian Cx46, Cx50, and Cx43, respectively. These three zebrafish connexins are all expressed in the adult lens. Whole mount *in situ* hybridization detected Cx48.5 expression throughout most of the lens, except the lateral epithelium, at 36 hpf and 2 dpf. Cx48.5 expression was only detected in differentiating secondary lens fibers in the medial and equatorial regions by 3 and 4 dpf. Cx44.1 was expressed in a similar pattern as Cx48.5, except its transcripts in the lens were detected as early as 21 hpf. Cx43 expression was throughout the lens at 24 and 36 hpf, but became more restricted to the lateral epithelium and the equatorial differentiating cells at later stages. Thus in zebrafish, Cx43 transcription is restricted to the lateral epithelium and the early stage differentiating fibers, while Cx48.5 and Cx44.1 are abundantly expressed in the differentiating lens fibers. Cx44.1 transcription begins during the lens placode stage, while Cx48.5 expression was not detected until 36 hpf. This study supplies important information for future studies with antisense morpholinos and for the interpretation of lens mutant phenotypes that have already been identified in morphological screens of the visual system (Heisenberg *et al.*, 1996; Vihtelic *et al.*, 2001; Vihtelic and Hyde, 2002).

Table 2.1. Summary of Temporal and Spatial Expression Patterns of Cx48.5, Cx44.1, and Cx43 Transcripts in the Zebrafish Embryonic Lens

		24hpf	36hpf	2dpf	3dpf	4dpf
Cx48.5						
	Lateral epithelium	-	-	-	-	-
	Differentiating primary fibers	-	+	+	NA	NA
	Differentiating secondary fibers	NA	+	+	+	+
Cx44.1						
	Lateral epithelium	-	-	-	-	-
	Differentiating primary fibers	+	+	+/-	NA	NA
	Differentiating secondary fibers	NA	+	+	+	+
Cx43						
	Lateral epithelium	+	+	+	+	+
	Differentiating primary fibers	+	+	+/-	NA	NA
	Differentiating secondary fibers	NA	+	+	+/-	+/-

+ indicates a strong signal; – indicates absence of a detectable signal; +/- indicates a weak signal; NA indicates not applicable. Differentiated fibers were negative for all three transcripts.

Table 2.2. RT-PCR Primers

EF1α	F 5'-CAAGGGCTCCTTCAAGTACGCCTG-3' R 5'-GGCAGAATGGCATCAAGGGCA-3'
Cx48.5	F 5'-GCAGACTGTACTTTCTCTCTAG-3' R 5'-TCTTTCTCCTCCTGGAGC-3'
Cx44.1	F 5'-TTGGAGGAGGACAAATCCAC-3' R 5'-GGATGATGCCCTGACAGTTT-3'
Cx43	F 5'-CCTACAGGGCTCTCCACTC-3' R 5'-ACGGTTGAGTTTCTCCTCC-3'
Cx45.6	F 5'-GCTCTGTATCCATGTTCAATGC-3' R 5'-GCTCTGATACAGATTCTTCCC-3'
Cx35	F 5'-GAGGGCATTCTCCAGGTTTTAC-3' R 5'-TCACTTACGGTGCTCAGC-3'
Cx43.4	F 5'-GGCTCCAGAGAAGTCTGC-3' R 5'-TCTGCTCGACAGCAGTGC-3'

F = forward primer

R = reverse primer.

Figure 2.1

The phylogeny of lens connexins. Sequence analysis showed that zebrafish (zf) Cx48.5, mouse (ms) Cx46, and chicken (ch) Cx56 are grouped into one subfamily, zfCx44.1, msCx50, and chCx45.6 belong to another subfamily, and zfCx43, msCx43, and chCx43 are in a third subfamily. Zebrafish Cx48.5, Cx44.1, and Cx43 share 61%, 62%, and 80% amino acid identity to their mouse orthologues respectively. Zebrafish Cx35, a non-lens connexin, was used as an outlier.

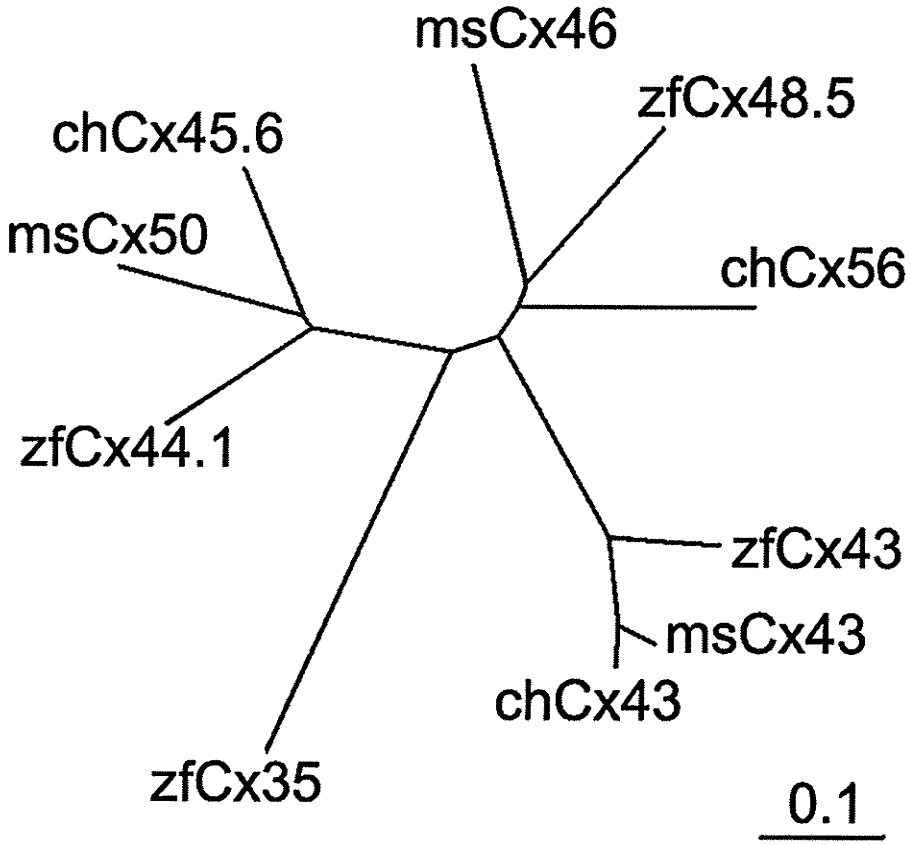
msCx46
zfCx48.5
chCx45.6
msCx50
chCx56
zfCx44.1
zfCx43
msCx43
chCx43
zfCx35
0.1

Figure 2.2

RT-PCR analysis of connexin expression in the adult lens. RT-PCR was performed with zebrafish adult lens and liver total RNA. Cx48.5 and Cx44.1 expression was detected in the adult lens. Cx43 expression was detected in both lens and liver. Zebrafish elongation factor 1 α was used as a positive control, and was detected in both tissues.

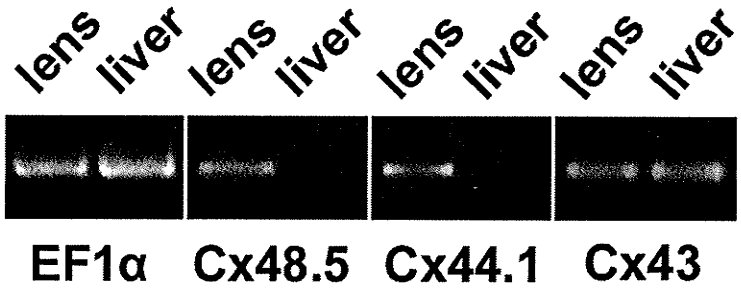
lens
liver
lens
liver
lens
liver
lens
liver
EF1α
Cx48.5
Cx44.1
Cx43

Figure 2.3

In situ hybridization analysis of connexin expression in the developing lens. Panels A-E shows images of eyes from embryos hybridized with sense control probes. Panels F-J show images of eyes from embryos hybridized with the Cx48.5 antisense probe. Panels K-O show images of eyes from embryos hybridized with the Cx44.1 antisense probe. Panels P-T show images of eyes from embryos hybridized with the Cx43 antisense probe. Arrowheads indicate the lateral epithelium, long arrows indicate differentiating primary fibers, short arrows indicate differentiating secondary fibers and asterisks indicates differentiated fibers. Bar, 50 μm.

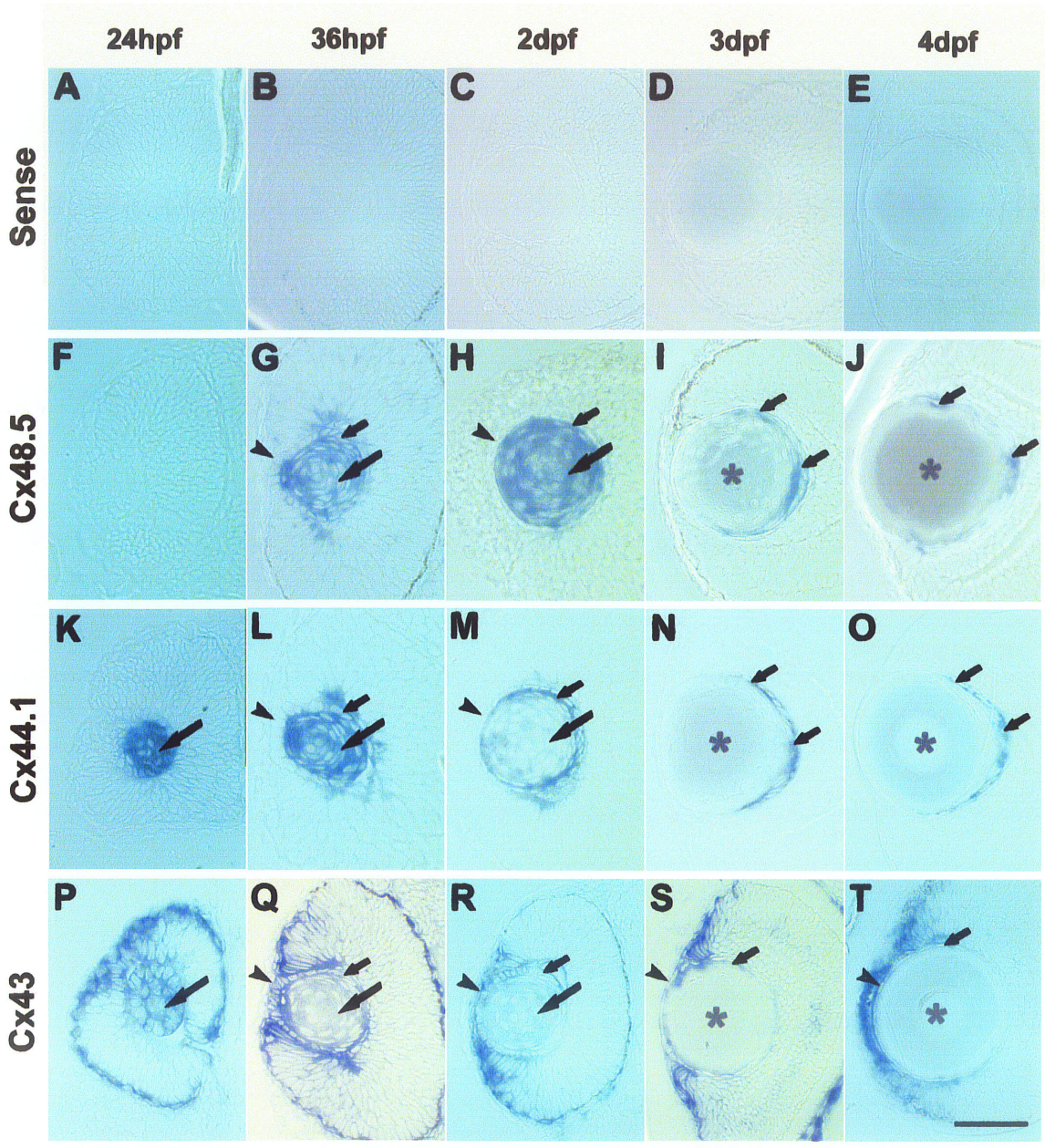
24hpf
36hpf
2dpf
3dpf
4dpf
Sense
Cx48.5
Cx44.1
Cx43
A
B
C
D
E
F
G
H
I
J
K
L
M
N
O
P
Q
R
S
T

CHAPTER III

CONNEXIN48.5 IS REQUIRED FOR NORMAL CARDIOVASCULAR FUNCTION AND LENS DEVELOPMENT IN ZEBRAFISH EMBRYOS

3.1 Rationale

Mouse knockout experiments have shown that Cx46 is required for lens homeostasis, but not lens growth (Gong *et al.*, 1997). Whether or not the function of Cx46 is conserved in other species, such as zebrafish, is unknown. It is also not clear if Cx46 has functions in organ systems other than the lens. Cx43, Cx40, Cx45 and Cx37 are the major connexins expressed in the mammalian heart, and mouse knockout experiments have demonstrated that they are all essential for cardiac development and function (Reaume *et al.*, 1995; Simon *et al.*, 1997; Kirchhoff *et al.*, 1998; Simon *et al.*, 1998; Kruger *et al.*, 2000; Kumai *et al.*, 2000). However, evidence also suggests other connexins may play a role in heart development and function. For example, despite the fact that Cx45 is the earliest connexin known to be expressed in the heart, cardiac function is initiated normally in Cx45 knockout mice (Kumai *et al.*, 2000). Also, in addition to Cx43, Cx40, Cx45 and Cx37, expression of two other connexins has been reported in the heart. Cx50 was detected in the atrioventrcular valves of the rat heart by immunohistochemistry (Gourdie *et al.*, 1992), whereas Cx46 mRNA was detected in the

rat heart by northern blotting (Paul *et al.*, 1991), and Cx46 protein was detected in the rabbit sinoatrial node by immunohistochemistry (Verheule *et al.*, 2001). Low amount of Cx46 protein was also found between occasional atrial and ventricular myocytes in the human heart (Davis *et al.*, 1995). However, no heart defects have been reported in the Cx50 and Cx46 knockout mice, and the function of these two connexins in the heart has remained a mystery.

In this study, we cloned the zebrafish Cx48.5 (orthologue to mammalian Cx46), and analyzed its expression. The function of Cx48.5 in the lens and cardiovascular system was examined by the morpholino knockdown technique. The antisense morpholino injected embryos developed cataracts as predicted. Unexpectedly the knockdown experiments also revealed two novel functions for this connexin in that the knockdown embryos also developed both microphakia and microphthalmia, and severe cardiovascular abnormalities. Our study provides the first functional evidence for a role for this orthologous group of connexins in ocular growth and cardiovascular function.

3.2 Materials and Methods

3.2.1 Screening of a zebrafish PAC library

A rat Cx46 cDNA probe (Paul *et al.*, 1991) was used to screen a zebrafish PAC library (German Human Genome Project, RZPD) at low stringency according to instructions supplied with the library. Two positive PAC clones were digested with Pst I and EcoR I and subcloned into the pBluescript II SK +/- vector (Stratagene, La Jolla, CA). Subclones were re-screened with the rat Cx46 probe under the same conditions, and

one positive subclone from each of the two original PAC clones was sequenced completely on both strands.

3.2.2 RT-PCR analysis with adult and embryonic tissues

Total RNA was isolated from adult tissues and whole embryos using TRIzol Reagent (Invitrogen, Burlington, ON). Total RNA (2 μg of each sample) was reverse transcribed using SuperScript II reverse transcriptase (Invitrogen), and a portion of the reverse transcription reaction was used for PCR with Taq polymerase (Invitrogen). For RT-PCR of 4 dpf embryonic hearts and lenses, tissues were dissected with extra fine needles and transferred to 200 μl PCR tubes with micropipettes. The tissues were washed once with PBS, and then immediately processed for RT-PCR with the Cell-to-cDNA II kit (Ambion, Austin, TX). Two embryonic lenses or hearts were used for each sample and the tissues were lysed in 6 μl Cell Lysis II buffer. The lysate was split into two parts: 4 μl were used for the reverse transcription and the remaining 2 μl were used as a negative control (no reverse transcriptase added). The total volume of each reverse transcription reaction was 8 μl; 4 μl of the reaction was used for Cx48.5 PCR and the other 4 μl for PCR with eF1α control primers. The primers used for Cx48.5 and eF1α control are the same ones used in Chapter II, listed in Table 2.2.

3.2.3 Whole mount *in situ* hybridization (WMISH) and whole mount immunohistochemistry (WMI)

WMISH was carried out as described in Chapter II. The Cx48.5 probe was 775 bp long extending from 612 nucleotides downstream of the start codon to 81 nucleotides

downstream of the stop codon, and the cmlc2 probe (generous gift from Dr. Didier Stainier, UCSF, CA) was about 1 kb long fragment from the 3' end of the cmlc2 cDNA (Yelon *et al.*, 1999). The alkaline phosphatase color reaction was allowed to proceed for 10 and 2 hours for the Cx48.5 and the cmlc2 probes, respectively. WMISH embryos were imaged on a Leica MZ8 steriomicroscope. WMI with the MF20 monoclonal antibody (Developmental Studies Hybridoma Bank, Iowa City, IA) was carried out according to the whole mount staining protocol in The Zebrafish Book (Westerfield, 1995). The secondary antibody used was a goat anti-mouse IgG labeled with Alexa Fluor 546 (Molecular Probes, Eugene, OR). The fluorescence images were collected on the Zeiss Axioskop FS microscope equipped with a rhodamine filter set. All images were captured with a SONY DXC-950 CCD color video camera and Northern Eclipse software (Empix, Mississauga, ON).

3.2.4 Microinjection of morpholino oligos

Cx48.5 antisense and control morpholinos were obtained from Gene Tools, LLC (Philomath, OR). Two non-overlapping antisense morpholinos were used. Both were targeted against non-coding sequences in 5'-UTR. The targeted sequences were 5'-GCTTCACGATTTCTAGCCTAGAGAG-3' and 5'-AACAGAGAGGATTCATTGAGAACTA-3'. The standard control morpholino sequence was 5'-CCTCTTACCTCAGTTACAATTTATA-3'. The standard control morpholino contains a random sequence, and has no significant antisense activity in the zebrafish system, as shown by previous studies [e.g., (Nasevicius and Ekker, 2000)]. Morpholino stock solutions were prepared according to (Nasevicius and Ekker, 2000),

and the working solution was 1 ng/nl. 1-cell stage zebrafish embryos were orientated in a holding chamber prepared according to The Zebrafish Book (Westerfield, 1995), and microinjected with a Narishige Pressure Microinjection System (Carsen Medical & Scientific Co. Ltd.) on a Nikon Eclipse TE300 inverted microscope.

3.2.5 Morphological analyses

For histological analysis the embryos were embedded in JB-4 (Polysciences, Warrington, PA), sectioned at 3 μm, stained with toluidine blue (1% in aqueous 1% borax), and imaged with a Zeiss Axioskop FS microscope. Observations of live embryos were performed with differential interference contrast optics (DIC) on a Zeiss Axioskop FS microscope, and dark field observations of dissected lenses were performed with a Leica MZ8 stereomicroscope. All images were acquired with a SONY DXC-950 CCD color video camera and Northern Eclipse Software.

3.2.6 Growth and heart rate measurements

For the measurements of the lens, eye, body length, and otic vesicles, embryos were anaesthetized according to The Zebrafish Book (Westerfield, 1995), and then placed in a viewing chamber constructed of a microscope slide and a supported cover glass. The space between the slide and the cover glass was about 1 mm, so that the zebrafish embryos were almost parallel to the slide. Images of lenses, eyes, and otic vesicles were collected as described above, and measured with the Northern Eclipse Software. Body lengths were measured by putting the slides against a ruler on a Leica MZ8 steriomicroscope. For the measurements of heart rates, the embryos were placed in 24-

well plates and allowed to equilibrate to room temperature (24°C). The plates were then placed on a Leica MZ8 steriomicroscope and the heart rates were counted. The embryos destined for heart rate measurements were not anaesthetized because this seemed to raise variation in the heart rate. Statistical comparisons were made between control and antisense injected embryos using an unpaired t-test. The default alpha level was 0.05 unless otherwise specified. N=12 for all comparisons except the heart rate where n=15.

3.2.7 .Movies

The movies show the heart beat in a 1.5 dpf Cx48.5 morphant embryo (Movie 1) and a 1.5 dpf control embryo (Movie 2). The trunk circulation in a 1.5 dpf Cx48.5 morphant embryo (Movie 3) and a control embryo (Movie 4) is also shown.

3.3 Results

3.3.1 Isolation of the zebrafish Cx48.5 gene

We are using comparative gene function analysis in our continued effort to understand the role of specific connexins in the development and function of the vertebrate ocular lens. We previously reported the cloning and characterization of Cx44.1, the zebrafish orthologue of rodent and human Cx50 (Cason *et al.*, 2001), and here we report the isolation and functional characterization of the zebrafish orthologue of rodent and human Cx46. The isolated genomic sequence contains a coding region of 1305 nucleotides within one single exon, coding for 434 amino acids. The protein has a predicted molecular weight of 48,492 Da, and is therefore named Cx48.5. Amino acid

sequence comparisons indicated that Cx48.5 belongs to the Cx46 orthologous group of connexins (61% amino acid identity to mouse Cx46, see chapter II). The amino acid sequence of Cx48.5 is consistent with the typical structure of a connexin (Yeager *et al.*, 1998; Unger *et al.*, 1999), with four transmembrane segments, a cytoplasmic loop between transmembrane segments 2 and 3, cytoplasmic amino and carboxy termini, and two extracellular loops with three conserved cysteines in each. Alignment of the amino acid sequences of the Cx48.5, mouse Cx46 and chicken Cx56 orthologs (Fig. 3.1) demonstrated conservation in the location of the six extracellular loop cysteines, and the two amino acids that have been shown to be mutated in human Cx46 linked congenital cataracts (N63 and P187) (Mackay *et al.*, 1999; Rees *et al.*, 2000). Analysis of the amino acid composition of Cx48.5 revealed that this connexin has an unusually low isoelectric point (pI; 5.64) and contains an unusually high proportion of glutamic acid (9.4%). Most members of the Cx46 orthologous group (mouse, sheep, cow, chicken) have a significantly higher pI (7.04-9.85) and much lower proportion of glutamic acid (5.2-6.7%). In contrast to this, most members of the Cx50 orthologous group (human, mouse, sheep, chicken, zebrafish) have low pI (5.01-5.44) and a much higher content of glutamic acid (10.0-13.2%). With respect to pI and glutamic acid content Cx48.5 therefore resembles the Cx50 orthologous group more closely than the Cx46 orthologous group, despite the fact that overall amino acid comparisons indicate clearly that Cx48.5 belongs to the Cx46 group.

3.3.2 Cx48.5 mRNA expression in embryos and adult tissues

RT-PCR was performed with RNA samples isolated from adult tissues, whole embryos, and embryonic hearts and lenses. Cx48.5 transcripts were not detected in 8 hpf whole embryo RNA, but were readily detected at 1 dpf and at later stages (Fig. 3.2A). In adult tissues Cx48.5 transcripts were detected in the lens and heart, and weak RT-PCR product was also amplified from testis mRNA. Cx48.5 mRNA was not found in the adult liver, ovary, brain, or retina. We also detected Cx48.5 transcripts in RNA isolated from 4 dpf embryonic hearts and lenses (Fig. 3.2B). Zebrafish elongation factor 1α (eF1α) primers were used to show that comparable amounts of cDNA were included in each reaction, and the absence of genomic DNA contamination from all the samples. The eF1α primers span an intron and produce a PCR product of smaller size from cDNA than genomic DNA (569 bp vs 733 bp) (Fig. 3.2A and B).

Whole mount *in situ* hybridization (WMISH) was performed with embryos from 24 hpf to 4 dpf. A strong signal was detected in the otic vesicles in 24 hpf embryos (Fig. 3.2C and D). The otic vesicle expression appeared to be transient since it was not detected at any of the later stages (36 hpf to 4 dpf). To our knowledge the expression of a Cx46 family member in the auditory system has not been reported before. In contrast to the signal in the otic vesicles, expression of Cx48.5 in the lens was barely above background at 24 hpf (Fig. 3.2C). Instead, strong expression of Cx48.5 in the lens was observed at 36 hpf (Fig. 3.2E and F), and later stages. Although, by WMISH, Cx48.5 expression was only detected in the otic vesicles and the lens, we cannot exclude the possibility of expression in other tissues, due to the sensitivity of the WMISH protocol used.

3.3.3 Antisense morpholino knockdown of Cx48.5 expression

Microinjection of antisene morpholinos into 1-2 cell stage zebrafish embryos has been widely used for targeted inhibition of zebrafish gene expression (Ekker and Larson, 2001; Heasman, 2002; Nasevicius and Ekker, 2000). Embryos that have had the expression of a specific gene inhibited with morpholinos are termed morphants (Ekker, 2000). In this study, two non-overlapping antisense morpholinos (MO-1 and MO-2) were targeted against sequences upstream of the Cx48.5 coding sequence. Comparisons of the morpholino sequences to all zebrafish sequences in GenBank failed to identify any sequences with significant similarities to either morpholino. In preliminary dose-response experiments the effective dose for producing a specific phenotype (see below) was 3-5 ng, when either MO-1 or MO-2 was injected individually. However, the same phenotype was produced with only 1 ng of each morpholino when the two morholinos were co-injected. The morphants data presented in the following sessions were analyzed with embryos co-injected with 1 ng of each antisense morpholino. Synergistic effects between two non-overlapping morpholinos are frequently observed in zebrafish embryos (Ekker and Larson, 2001). Whether individually injected or co-injected, the morpholinos clearly produced the same phenotype, while embryos injected with the same amount of non-specific control morpholino never displayed any developmental abnormalities. Hence we conclude that the phenotype obtained is specific for Cx48.5 targeting. However, the age at which the phenotype became detectable and the severity of the phenotype varied slightly between individual embryos, presumably due to slight variability in the volume injected and individual differences in the rate of development.

3.3.4 Cataract formation, microphakia and microphthalmia in Cx48.5 morphants

The center region of the lens in Cx48.5 morphants became visibly abnormal in live embryos by 3–4 dpf. The lenses in live Cx48.5 morphants appeared uneven and rough when viewed with DIC optics, in contrast to the very smooth appearance of the lenses in the control embryos (Fig. 3.3A and B). Sectioning of the morphant eyes also revealed histological abnormalities. In the control lenses at 3 dpf, the primary lens fibers in the center region were mature, and less intensely stained with toluidine blue than the cortical fibers. The less intense staining in the central fibers in the normal control lenses reflects the loss of basophilic materials such as ribosomes and nuclei during the differentiation process. The differentiating secondary fiber cells elongate medially from the equatorial region, and form the long, smooth and tightly packed fibers of the normal lens (Fig. 3.3D). However, this differentiation process was disrupted in the Cx48.5 morphants. The primary and secondary fibers in the Cx48.5 morphants did not gain the same long, thin, and smooth shape by 3 dpf. Instead most of the fibers remained nucleated and the entire core of the lens appeared disorganized (Fig. 3.3C). Cx48.5 morphant and control lenses were dissected from embryos at a series of stages, and observed with a microscope equipped with darkfield optics. Nuclear opacities (cataracts) first appeared in the Cx48.5 morphant lenses by 5.5- 7.5 dpf. The cataractous lens shown in figure 3.3E was photographed at 9.5 dpf. The size of the cataracts in the lenses of the Cx48.5 morphants also varied. The retina also appeared to be abnormal in the Cx48.5 morphants. All the retinal cell layers were present in the Cx48.5 morphants, but they appeared to be thinner and less well developed than in the control retinas (Fig. 3.3C).

Previous work has demonstrated that Cx50, but not Cx46, is required for the development of normal lens and eye size in mice (Gong *et al.*, 1997; White *et al.*, 1998; Rong *et al.*, 2002; Martinez-Wittinghan *et al.*, 2003). To determine if this was an ancient or derived feature of the function of these genes in the lens we investigated the size of ocular structures in the Cx48.5 knockdown zebrafish embryos. Measurements of lens and eye size revealed that both were significantly smaller in the Cx48.5 morphants than in the controls ($p<0.001$). At 3.5 dpf, when the lens abnormality was first becoming noticeable, the Cx48.5 morphant lenses were 6.3% smaller in diameter than the control lenses (Fig. 3.3G). By using the lens diameter measurements to calculate lens volume (assuming a that the lens is a sphere), the lenses in the Cx48.5 morphants were found to be 17.7% smaller in volume than the controls at 3.5 dpf. By 6.5 dpf the morphant lenses were 13.7% smaller in diameter than the controls, and 35.7% smaller in volume (Fig. 3.3G). The size of the eye was also significantly smaller in the Cx48.5 morphants (Fig. 3.3H). The anterior-posterior diameter of the morphant eyes was 10.5% and 7.2% smaller than the diameter of the control eyes at 3.5 and 6.5 dpf, respectively. No significant difference was observed in the length of the whole embryo between the Cx48.5 moprhants and the controls (Fig. 3.3I), indicating that the smaller lens and eye in Cx48.5 morphants was not due to undergrowth of the embryo as a whole. Since we observed Cx48.5 expression in the otic vesicles only early on, we measured their size at 2.5 and 3.5 dpf. No significant difference was found in the size of otic vesicles between the Cx48.5 morphants and the controls (Fig. 3.3J).

3.3.5 Abnormal cardiac contractions and circulation blockage in Cx48.5 morphants

In addition to the ocular abnormalities described above, we also observed severe cardiovascular dysfunction in the Cx48.5 morphants (Fig. 3.4). The abnormal cardiovascular function became apparent about 1.5 dpf, much earlier than the lens dysmorphology. Prior to 1.5 dpf cardiovascular development in the Cx48.5 morphants appeared normal, including the initiation of cardiac contractions around 22-24 hpf. At 1.5 dpf the normal zebrafish heart is a simple tubular structure, and neither the bulbus arteriosus, nor the cardiac valves, have developed yet. Blood is pumped unidirectionally through the heart by alternate atrial and ventricular contractions. In each chamber contractions are initiated caudally and a wave of contractions then travels anteriorly while the posterior portion of the chamber remains contracted. This process culminates in the near obliteration of the chamber lumen, thereby minimizing backflow (this study, and (Hu *et al.*, 2000; Hove *et al.*, 2003)) (Fig. 3.4F-J; Movie 1). By contrast, contractions in the morphant atria appeared less coordinated and as a consequence the full contraction of the entire atrium as seen in the controls was never achieved. Frequently the posterior end of the atrium was already relaxing by the time the contractile wave reached the anterior end, thereby causing the blood to move back and forth within the atrium (Fig. 3.4A-C) (see Movie 2). In control embryos the ventricles could be seen to expand in volume and fill very rapidly and forcefully during diastole (Fig. 3.4I-J; Movie 1). This is likely aided by the rapid fall in intraventricular pressure to near zero that occurs at the end of systole (Hu *et al.*, 2000). Contractions in the morphant ventricles appeared very uncoordinated. In addition the ventricle appeared to expand much less than the control ventricles during

diastole and as a result the extent of ventricluar filling was much lower than normal (Fig. 3.4D-E) (Movie 2).

Accompanying the cardiac abnormality was a block in the systemic circulation (compare Movies 1 and 2, and Movies 3 and 4) that was evident between 1.5 and 3.5 dpf. Blood cells did not move through the heart during this period, and starting from 1.5 dpf, blood accumulation was seen in the common cardinal vein distal to the atrium in the Cx48.5 morphants (Fig. 3.5A and B). Between 2 and 4 dpf, blood accumulation was seen in the trunk veins of the morphant embryos and in the atria of some of them (Fig. 3.5C). Arrhythmia, tachycardia, enlarged atria, and pericardial edema developed frequently between 3 and 5 dpf; these are possibly secondary effects of the primary cardiac dysfunction evident at 1.5 to 2 dpf. However, most of the Cx48.5 morphants recovered from the cardiovascular symptoms by 5 to 6 dpf. The recovery of the Cx48.5 morphants from cardiac dysfunction is possibly due to withdrawal of the antisense morpholino effects. Antisense morpholinos are typically effective for the knockdown of translation of the targeted mRNA during first a few days of zebrafish development only (Ekker and Larson, 2001; Heasman, 2002).

Overall, the duration of each cardiac cycle appeared longer in the morphant hearts (compare Movies 1 and 2). We quantified this difference by comparing the heart rates in the Cx48.5 morphants and the control embryos. The Cx48.5 morphants had significantly slower heart rates than the control embryos at 1.5 and 2.5 dpf ($p<0.001$), but at 3.5 dpf the rates had become faster than the controls (Fig. 3.5G) ($p<0.01$). Heart rate measurements were not carried out with older embryos because the morphant cardiac phenotype was much more varied in later stages (including arrhythmia, tachycardia,

pericardial edema, and occasional bradycardia), rendering group comparisons less meaningful. The lengthening of the cardiac cycle in the morphants appeared to arise primarily from the slowing of the caudal to cephalic waves of atrial and ventricular contractions.

Although the cardiovascular function of the Cx48.5 morphants was severely impaired, no gross morphological abnormalities were seen in the morphant hearts in the early stages (1.5 to 3 dpf). However, some of the morphant hearts became morphologically atypical later on (3 to 5 dpf), possibly induced by the early stage heart dysfunction. To confirm whether the morphant hearts were morphologically normal and had reached normal extent of differentiation at the time of the cardiovascular dysfunction onset, we examined the expression of two cardiac markers in the Cx48.5 morphants: cardiac myosin light chain 2 (cmlc2)(Yelon *et al.*, 1999), and myosin heavy chain (MF20)(Bader *et al.*, 1982; Alexander *et al.*, 1998). These markers are expressed in both the atrium and the ventricle (Yelon *et al.*, 1999). We carried out a whole mount *in situ* hybridization with a cmlc2 antisense RNA probe at 1.5 dpf, and the MF20 antibody was used in whole mount immunohistochemistry at 1.75 dpf. The expression of cmlc2 and MF20 appeared to be typical in the Cx48.5 morphants (Fig. 3.6A and C). Hence we conclude that the functional cardiovascular defect displayed by the Cx48.5 morphants at the early stages is not caused by abnormal cardiac morphology nor defective differentiation of the myocardium.

3.4 Discussion

We report here the identification and characterization of Cx48.5, a novel member of the zebrafish connexin gene family. Cx48.5 is predicted to possess all the typical features of connexin family members, such as four α-helical transmembrane segments and two extracellular loops with three conserved cysteine residues in each. Sequence comparisons indicated that Cx48.5 shares the highest degree of sequence identity with the Cx46 orthologous group of connexins. The electrophysiological properties of the gap junction channels composed of Cx48.5 were also found similar to the Cx46 group (appendix B), supporting the notion that Cx48.5 belongs to the Cx46 subfamily. An unusual feature of Cx48.5 is its low isoelectric point and high content of glutamic acid residues. With regards to these two features Cx48.5 resembles more closely the Cx50 orthologous group of connexins than the Cx46 subgroup. How these differences might influence the function of Cx48.5 relative to its orthologs is not clear, but they may contribute to some of the phenotypic differences between Cx46 knockout mice and our Cx48.5 knockdown zebrafish.

Previous research on the *in vivo* function of Cx46 family members has primarily focused on the expression and role of this connexin in the development and maintenance of the ocular lens. In fact, Cx46 has frequently been considered a lens specific connexin. This view has been reinforced by the apparent absence of non-ocular abnormalities in Cx46 knockout mice (Gong *et al.*, 1997). However, several studies, including ours, have documented the expression of Cx46 members in tissues other than the lens, including: heart (Paul *et al.*, 1991; Davis *et al.*, 1995; Verheule *et al.*, 2001), kidney (Paul *et al.*,

1991; Silverstein *et al.*, 2003), alveolar epithelial cells (Abraham *et al.*, 2001), osteoblastic cells (Koval *et al.*, 1997) and degenerating Schwann cells (Chandross *et al.*, 1996). In this study we demonstrate that in addition to the lens, Cx48.5 is expressed in the embryonic and adult heart, in the early otic vesicles, and adult testes. We have recently reported a detailed description of the Cx48.5 WMISH expression pattern in the developing zebrafish lens (Chapter II). We did not observe any gross morphological abnormality in the otic vesicles of the Cx48.5 morphants and the question of whether Cx48.5 has a role in inner ear development and function is yet to be answered. Neither do we know what possible role Cx48.5 might play in the testis as the antisense morpholino effects will have worn off by the time the testes fully develop.

The Cx48.5 knockdown embryos reproduced the cataract phenotype seen in the Cx46 knockout mice (Gong *et al.*, 1997). Somewhat surprisingly however, the Cx48.5 morphants also developed abnormally small lenses and eyes, features that were observed in the Cx50, but not the Cx46 knockout mice (Gong *et al.*, 1997; White *et al.*, 1998; Rong *et al.*, 2002). Further insight into the contribution of Cx46 and Cx50 to ocular growth has been gained from recent knockin and knockover experiments. Homozygous replacement of the Cx50 coding sequence with the Cx46 coding sequence did not rescue the growth defect, regardless of whether the native Cx46 locus was intact or not (White, 2002; Martinez-Wittinghan *et al.*, 2003). On the other hand lens growth was normal in mice with one native Cx50 allele intact, whether the second allele was deleted, or replaced with Cx46 (White, 2002; Martinez-Wittinghan *et al.*, 2003). Thus it appears that the role of connexins in lens growth in mice is primarily served by Cx50, and that the role of Cx46 in this process is negligible. From the present study it is clear that zebrafish Cx48.5,

by several criteria a Cx46 orthologue, has a growth regulatory role in the lens. Whether or not Cx44.1, the zebrafish orthologue of mouse Cx50, also plays a role in lens growth is currently under investigation in this lab. My preliminary data (see appendix Fig. 1) suggest that Cx44.1 contributes to both lens growth and homeostasis. Our data also suggest a role for Cx48.5 in retinal development, since smaller retinas developed in the Cx48.5 morphants. Currently we do not know the underlying cause of the retinal defect, but it may be that the aberrant development of the Cx48.5 knockdown lenses interferes with signaling between the lens and the retina. A number of studies have demonstrated that signals emanating from the lens are required for normal growth of the retina (Coulombre and Coulombre, 1964; Breitman *et al.*, 1987; Yamamoto and Jeffery, 2002)

Although Cx46 mRNA or protein has been detected in the adult rat, rabbit and human heart (Paul *et al.*, 1991; Davis *et al.*, 1995; Verheule *et al.*, 2001), no cardiac defects were reported in the Cx46 knockout mice (Gong *et al.*, 1997). This is in contrast to the cardiac dysfunction we observed in the Cx48.5 knockdown embryos. Several possible explanations exist for the apparent discrepancy between the mouse and zebrafish data with respect to cardiac function. The most straightforward explanation is that Cx46 is either not expressed, or does not carry out an essential physiological function in the fetal, neonatal or adult mouse heart. We are currently investigating this possibility. Alternatively, Cx46 may have an essential role in the heart at some stage in the life of the mouse, but in its absence this role can be covered by one of the other connexins expressed in the heart. Another possibility is that the Cx46 knockout mice may have suffered a cardiac abnormality in early fetal life that was both transient and non-lethal, and therefore went undetected. We can not exclude the possibility that the role of Cx48.5

in zebrafish cardiovascular function is transient and non-essential as well, because we do not know whether the recovery of function we observed is due to reduction in the knockdown effect caused be cellular dilution of the morpholino, or due to a diminished role for Cx48.5 in cardiac function as the heart matures.

The cause of the abnormalities we observed in the cardiovascular system is most consistent with a defect in some aspect of the generation or propagation of chamber activation. The underlying molecular and cellular mechanisms are not known at this time, but it is interesting to note that several of the mutants identified in the initial large scale screens displayed cardiovascular defects resembling the cardiovascular problems of the Cx48.5 morphants (Chen *et al.*, 1996; Stainier *et al.*, 1996). Adult zebrafish hearts do not appear to contain a histologically discrete conduction system such as the His-Purkinje system of mammals. Instead, the ventricular trabeculae appear to be the functional equivalents of the specialized conduction system in mammals (Sedmera *et al.*, 2003). Although extensive network of ventricular trabeculae have begun to form by 5 dpf, at 2 dpf when the cardiovascular abnormalities in the Cx48.5 morphants were at their peak, the ventricle is devoid of trabeculae (Hu *et al.*, 2000). The conduction requirements of the 2-3 dpf zebrafish hearts may therefore be quite different from 5 dpf hearts in which trabeculae have formed. Perhaps this early requirement is partially fulfilled by Cx48.5, but once trabeculae form, impulse conduction can proceed through gap junctions composed of other connexins. A similar situation may exist in mice. Cx45 is the earliest known connexin to be expressed in the heart tube, yet cardiac contractions are initiated at the correct time in Cx45 knockout mice (Kumai *et al.*, 2000). It will be interesting to determine if the cardiac contractions in the early Cx45 knockout embryos are mediated

by Cx46. In this report we have placed less emphasis on the cardiovascular abnormalities observed in later stage Cx48.5 morphants, because it is not possible based on our data to distinguish whether these were primary effects due to Cx48.5 knockdown or secondary effects arising from the earlier defects in blood flow. In particular, it has been shown that the fluid forces from the blood circulation are necessary for the zebrafish heart to develop properly (Hove *et al.*, 2003). Hence, the developmental and functional abnormalities observed at later stages were possibly at least partially due to secondary effects, and therefore less indicative to the function of Cx48.5 in the zebrafish heart.

3.5 Summary

Sequence analysis showed that Cx48.5 is is the zebrafish orthologue of mammalian Cx46. RT-PCR detected Cx48.5 expression in both adult and embryonic lens and heart, and adult testis. Whole mount *in situ* hybridization detected Cx48.5 expression in the otic vesicles by 1 dpf, and the lens starting from 1.5 dpf. Cx48.5 expression was disrupted in the embryos microinjected with antisense morpholinos. Cx48.5 morphants developed cataracts by 5.5 to 7.5 dpf, as well as smaller lenses and eyes. The heart of the Cx48.5 morphant developed normally at the early stage, but exhibited severe abnormalities in the cardiac contraction, and resulted in a failure of blood circulation. These results are the first indication that members of the Cx46 orthologous group of connexins play a significant role in ocular growth regulation and cardiovascular function.

Figure 3.1

Sequence alignment of Cx46 orthologs from mouse, zebrafish, and chicken. Solid lines over the sequences delineate the four transmembrane regions of connexins. The X symbols indicate the six conserved cysteines within the two extracellular loops. The two bold black dots above the sequences show the conserved Asn and Pro residues that are mutated in humans with congenital cataracts (N63 and P187). Amino acid identity between all three sequences is indicated with (*), strong conservation with (:), and weak conservation with (.).


50
100
150
200
250
300
350
400
450
500
msCx46 MGDWSFLGRLLENAQEHSTVIGKVWLTVLFIFRILVLGAAAEEVWGDEQSDFTCNTQQPGCENVCYDRAFPISHIRFWALQIIFVSTPTLIYLGHVLHIVRME
zfCx48.5 MGDWSFLGRLLENAQEHSTVIGKVWLTVLFIFRILVLGAAAEEVWGDEQSDFTCNTQQPGCENVCYDEAFPISHIRFWVLQIIFVSTPTLIYLGHVLHIVRME
chCx56 MGDWSFLGRLLENAQEHSTVIGKVWLTVLFIFRILVLGAAAEEVWGDEQSDFTCNTQQPGCENVCYDKAFPISHIRFWVLQIIFVSTPTLIYLGHVLHIVRME
msCx46 EKKKEREEELLRRDNPQ--------HGRGREPMRTGS--------PRDPPLRDDRGKVRIAGALLRTYVFNIIFKTLFEVGFIAGQYFLYGFQLQPLYRCDRW
zfCx48.5 EKRKEREEELRKASRLQEEKELLYRNGGGGEPGGRGGGGK-----KEKPPIRDEHGKIRIRGALLRTYVFNIIFKTLFEVGFILGQYFLYGFQLRPLYKCARW
chCx56 EKRKEKEEELKKRGSVKDNNYPGAATSGGGSGGGNNFKDPPIKMGKEKLPIRDERGRIRMGGALLRTYIFNIIFKTLFEVGFIVGQYFLYGFELKPVYQCSRP
msCx46 PCPNTVDCFISRPTEKTIFVIFMLAVACASLVLNMLEIYHLGWKKLKQGVTNHF----------NPDASEARHKPLDPLPAATSSGP
zfCx48.5 PCPNTVDCFISRPTEKTIFIIFMLVVACVSLLLNLLEIYHLGWKKVKQGMTNEF----------APDR-ESLPEADEAEPESPRTAP
chCx56 PCPHTVDCFISRPTEKTIFIIFMLVVASVSLLLNMLEIYHLGWKKLKQGMTSQYSLEMPVTTLTPVMVTGESKPVSLPPPAPPVVVTTTAPAPVLPDTRAVTP
msCx46 PSVSIGFPPYYTHPAC----PTVQGKAIGFPGAPLSPAD----------FTVVTLNDAQGRNHP--VKHCNG-HHLTTEQNWTRQVAEQQT---PASKPSSAA
zfCx48.5 P--TLSYPPDYTEVA-------VAGGAFLQPVSAPSTAE----------FKMDPLREELEESSPFYISNNNN-HRLAAEQNWANLATEQQTREMNATSPCSSS
chCx56 LLAPVTMAPYYAAAAPRTRPPSNTASMASYPVAPPVPENRHRAVTPTPVSTPVTIQRPYPTPTPAIINYFNSKRMLAARQNWVNMAAEQQGKAPSSSAGSSTP
msCx46 S--SPDGRKG----------LIDS----SGSSLQESALVVTPEEGEQ---------ALATTVEMYSPPLVLLDP---GRSSKSSNGRARPGDLAI
zfCx48.5 SSCSSDNVRQ----------SKDAAQLASTPSSAGGGLSTGPEEG----------HVTTTVEMHEPPVIFTDARRLSRASKASSVRARPNDLAV
chCx56 SSVRHPLPEQEEPLEQLLPLPAGPPITTTNSGSSTSLSGASGSKWDVEGEEELAEERPISATCTTVEMHEPP-LLVDTRRLSRASKSSSSRARSDDLAV

Figure 3.2

Cx48.5 expression in embryos and adult tissues. RT-PCR was performed with RNA samples isolated from embryos and adult tissues. Cx48.5 specific products were amplified from RNA isolated from 1to 5 dpf whole embryos (A), the adult lens, heart, and testis, and the embryonic (4 dpf) lens and heart (B). The eF1α primers amplified a single 569 bp fragment in all the samples, demonstrating the presence of cDNA, and the absence of genomic DNA from all samples. Whole mount *in situ* hybridization detected Cx48.5 transcripts in the otic vesicles (OV) in 24 hpf embryos (C and D), but not in 36 hpf embryos. Cx48.5 transcripts were not detected in the lens until 36 hpf (E and F). In the 36 hpf lens, Cx48.5 is transcribed in the differentiating primary lens fibers (PF), but not in the lateral epithelium (LE).

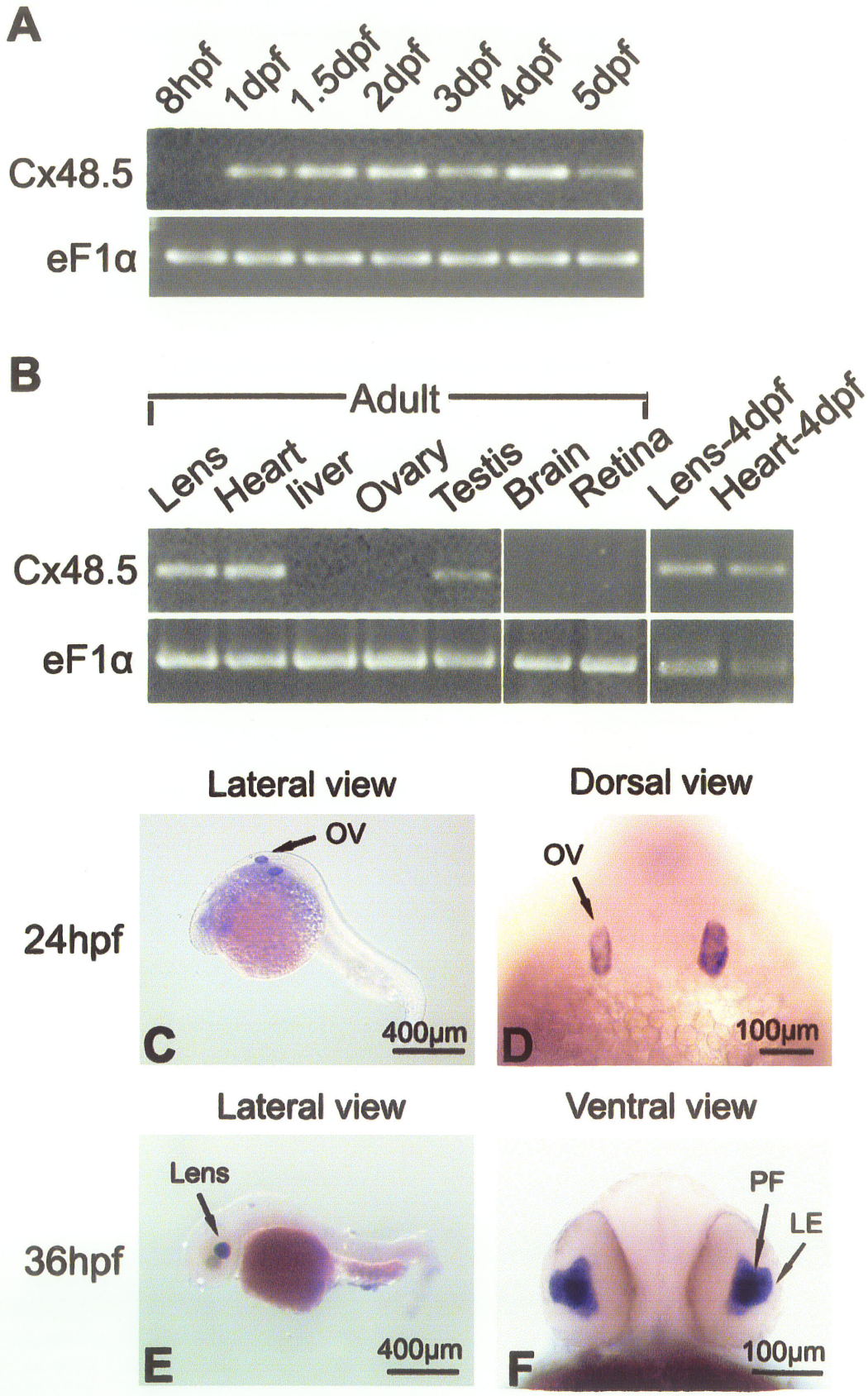
A
8hpf
1dpf
1.5dpf
2dpf
3dpf
4dpf
5dpf
Cx48.5
eF1α
B
Adult
Lens
Heart
liver
Ovary
Testis
Brain
Retina
Lens-4dpf
Heart-4dpf
Cx48.5
eF1α
Lateral view
Dorsal view
24hpf
OV
OV
C
400μm
D
100μm
Lateral view
Ventral view
36hpf
Lens
PF
LE
E
400μm
F
100μm

Figure 3.3

Cx48.5 morphants developed cataracts and smaller lenses and eyes. Microscopic observations of the Cx48.5 morphants with DIC optics revealed marked irregularities and roughness in the lens core by 3 dpf (A), which was in strong contrast to the smoothness of the control lenses (B). Sections of those lenses revealed that lens fiber differentiation was abnormal and immature in the Cx48.5 morphants (C), while the lens fibers in the core region of the control lenses had fully differentiated by this time (D). Note also that the retina in the Cx48.5 morphants (C) is smaller than in the controls. Lenses were dissected from 9.5 dpf embryos, and observed with a darkfield microscope. The morphant lenses developed nuclear opacities (cataract, E), while the control lens is transparent (F). Lens, eye, and otic vesicle size, as well as body length, were compared between the Cx48.5 morphants and the controls. The Cx48.5 morphant has significantly smaller lenses and eyes at 3.5 and 6.5 dpf (G and H, $p<0.001$). However, no significant difference in whole body length was detected between the Cx48.5 morphants and the controls at 3.5 and 6.5 dpf (I), and neither does the size of the otic vesicles differ between the morphants and the controls at 2.5 and 3.5 dpf (J). The * sign indicates significant difference existing between the morphant and control groups. Data are presented as means ± SD. Bar, 50 μm.

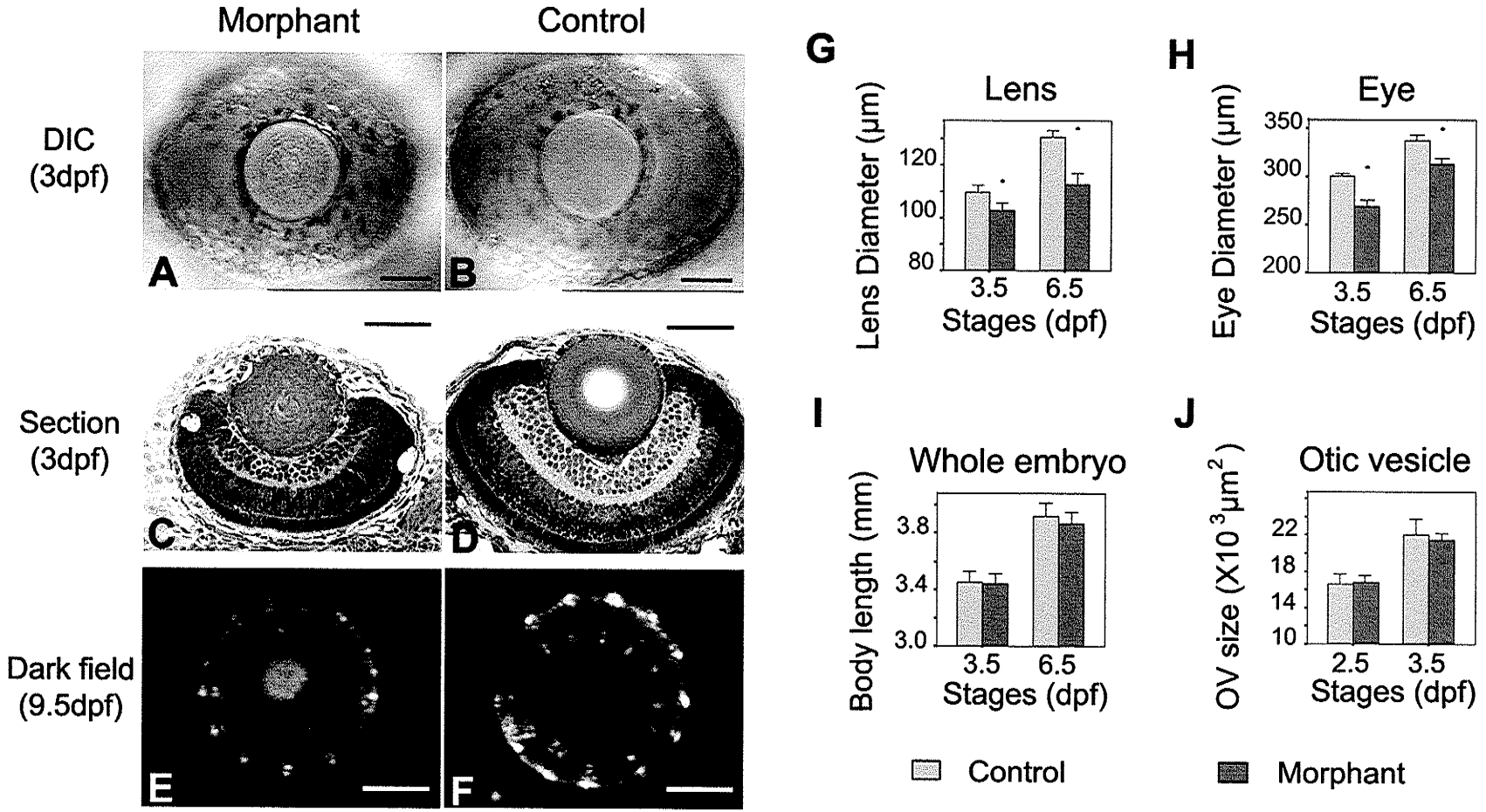
Morphant
Control
DIC
(3dpf)
Section
(3dpf)
Dark field
(9.5dpf)
A
B
C
D
E
F
G
Lens
Lens Diameter (µm)
120
100
80
3.5
6.5
Stages (dpf)
H
Eye
Eye Diameter (µm)
350
300
250
200
3.5
6.5
Stages (dpf)
I
Whole embryo
Body length (mm)
3.8
3.4
3.0
3.5
6.5
Stages (dpf)
J
Otic vesicle
OV size (X10 3µm2)
22
18
14
10
2.5
3.5
Stages (dpf)
Control
Morphant

Figure 3.4

Cx48.5 morphants exhibited cardiac abnormalities by 1.5 dpf. All panels are ventral views, head up. Panels A-C (Cx48.5 morphant embryo) and F-H (control embryo) show images of atria at different stages of the cardiac cycle. The atria are demarcated with dashed lines. The contractile wave in the Cx48.5 morphant is initiated normally at the posterior end of the atrium (B) but as it travels towards the anterior end the posterior portion of the atrium begins to relax (C), so that contractions in the anterior and posterior regions of the atrium are not synchronized. Arrowheads show a region of the morphant atrium undergoing contraction, while other parts of the atrium are in a relaxed state. In contrast, the posterior portion of the atrium in the control embryos remains contracted as the wave travels in the anterior direction such that the entire atrium is contracted at the end of the cycle (G and H). Panels D-E (Cx48.5 morphant embryo; from Movie 2) and I-J (control embryo; from Movie 1) show images of ventricles at two stages of the cardiac cycle. The ventricles are outlined with dash lines. The atria are labelled with a small font letter A. Panel I shows a fully distended ventricle in a control embryo at the end of diastole and panel J shows the same ventricle at the end of systole. These panels show that the volume of the ventricle increases significantly during diastole. However, in the Cx48.5 morphant the ventricular volume difference between diastole and systole was greatly reduced and the ventricle became somewhat misshapen (D and E). Bar, 100 μm.

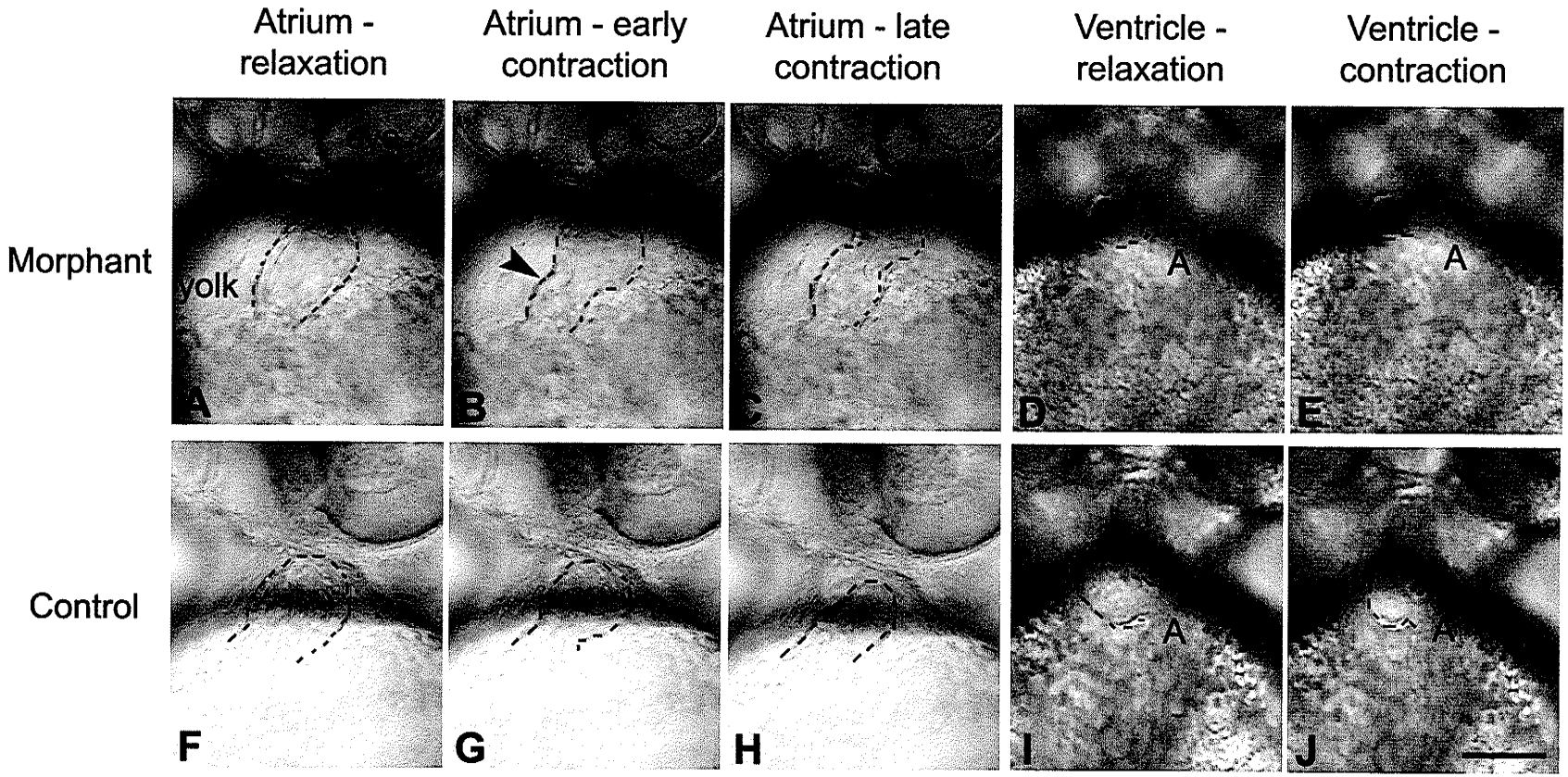
Atrium - relaxation
Atrium - early contraction
Atrium - late contraction
Ventricle - relaxation
Ventricle - contraction
Morphant
Control
yolk
A
B
C
D
E
F
G
H
I
J

Figure 3.5

Cardiac dysfunction and blood circulation blockage in the Cx48.5 morphants. By 1.5 dpf blood had begun to accumulate in the common cardinal vein in the Cx48.5 morphants (A and B, arrowhead). The morphology of the heart appeared normal at this stage (B and E). Blood accumulation was also seen in the caudal vein and other vessels in the trunk (C). Blood circulation was almost completely blocked at this stage (see Movie 3). The Cx48.5 morphants had significant slower heart rate than the controls at 1.5 and 2.5 dpf (G, $p<0.001$), but had faster heart rates than the controls at 3.5 dpf (G, $p<0.01$). Panels A-F are lateral views with the head to the left. The * sign indicates significant difference existing between the morphant and control groups.

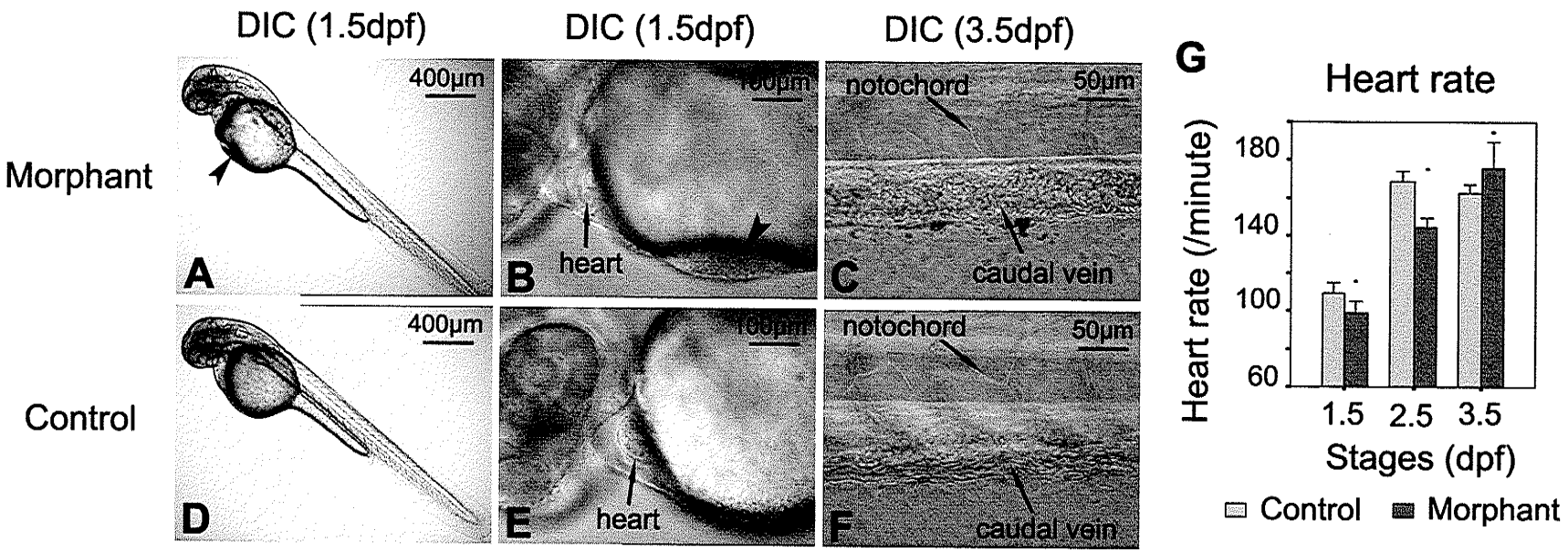
DIC (1.5dpf)
DIC (1.5dpf)
DIC (3.5dpf)
Morphant
Control
400μm
400μm
heart
heart
notochord
notochord
50μm
50μm
caudal vein
caudal vein
A
B
C
D
E
F
G
Heart rate
Heart rate (/minute)
180
140
100
60
1.5
2.5
3.5
Stages (dpf)
Control
Morphant

Figure 3.6

The expression of cardiomyocyte markers is normal in the early Cx48.5 morphant hearts. The expression of the cardiomyocyte differentiation markers cmlc2 and MF20 was examined at 1.5 and 1.75 dpf, respectively. Both markers were expressed normally in the Cx48.5 morphants (A and C), indicating that differentiation of the myocardium was not disrupted by the knockdown of Cx48.5 expression. V = ventricle, A = atrium. All panels are ventral views with the head pointing up.

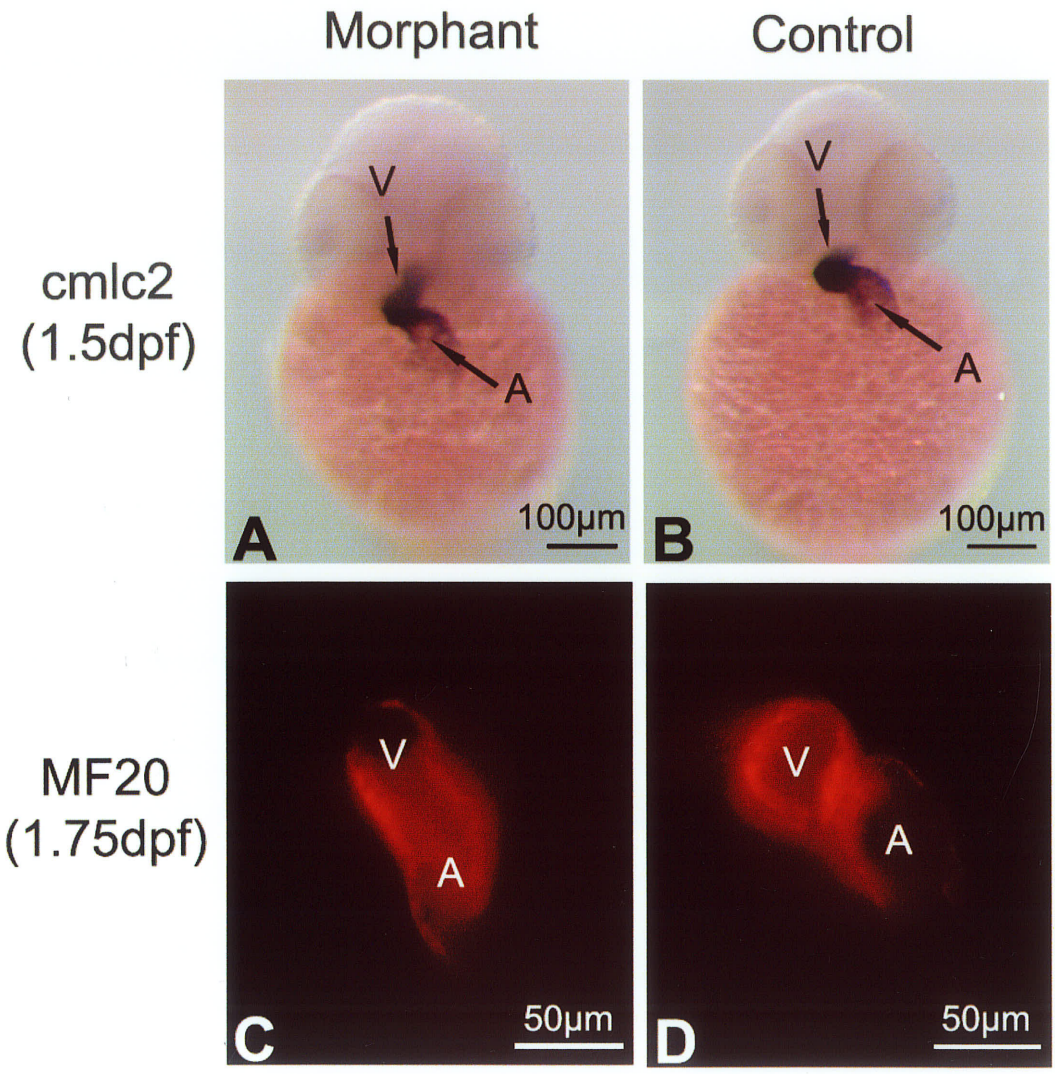
Morphant
Control
cmlc2
(1.5dpf)
MF20
(1.75dpf)
V
A
100μm
A
B
C
D
50μm

Movie 3.1

Cardiac contractions in a Cx48.5 morphant. Movie shows the cardiac cycle in a Cx48.5 morphant. Notice that the contractions are disorganized in both atrium and ventricle, and the reduced ventricular filling (compare to Movie 2). Movie was collected at 33 frames/second and played at one fifth of the original speed. Figure 3.4D-E are still images from Movie 1.

Movie 3.2

Cardiac contractions in a control embryo. Movie shows cardiac cycles in the control embryo. Notice the large ventricular volume increase during diastole. Movie was collected at 33 frames/second and played at one fifth of the original speed. Figure 3.4I-J are still images from Movie 2.

Movie 3.3

Blood circulation in a Cx48.5 morphant. Movie shows blood circulation in the caudal vein of a Cx48.5 morphant. Notice the near absence of blood cell movement through the vein (compare to Movie 4). Movie was collected at 33 frames/second and played at one fifth of the original speed.

Movie 3.4

Blood circulation in a control embryo. Movie shows blood circulation in the caudal vein of a control embryo. Notice the fast movement of blood cells through the vein. Movie was collected at 33 frames/second and played at one fifth of the original speed.

CHAPTER IV

POTENTIAL DOUBLE KNOCKDOWN OF CONNEXIN44.1 AND CONNEXIN48.5 IN ZEBRAFISH LENS LEADS TO REDUCED LENS GROWTH AND THE FORMATION OF CATARACTS BY APOPTOSIS

4.1 Rationale

Whether or not Cx44.1 and Cx48.5 have redundant functions in lens development and homeostasis can be determined by creating zebrafish embryos deficient for both connexins. In the study presented in this chapter, I used an antisense morpholino targeting Cx44.1, but that potentially also targeted Cx48.5. The first 25 nucleotides (nt) of the two connexins are highly conserved, and this antisense morpholino is complementary to this region. Western analysis showed that the expression of Cx44.1 was knocked down in the antisense injected embryos, while Cx43 expression remained intact. Whether or not the expression of Cx48.5 protein was also knocked down still needs to be determined, once antibodies become available (currently being developed). The antisense morpholino injected embryos exhibited reduced lens growth and cataract formation that resembled the phenotype of the "pure" Cx48.5 knockdowns. However the underlying pathology was strikingly different. These embryos exhibited severely disrupted lens fiber differentiation, and an apoptosis like process was triggered in the lens nuclear region. As a consequence, lens growth was delayed and nuclear cataracts formed.

4.2 Materials and Methods

4.2.1 Microinjection of morpholino

An antisense morpholino complementary to the sequence of the Cx44.1 mRNA from the start codon to the 25th nucleotide (5'-TGCCCAAGAAACTCCAGTCACCCAT-3') was obtained from Gene Tools, LLC (Philomath, OR). This morpholino has a 1 nt mismatch with Cx48.5 within the first 24 nt (see below). The preparation of morpholino solutions, control morpholino, and the protocol of microinjection was the same as described in Chapter III. Each embryo was injected with 2 ng of morpholino.

```
Cx44.1   1ATGGGTGACTGGAG –TTTCTTGGGCA25
         |||||||||||||| |||||||||||
Cx48.5   ATGGGTGACTGGAGCTTTCTTGGGCG
```

4.2.2 DNA Constructs

To create a Cx44.1 expression construct, a 1.7 kb DNA fragment, including the 1,176 bp coding sequence and flanking regions, was PCR amplified (forward primer: 5'-TCTGCCTGCTTTCAAACATC-3'; reverse primer: 5'-GGATGATGCCCTGACAGTTT-3') from genomic DNA with *Pwo* DNA polymerase (Roche Diagnostics, Laval, Quebec,), cloned into the pCR2.1 cloning vector (Invitrogen, Carlsbad, California), and then subcloned into the pCS2+ expression vector with BamHI and XbaI (Cason *et al.*, 2001; Turner and Weintraub, 1994). Positive clones were verified by restriction enzyme digestion and sequencing. The verified clone was named pCS2+44.1. Prior to microinjection pCS2+44.1 was linearized with PvuII, phenol-

chloroform extracted and ethanol precipitated. Its transcriptional capability was tested with the mMESSAGE mMACHINE Large Scale In Vitro Transcription Kit (Ambion, Austin, Texas). To obtain a green fluorescent protein (GFP) tagged Cx44.1, the coding region of Cx44.1 was PCR amplified from the pCR2.1-44.1 clone with Pwo DNA polymerase. The forward primer was zfCx44.1/F/3, 5'-TCTGCCTGCTTTCAAACATC-3', starting 53 bp upstream of the start codon. The reverse primer zfCx44.1/R/8, 5'-TCTAGAACCGTCAAGTCATCTGAC-3', matched the last 19 nucleotides of the coding sequence of Cx44.1, except that an XbaI site was added to the 5' end, replacing the stop codon. The PCR product was subsequently cloned into the pCR2.1 vector, and verified by sequencing. This clone was digested with XbaI, yielding the entire zfCx44.1 coding region, except the stop codon. This fragment was subcloned into the GFP tagged expression vector, pCS2PeGFPX/P (a generous gift from Robert Davis, Harvard Medical School), linearized with XbaI, 13 bp upstream of the GFP coding region. The reading frames of the two coding regions were identical. This construct was named pCS2+44.1-GFP.

4.2.3 Western blot analysis

For each of the stages examined, 30-40 embryos were collected, the chorion and yolk were removed, and the embryos were homogenized in a buffer containing 0.1M NaCl, 20mM HEPES (pH 7.2), 2mM EDTA, 0.5m phenyl methylsulfonyl fluoride (PMSF), and protease inhibitor cocktail (Roche Diagnostics). The homogenates were spun at 3,000 g for 5 minutes to remove large debris, and the supernatant was used for analysis. Protein concentrations were determined by the *DC* Protein Assay kit (Bio-Rad

Laboratories, Missisauga, Ontario). The proteins were separated by electrophoreses in a 12% SDS-polyacrylamide gel (30%T, 2.67%C), with 40 μg of sample loaded per lane. The proteins were electroblotted onto Immobilon-P Transfer Membrane (Millipore, Nepean, Ontario). For the Cx44.1 expression analysis, the blot was incubated with 1:300 dilution of the monoclonal primary antibody 6-4-B2-C6 (Kistler *et al.*, 1985) overnight at 4°C. The primary antibody was detected with a HRP-goat anti-mouse IgM secondary antibody (Zymed Laboratories, Inc., San Francisco, California), and visualized with a Renaissance Western Blot Chemiluminescence Reagent Plus kit (NEN Life Science Products, Inc., Boston, Massachusetts). Equal loading of protein samples was assessed by Ponceau S staining. For Cx43 expression analysis, a primary antibody raised against a mouse Cx43 peptide (aa. 302-319, sequence highly conserved between mouse and zebrafish; De Sousa *et al.,* 1993) was used at 1:200 dilution, and detected by a HRP-F(ab')2-goat anti-rabbit IgG (H+L) antibody (Zymed Laboratories, Inc., San Francisco, California), and visualized as above. To assess the loading of protein samples, the same blot was then reused to detect α-Tubulin protein expression with a monoclonal anti-acetylated tubulin clone 6-111B-1 antibody (Sigma Chemical Co.).

4.2.4 Light microscopy

Morphological studies of lenses *in situ* in live embryos were carried out at a series of stages (1, 1.5, 2, 2.5, 3.5, 4.5, 5.5, 7.5 dpf) on a Zeiss Axioskop FS microscope with differential interference contrast optics (DIC). GFP fluorescence was observed with the fluorescein filter set. To obtain semi-thin sections for histological study, embryos were fixed in a modified Karnovsky's fixative containing 1% paraformaldehyde, 3%

glutaraldehyde, and 0.2% $CaCl_2$ in 0.1M phosphate buffer (pH 7.3) overnight at 4°C, and embedded in JB-4™ Embedding Medium (Polysciences, Inc., Warrington, Pennsylvania) according to the manufacturer's instructions. Sections were obtained at 1.5 μm and stained with toluidine blue (1% in aqueous 1% borax). Images of tissue sections were obtained with a 63X objective (NA=1.4).

4.2.5 Measurements and statistics

. For measurements of lens and eye diameter, and body length, the zebrafish embryos were dechorionated at 24 hpf. At the desired stages, embryos were anesthetized according to the Zebrafish Book (Westerfield, 1995), and then placed in a viewing chamber composed of a microscope slide and a supported cover glass. The space between the slide and the cover glass was about 1 mm, so that the zebrafish embryos were almost parallel to the slide. Lens size was estimated from the maximum lens diameter. Eye size was estimated by the anterior to posterior diameter. The data were analyzed with a 3 (Group: knockdown (KD), Wild Type, Control) X 8 (Stage: 1, 1.5, 2, 2.5, 3.5, 4.5, 5.5, 7.5 dpf) analysis of variance (ANOVA) with repeated measures on the second factor. Significant effects and interactions were followed up with Tamhane's T2 Post Hoc Tests. Each group included 10 embryos. An alpha level of 0.05 was adopted for all analyses.

4.2.6 TUNEL analysis

Embryos were fixed in 2% paraformaldehyde in PBS for 6 hours and then processed for paraffin embedding according to standard protocols. Slides containing 7 μm sections were obtained and processed for the TUNEL assay according to the

manufacturer's instructions (*In situ* Cell Death Detection Kit, TMR red; Roche), and images were obtained with the rhodamine filter set. Following the TUNEL reaction, the sections were incubated with 10μg/ml Hoechst 33452 (stains nuclei) for 15 minutes and washed with PBS. All images were captured with the Zeiss Axioskop FS microscope equipped with the appropriate filter set and the Northern Eclipse imaging software.

4.3 Results

4.3.1 Connexin expression in antisense morpholino injected embryos

Each 1-2 cell zebrafish embryo was injected with 2 ng of the antisense morpholio. Western analysis was carried out to assess the protein levels of connexins in the injected embryos. Since an antibody against Cx48.5 is not available yet, only Cx44.1 and Cx43 protein expression levels were assessed.

We assessed the effects of the antisense morpholino on Cx44.1 protein levels by western blotting using the monoclonal antibody 6-4-B2-C6 (Kistler *et al.*, 1985). This monoclonal antibody was originally raised against sheep MP70 (Cx49), but also cross-reacts with rat and mouse Cx50 (White *et al.*, 1992), as well as bovine Cx44 (Konig and Zampighi, 1995). Figure 4.1A shows Cx44.1 protein levels at 2 and 3dpf in the morpholino injected embryos, control morpholino injected embryos, and wild type (non-injected) embryos (lane 1 to 6). A 48 KDa band, corresponding to Cx44.1, was detected. Cx44.1 protein was strongly detected in both control morpholino injected and wild type embryos (Fig. 4.1A lane 3 to 6). In the antisense morpholino injected embryos, Cx44.1 protein was barely detectable at 2dpf, and while the levels had increased by 3 dpf (Fig.

4.1A lane 1 and 2), they were still substantially lower than in the controls. To provide further evidence that this 48 KDa band truly represent Cx44.1, the Cx44.1 expression plasmid, pCS2+44.1, was injected into 1 to 2 cell stage embryos. Protein extracts from injected embryos were obtained at 8 hpf and used for western analysis. Wild type (non-injected) embryos were used as a negative control. A strong 48 KDa band was detected in the injected embryo protein extract, and but not in the wild type embryos (Fig. 4.1A lane 7 and 8).

The efficiency of gene knockdown was further tested by co-injecting the antisense morpholino with a GFP tagged Cx44.1 expression construct, pCS2+44.1-GFP. The GFP fluorescence was greatly reduced in the embryos co-injected with antisense morpholino and pCS2+44.1-GFP (Fig. 4.1C and E), compared to the embryos injected with pCS2+44.1-GFP alone (Fig. 4.1B and D). The difference in the intensity of GFP fluorescence between the two groups was reduced after 3 dpf. The above results demonstrate that the antisense morpholino was effective in targeting Cx44.1 expression in the early stage embryos.

To test if the Cx43 expression was unaltered in the morpholino injected embryos, western analysis was also carried out with a Cx43 antibody (Fig. 4.1F). The embryos in this western analysis were collected at 1.5, 2.5, and 3.5 dpf, and the protein level of α-tubulin was used as the loading control. No apparent change in Cx43 expression was detected in the morpholino injected embryos (Fig. 4.1F lane 1, 3, and 5), compared to the controls (lane 2, 4, and 6).

4.3.2 Cataract formation in the knockdown zebrafish

The morphological development of three groups of zebrafish embryos was compared: embryos injected with the antisense morpholino (knockdown (KD) group), embryos injected with the control morpholino (control group), and non-injected wild type embryos (wild type group). Development in these three groups of embryos appeared to be identical, except that cataracts and small lenses developed in the knockdown embryos. No differences were observed between the control morpholino injected embryos and non-injected wild-type embryos. Hence, only figures of knockdown and control embryos are presented. Figures 4.2A-D are DIC images of lenses at 2.5 dpf, 3.5 dpf, 4.5 dpf, and 5.5 dpf, respectively, from embryos injected with the control morpholino. Throughout this developmental period the control lenses exhibited the same smooth appearance that is typical of non-injected wild type lenses. This smoothness was evident in all focal planes through the lens. No lens abnormalities were observed in the knockdown embryos before 2dpf. However, beginning at 2.5 dpf, the surfaces of the knockdown lenses lost some of their smoothness compared to the control lenses (Fig. 4.2E). At 3.5 dpf, abnormalities appeared in the nuclear region of the knockdown lenses. The fibers became dysmorphic, with significant loss of smoothness and the acquisition of a rough, uneven appearance (Fig. 4.2F). This feature reached a maximum at about 4 dpf. At 4.5 dpf, the bumpy region had lost some of its roughness, especially in the core area (Fig. 4.2G). This process continued along the following day. At 5.5 dpf, the uneven region was almost completely smooth again, with only some sporadic, minor unevenness left in the previously bumpy

region (Fig. 4.2H). This pattern remained unchanged up to 12 dpf when observations were discontinued.

Lenses dissected from antisense morpholino injected embryos at both 5.5 dpf and 12 dpf and viewed with darkfield optics showed nuclear opacities, also known as nuclear cataracts (Fig. 4.2J). The lenses from the control morpholino injected embryos were transparent (Fig. 4.2I). The penetrance of the cataractous phenotype was over 95% in the antisense morpholino injected embryos. The timing of the morphological changes in the nuclear region differed slightly between individual embryos, by a maximum of half a day. The severity of the opacity also differed slightly between individuals. However, no differences were observed in the two lenses of an individual embryo, suggesting that any differences in the extent of cataract formation between individual embryos were due to either slight variation in the rate of development between individual embryos, or the amount of antisense morpholino injected. These results suggest that connexin expression is required for normal lens development.

4.3.3 Abnormal lens fibers differentiation in the knockdown embryos

To examine in more detail the morphological changes we observed in the lenses of live knockdown embryos, semi-thin sections of 1.5-5.5 dpf lenses were obtained to examine the histology. The sections revealed changes in cellular morphology beginning as early as 2 dpf. At 1.5 dpf, both the knockdown lenses and the control lenses were composed of elongated fiber cells in the core region (Fig. 4.3A and E). There was no apparent difference in fiber shape or numbers. Fiber cells with vacuolated nuclei and condensed chromatin were evident in the nuclei of both types of lenses. However,

starting from 2 dpf, the nuclear fibers in the knockdown lenses became abnormal compared to the lenses from the control morpholino injected embryos. In the control lenses (Fig. 4.3A-D and I-L), the nuclei of the core fibers were vacuolated, many with sparse or no visible condensed chromatin. Far fewer fiber cell nuclei were present in the anterior region of the lens core than the posterior core, although these latter nuclei eventually disappeared. At the same time, the equatorial epithelial cells elongated, adding new fibers around the primary fibers. As the enucleated primary fiber cells matured they became less densely stained by toluidine blue compared to the differentiating fibers in the cortical region. This less densely stained region enlarged as development proceeded. By 4.5 dpf, most of the lens fibers had matured and stained only faintly in the sections. Only the epithelium and the differentiating fibers in the outer cortical region were strongly stained by toluidine blue. This staining pattern remained at 5.5 dpf, as well as 12 dpf (data not shown). This suggests that the zebrafish lens has functionally matured by 4.5 dpf. The absence of staining in the core of these lenses was not due to poor fixation as we were able to clearly see fibers in these sections with DIC optics. The explanation for the lack of staining is probably that toluidine blue is a basic dye, and as such stains acidic cell components such as RNA and DNA and these cell components are largely absent in mature fibers.

In the knockdown lenses two separate phenomena were observed (Fig. 4.3E-H and M-P). In the nuclear region at 2 dpf the vacuolated fiber cell nuclei contained more condensed chromatin than the controls. No difference in the number of fiber nuclei was evident between the anterior and posterior core areas. Both the fiber nuclei, and the fiber cells as a whole, became more condensed with time. This reached maximum severity at

3.5-4 dpf (Fig. 4.3M-N). The nuclear abnormality observed in the sections corresponds to the abnormal morphology observed in the DIC images (Fig. 4.2). The abnormal lens fibers stained strongly with toluidine blue when compared to the controls. At 4 dpf, the fibers in the center of the lens appeared to be dying, leaving a less densely stained core area. This pattern became more evident at 4.5 dpf. From this stage onward, more new fibers were added from the cortical region, and the pace of lens growth increased. At 5.5 dpf, the knockdown lens sections revealed a core area largely free of cells and debris, instead it was occupied by pale staining, amorphous material, with strongly staining punctuate spots, which may be the direct cause of the nuclear opacity. Lens sections at 12 dpf were also examined (data not shown). At 12 dpf, differentiation of the knockdown lens cortical fibers was indistinguishable from the controls. However, the punctate, amorphous material in the nuclear region and the nuclear opacity remained. Thus the histological analysis revealed abnormal fiber differentiation in the knockdown embryos.

4.3.4 Lens growth is retarded in the knockdown zebrafish

From the DIC images, knockdown lenses appeared to be smaller than the control lenses. To quantify these differences the diameters of lenses from non-injected wild type, control morpholino and antisense morpholino injected embryos were measured and compared, from 1 to 7.5 dpf (Fig. 4.4A). Statistical analysis showed the knockdown lenses to be growth retarded. The lens growth retardation first became significant at 2 dpf ($n=10$; $p<0.05$; ANOVA). The lens diameter difference between the knockdown and control morpholino injected zebrafish embryos became greater as development continued, and reached maximum at 3.5 dpf. At this stage, the lens diameter of the

knockdown embryos was 18.1% smaller than the lens diameter in the control morpholino injected embryos. Assuming equal mass density, the knockdown lenses had 45.1% less mass than the controls at this stage. The difference in lens size stabilized after 3.5 dpf and was maintained up until 12 dpf, when observations were discontinued. No size difference was found between the lenses from control morpholino injected embryos and non-injected wild type embryos. From the growth profile of the knockdown lenses, it appeared the smaller lenses of the knockdown zebrafish were due to a slower growth rate during the 1.5-3.5 dpf stage. We confirmed this by calculating growth rates. It can be seen in Figure 4.4B that the growth rate of the lenses from knockdown embryos was slower than control morpholino injected and non-injected wild type lenses at 1.5-3 dpf, but after this period the growth rates were similar in all three groups. These results suggest that the lens growth in the knockdown embryos was mainly disrupted during the early stages, possible due to the loss of morpholino effect as the cellular concentration of the morpholino was reduced as the embryos grew.

To determine whether the retardation of lens growth was associated with any effect on eye growth, eye size in the three groups of embryos was measured at the 3.5 and 7.5 dpf stages (Fig. 4.4C). We observed a small, but significant, reduction in eye size in the knockdown embryos compared to the control morpholino injected embryos, and the non-injected wild type embryos at 3.5 dpf ($n=10$; $p<0.05$; ANOVA). However, no significant difference was found at 7.5 dpf ($n=10$; $p>0.05$; ANOVA). The slower growth of the eye might be due to two factors. One is a reduction in Cx44.1 and Cx48.5 expression in the developing retina, another factor is a possible disruption in signaling from the lens to the retina that is essential for normal eye growth. However, the

mechanism underlying the eye growth retardation is not the focus of this study. Semi-thin sections also revealed that the impairment in the retina is very mild compared to the lens. Figure 4.4E and F showed that the lens in the knockdown zebrafish is severely affected in the nuclear region, while the retinas developed normally except that they were slightly smaller than in the control embryos. Retinas from both antisense and control morpholino injected embryos had fully developed layers of rods and cones, outer and inner plexiform layers, bipolar layers, amacrine cell layers, and ganglion cell layers.

The overall growth of the embryos was assessed by total body length (Fig. 4.4D). There was no significant difference in body length between the three groups of embryos at either 3.5 dpf or 7.5 dpf ($n=10$; $p>0.05$; ANOVA). No other gross dysmophology was observed in the knockdown embryos except pericardial edema was seen in some cases.

4.3.5 TUNEL labeling in the knockdown lenses

To investigate whether the abnormal lens fibers in the knockdown zebrafish were undergoing an apoptosis-like process, 1.5 to 5.5 dpf embryos were processed for TUNEL labeling. The TUNEL assay is based on the ability of terminal deoxynucleotidyl transferase (TdT) to add labeled nucleotides to the 3'-OH ends of DNA fragments generated in the later stages of apoptosis (Gavrieli *et al.*, 1992). The TUNEL labeled sections were also labeled with the general DNA stain Hoechst to locate all nuclei. For each time point and treatment condition we examined lenses from 3-5 embryos. Fig. 4.5 shows the results from 2.5, 3.5, and 4.5 dpf embryos. Strong signals were observed in the nuclear region of all the lenses from 3.5 and 4.5 dpf knockdown zebrafish (Fig. 4.5I and

K). Only occasional, weak signals were detected in 5.5 dpf knockdown zebrafish lenses (data not shown), and no TUNEL positive nuclei were observed in the knockdown zebrafish lenses at 1.5 (data not shown) or 2.5 dpf (Fig. 4.5G). All the non-injected wild type zebrafish lenses were TUNEL negative throughout the developmental stages we investigated (Fig. 4.5A, C, and E). These data, coupled with the morphological observations in Fig. 4.3, indicate that extensive cell death occurred during the 3.5-4.5 dpf period in the knockdown embryos, immediately preceding the appearance of the lens nuclear opacity. The cellular mechanisms responsible for the fiber cell death appear to involve certain hallmark features of apoptosis, such as accumulation of nuclear DNA breakdown products with 3'-OH ends. The fact that we did not observe any TUNEL labeling in the non-injected wild type lenses also suggests that the normal lens fiber differentiation process is different from apoptosis in some respects, although they clearly share some similar features such as degradation of cellular organelles and nuclei.

4.4 Discussion

In this study, we used an antisense morpholino to target the expression of both Cx44.1 and Cx48.5. The antisense morpholino injected embryos developed severe lens abnormalities. The western analysis showed that the level of Cx44.1 protein was substantially reduced in the knockdown embryos during the early stages, while Cx43 expression appeared intact. Since the sequence of the antisense morpholino is highly conserved between Cx44.1 and Cx48.5 (96% over the first 24 nt), it is to be expected that Cx48.5 would also be knocked down by this morpholino. However, the Cx48.5 protein

level in the knockdown embryos needs to be determined in the future when antibodies become available.

The injected embryos developed a similar lens phenotype as seen in the Cx48.5 knockdowns described in chapter III. Those similarities included small lens, cataract formation, small eye, and abnormal lens fiber differentiation. However, in general, the phenotypes seen in this knockdown study were more severe than in the Cx48.5 knockdown. Firstly, the lens size was more reduced (18.1% in this study vs. 6.3% in the Cx48.5 knockdown). Secondly, the rough appearance of the knockdown lens under DIC microscopy was more pronounced, and cataracts formed earlier (5-5.5 dpf in this study, vs. 5.5-7.5 dpf in the Cx48.5 knockdown). Finally, a strong TUNEL signal was detected in the knockdown lenses in the present study, but not in the Cx48.5 knockdown lenses, indicating a different pathological mechanism underlying the cataract formation in these lenses. The phenotypic difference between this knockdown and the Cx48.5 knockdown suggests that Cx44.1 and Cx48.5 both have unique funtions during zebrafish lens development.

The TUNEL result strongly suggests that the abnormal lens fiber differentiation and the associated loss of these fibers from the nuclear region involve cell death by a process similar to apoptosis. Indeed, studies have shown that an imbalance of growth signals during lens fiber differentiation leads to cataract formation via an apoptotic pathway (Chen *et al.*, 2000). E2F1 and E2F2 are transcription factors involved in cell cycle regulation and generally stimulate cell proliferation. E2F1 and E2F2 transgenic mice have been generated in which lens fiber specific E2F1 and E2F2 overexpression was driven by the αA-crystallin promoter. This induced post-mitotic lens fibers to re-

enter the cell cycle, and stimulated p53-dependent apoptosis. These transgenic mice also had small lenses and disordered fibers (Chen *et al.*, 2000). In our experiments we observed a sharp increase in the number of TUNEL positive nuclei in knockdown lenses, suggesting the involvement of apoptosis-like cell death. However, several studies have shown that the normal lens differentiation process shares some features with apoptosis, including the formation of TUNEL-positive nuclei (Wride and Sanders, 1998; Cole and Ross, 2001), and the activation of the caspase family proteases (Wride *et al.*, 1999; Wride, 2000; Yin *et al.*, 2001) The fact that we never detected TUNEL labeling in the non-injected wild type zebrafish lenses during the developmental period investigated (1.5-5.5 dpf) demonstrates that the TUNEL labeling we observed in the knockdown lenses did not arise from normally differentiating fiber cell nuclei. We therefore regard the positive TUNEL staining in the knockdown lenses as evidence that these cells are apoptotic like. With regard to this last point it is worth noting that several research groups have reported the absence of TUNEL staining in normally differentiating lens fibers (Morgenbesser *et al.*, 1994; Chow *et al.*, 1995; Robinson *et al.*, 1995; Stolen and Griep, 2000). In Cole and Ross's study (2001), apotototic nuclei were frequently detected in zebrafish lens cells during a time window from 22 hpf to 1.5 dpf. However in the present study, TUNEL labeling did not detect any apoptotic-like cells at 1.5 dpf. This discrepancy might have arisen from variability in the rate of development between the embryos in these two studies, especially considering that Cole and Ross (2001) reported the complete absence of TUNEL positive cells after 1.5 dpf.

Given the evidence from chapter III that Cx48.5 is required for the heart function in zebrafish embryos, it is worth noting that cardiovascular abnormalities were

not typically seen in the knockdown embryos reported in this chapter.. One explanation is that the morpholino dosage (2 ng) used to trigger the lens phenotype in the "double knockdown" embryos was not high enough to set off the cardiac phenotype. Abnormal cardiac function did emerge when higher doses, such as 3 to 4 ng morpholino, was microinjected into 1-2 cell embryos.

4.5 Summary

Gap junctions are crucial for the proper lens development and function. Here we microinjected an antisense morpholino potentially targeting the expression of both Cx44.1 and Cx48.5 in the developing zebrafish. Western analysis found that the protein level of Cx44.1 was significantly reduced during early embryonic development, while Cx43 expression was not affected. The knockdown embryos developed nuclear cataracts and small lenses. The lens growth retardation started at 2 dpf, reached a maximum at 3.5 dpf and was maintained thereafter. The cataractous lenses were 18.1 % smaller than the control lenses at 3.5 dpf. The growth of the eye was also retarded at 3.5 dpf, but not at 7.5 dpf. Dramatic morphological changes were observed in the cataractous lenses that reached a maximum at about 4 dpf in living embryos. Tissue sections further revealed that the lens fibers in the nuclear region had differentiated abnormally and eventually died. TUNEL labeling showed that the death of the fiber cells was by apoptosis-like process.

Figure 4.1

(A) The level of Cx44.1 protein was greatly reduced at 2 dpf (2d), and moderately reduced at 3 dpf (3d) in the antisense morpholino injected embyos (MO), but was intact in the control morpholino injected embryos (control) and wild type (WT) non-injected embryos. The same band (48 KDa) was also detected in 8 hpf embryos microinjected with a Cx44.1 expression vector, pCS2+44.1, but not in the control 8 hpf embryos. The native Cx44.1 is not expressed at this stage. The lower panel shows the Ponceau S staining of the yolk proteins as the loading control (loading). (B-E). The efficiency of Cx44.1 knockdown was also assessed by coinjecting the antisense morpholino with a GFP tagged Cx44.1 expression plasmid, pCS2+44.1-GFP. The GFP fluorescence was strong in 2 and 3 dpf embryos injected with pCS2GFP+44.1 alone (B and D). In embryos injected with both pCS2+44.1-GFP and antisense morpholinos, the fluorescence was barely detectable at 2 dpf (C), and only slightly more intense at 3 dpf (E). (F) Western analysis of Cx43 protein expression at 1.5 dpf (1.5d), 2.5 dpf (2.5d), and 3.5 dpf (3.5d). No apparent change in Cx43 protein expression was seen in the antisense morpholino injected embryos (MO) compared to the controls. Lower panel shows the level of α-tubulin as an assessment the even loading of protein samples. Scale bar = 500μm

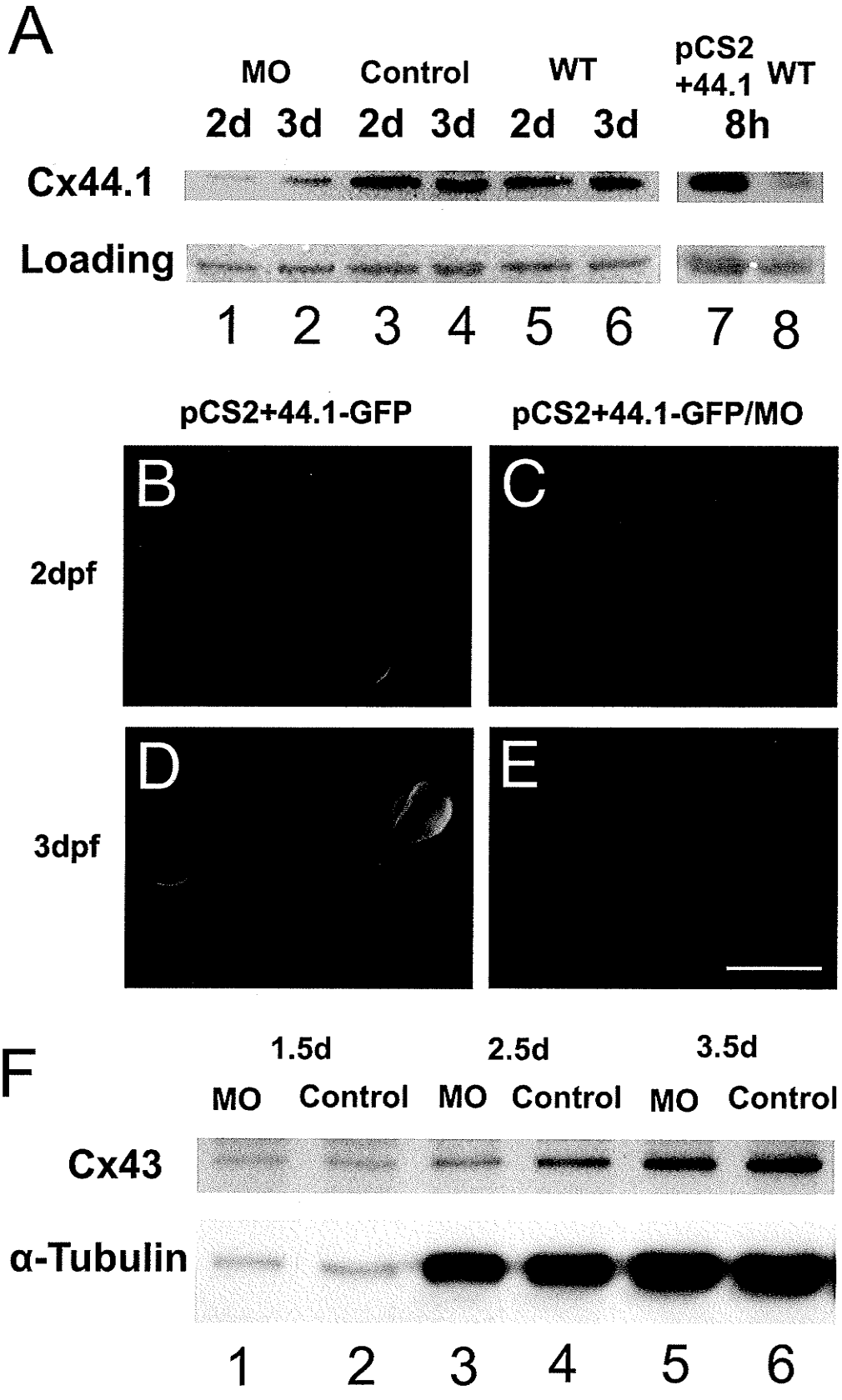
A
MO
Control
WT
pCS2 +44.1
WT
2d 3d 2d 3d 2d 3d
8h
Cx44.1
Loading
1 2 3 4 5 6 7 8
pCS2+44.1-GFP
pCS2+44.1-GFP/MO
B
C
2dpf
D
E
3dpf
F
1.5d
2.5d
3.5d
MO Control MO Control MO Control
Cx43
α-Tubulin
1 2 3 4 5 6

Figure 4.2

Morphological abnormalities and cataract formation in knockdown embryos. (A-H). DIC images of lenses in live embryos. Control embryos at 2.5, 3.5, 4.5, 5.5 dpf are shown in A, B, C and D, respectively. knockdown embryos at 2.5, 3.5, 4.5, 5.5 dpf are shown in E, F, G and H, respectively. The lenses in control embryos grew in size gradually, and appeared very smooth in all focal planes throughout this period (A-D). In the knockdown embryos, the lenses were smaller and not as smooth as the controls, beginning at 2.5 dpf (E). At 3.5 dpf, the center region of the lenses appeared very uneven (F). This feature then became reduced in severity at 4.5 dpf (G) and 5.5 dpf (H). Arrow shows the nuclear abnormality. (I-J). Lenses dissected at 12 dpf visualized with darkfield microscopy. (I) The control lenses were fully transparent. (J) The knockdown lenses were smaller, and opaque in the center region (arrowhead). The nuclear cataracts became visible with darkfield microscopy beginning at 5.5 dpf. The peripheral reflected light is due to light leaking from around the edge of the lenses. Scale bar = 50μm.

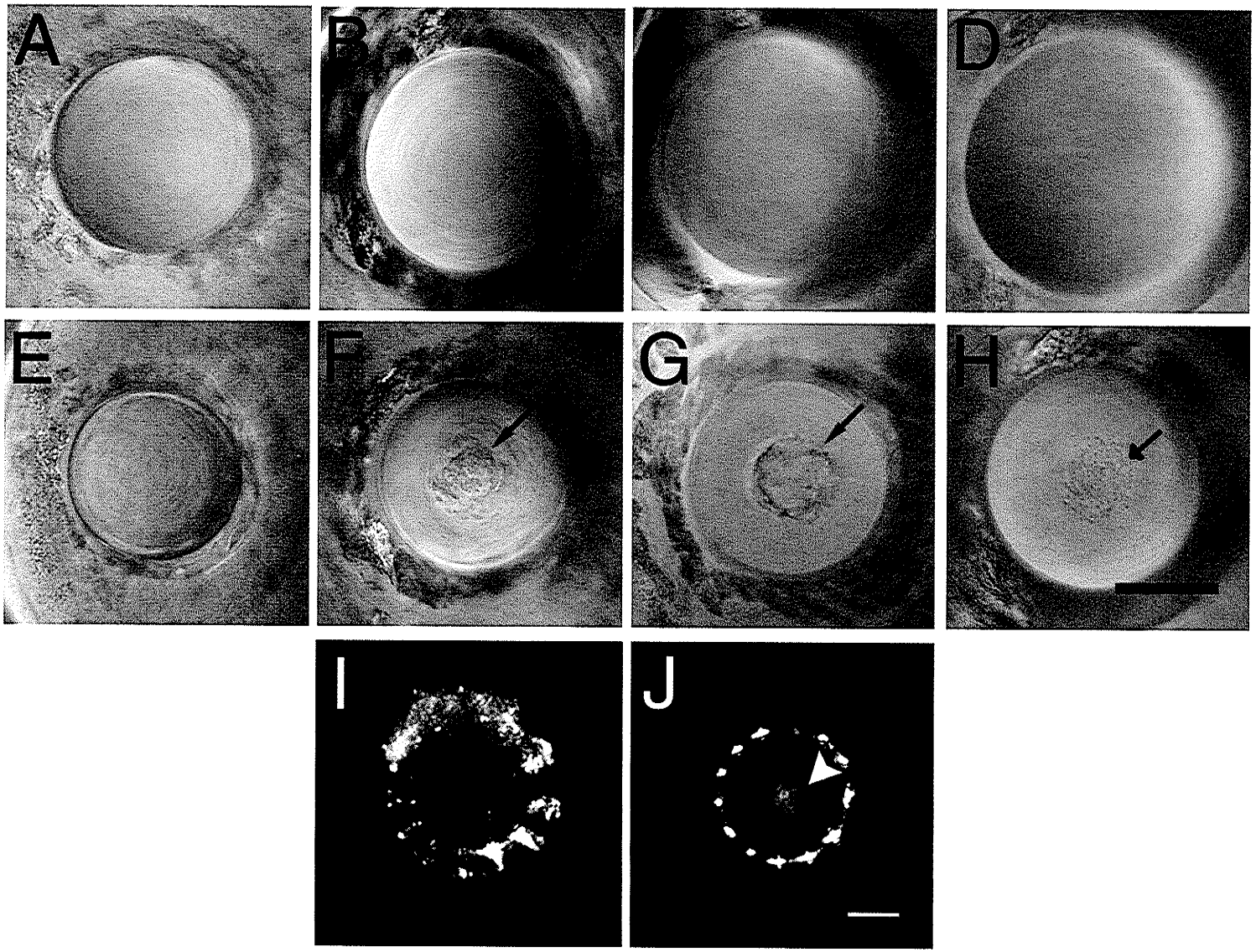
A
B
D
E
F
G
H
I
J

Figure 4.3

Time course and histology of cataractogenesis. Tissue sections show lens development in control morpholino injected and knockdown embryos. A-D and I-L show sections of lenses from control injected embryos at 1.5, 2.0, 2.5, 3.0, 3.5, 4.0, 4.5 and 5.5 dpf, respectively. E-F and M-P show the corresponding stages in the knockdown embryos. In control lenses, the core lens fibers have already begun to elongate at 1.5 dpf (A) indicating that the differentiation process has begun. As differentiation proceeds new fibers are continuously added (B-D and I-L). At 2.5 dpf, some of the nuclear fibers have already completed denucleation (C). After this the core region consisting of mature fibers enlarges (D, and I-L). In the Knockdown lenses, elongation of core fibers also began at 1.5 dpf (E). At 2-3 dpf, the nuclei of the core fibers are more condensed than in the controls and the differentiation process has become abnormal. Fewer new fibers are added (F-H). The abnormal core fibers die at 3.5-4 dpf (M and N), and many have disappeared by 4.5 dpf (O). Finally, by 5.5 dpf a number of new lens fibers have been added, but the nuclear region of the lens still contains punctate, amorphous material (P). The dissected lens at this stage shows a nuclear opacity with the darkfield microscope (Figure 4B). Arrow shows the nuclear, amorphous material. Scale bar = 25 μm.

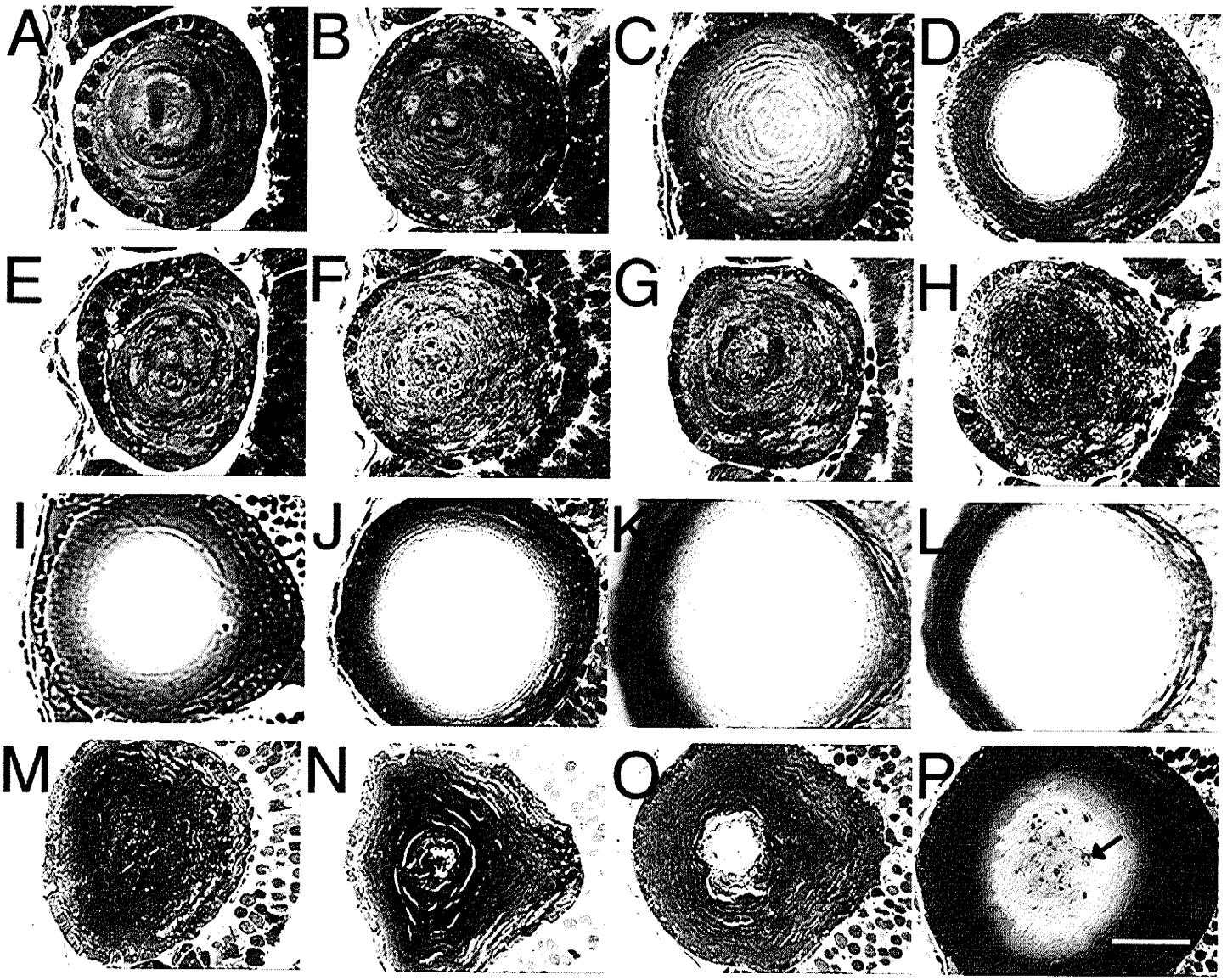
A
B
C
D
E
F
G
H
I
J
K
L
M
N
O
P

Figure 4.4

Growth in knockdown embryos. (A) There was no significant lens size difference between the control and wild type embryos from 1-7.5 dpf. The knockdown (KD) lens diameters were significant smaller starting from 2 dpf ($n=10$; $p<0.05$; ANOVA). (B) Lens growth rates were calculated from the data in (A). The lens growth rate in the knockdown embryos was lower than in the controls during 1-3 dpf, which led to an increasing difference in lens size. The lens growth rate in the knockdown embryos then caught up with the controls during 4-7 dpf. (C) Eye size was estimated by measuring the diameter of the eye in the anterior-posterior axis. At 3.5 dpf, the knockdown embryos had significantly smaller eyes than the control ($n=10$; $p<0.05$; ANOVA), but no significant difference was observed at 7.5 dpf stage ($n=10$; $p>0.05$; ANOVA). (D) The body length were measured and compared at 3.5 and 7.5 dpf. There was no significant difference between the three groups of fish at either stage ($n=10$; $p>0.05$; ANOVA). (E) Control eye at 4 dpf: the nuclear and inner cortical lens fibers are fully differentiated, and the retina has also undergone cell differentiation to form rod and cone layers, outer and inner plexiform layers, a bipolar layer, an amacrine cell layer, and a ganglion cell layer. (F) Knockdown eye at 4 dpf: the lens is smaller and the nuclear region is abnormal and undergoing cataractogenesis. The development of the retina appears unaffected, except that it is overall smaller than in the controls. Data are presented as means ± SEM. Scale bar = 50μm.

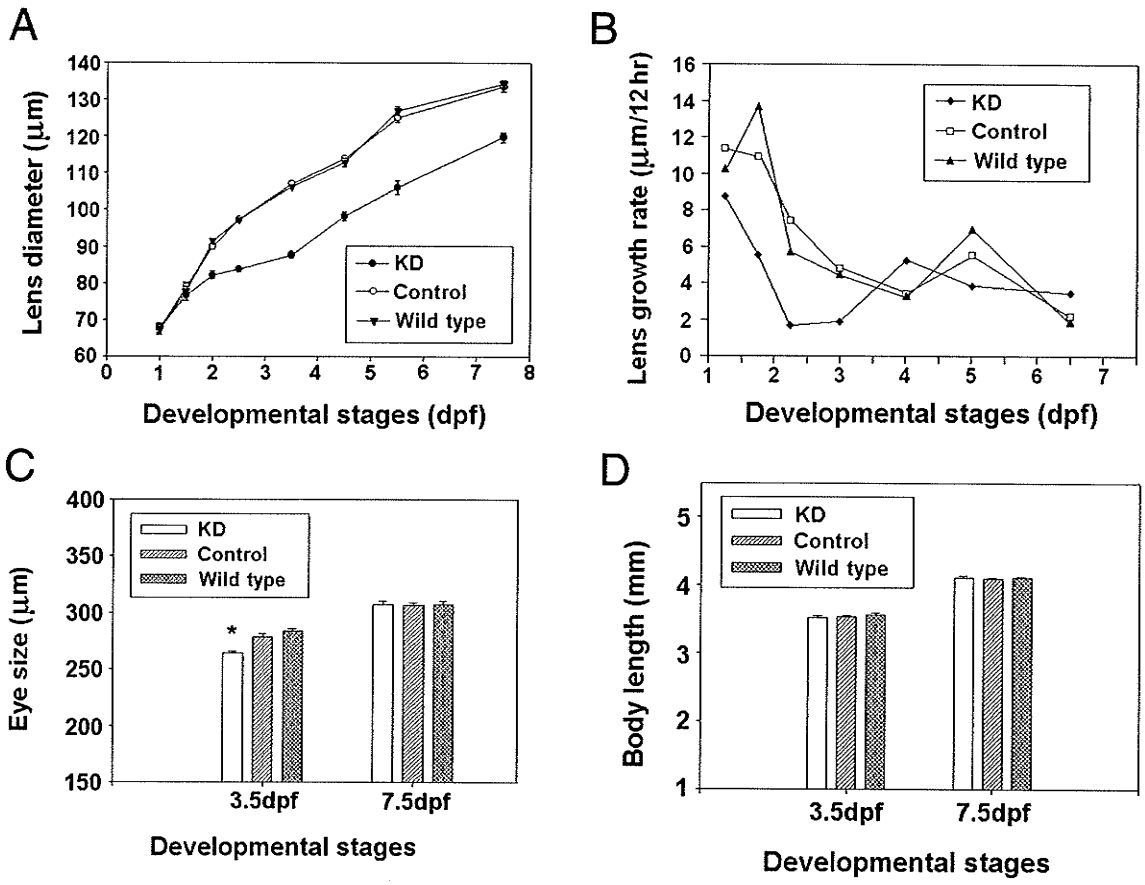
A
Lens diameter (μm)
Developmental stages (dpf)
KD
Control
Wild type
B
Lens growth rate (μm/12 hr)
Developmental stages (dpf)
KD
Control
Wild type
C
Eye size (μm)
*
3.5dpf
7.5dpf
Developmental stages
KD
Control
Wild type
D
Body length (mm)
3.5dpf
7.5dpf
Developmental stages
KD
Control
Wild type
E
F

Figure 4.5

TUNEL labeling in zebrafish lenses at 2.5, 3.5 and 4.5 dpf. The upper panel shows lenses from non-injected wild type embryos and the lower panel lenses from knockdown embryos. Parts A, C, E, G, I and K are TUNEL labeled sections (red) and B, D, F, H, J and L are the corresponding Hoechst stained sections (blue). TUNEL positive nuclei were only detected in 3.5 and 4.5 dpf knockdown lenses. Scale bar = 50μm.

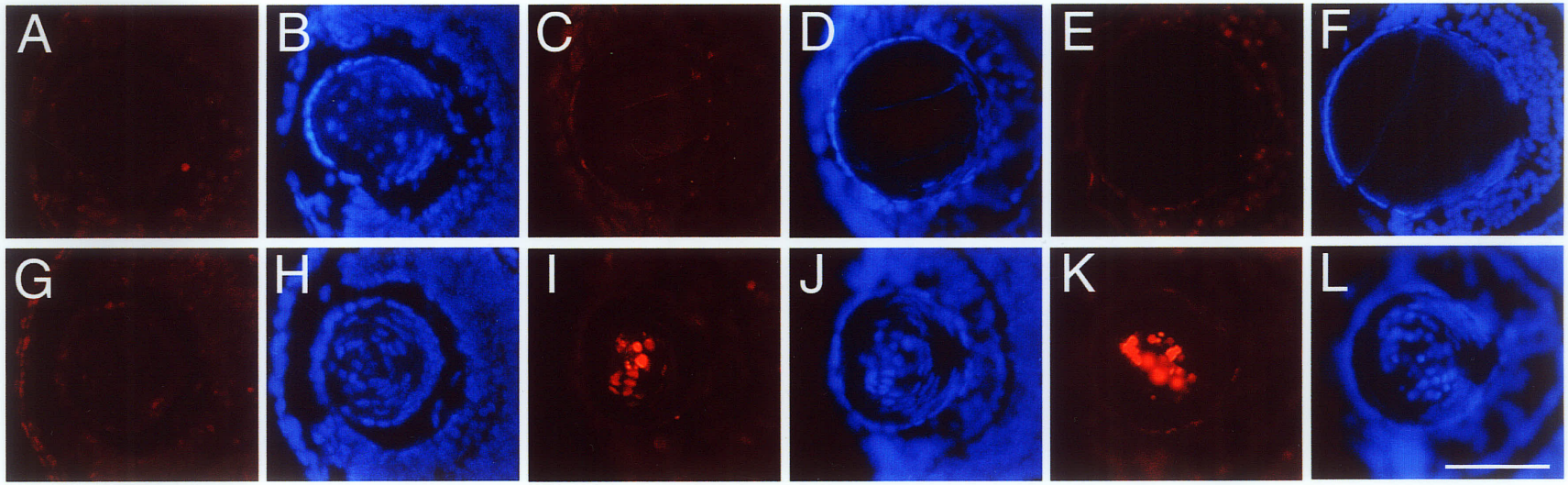
A
B
C
D
E
F
G
H
I
J
K
L

CONCLUSIONS

In this thesis, I investigated the detailed expression profiles of three connexins in the zebrafish lens, and have drawn a partial picture of the function of these connexins during development. I found that the zebrafish lens expresses the orthologues of all three connexins that have been found in the mammalian and chicken lens with similar, yet slightly different functions.

Zebrafish Cx43 is expressed in the lens epithelium and the differentiating lens fibers, as is the case in mammals and chicken. The function of Cx43 in the ocular lens is not clear. In the mouse, Cx43 expression in the anterior lens epithelium does not seem to be required for epithelial cell proliferation, since the embryonic lens growth was normal in the Cx43 knockout mice (Gao and Spray, 1998). However, the lens abnormality revealed by histological analysis in the mice suggests an essential role for Cx43 mediated intercellular communication between the epithelial and fiber cells.

Although sequence analyses and electrophysiological studies clearly indicate that Cx44.1 and Cx48.5 are the orthologues of mouse Cx50 and Cx46 respectively, their function in the zebrafish seems somewhat different than in the mouse. Firstly, we have observed that the Cx44.1 gene is turned on significant earlier than Cx48.5. The window of time when Cx44.1 is expressed in the absence of Cx48.5 expression coincides with the initiation of primary lens fiber differentiation. Hence, Cx44.1 might have a role during the initiation of primary lens fiber differentiation that is not shared with Cx48.5. Whether or not this scenario exists in the mouse is not clear. Secondly, in the mouse both Cx50 and Cx46 contribute to lens homeostasis, but only Cx50 is required for lens growth

(Gong *et al.*, 1997; White *et al.*, 1998). In contrast, Cx48.5 is required for both lens growth and homeostasis in zebrafish. My preliminary knockdown analysis of Cx44.1 function has revealed that Cx44.1 is also required for lens growth and homeostasis (see appendix A, Fig. 1). Thus, it appears that unlike in the mouse, Cx44.1 and Cx48.5 share roles in both lens growth and homeostasis. Similar pI and glutamic acid content has also been found between Cx44.1 and Cx48.5, but not between the other Cx46 and Cx50 members, suggesting a possible molecular basis for their functional overlap. However, regardless of the functional overlap between Cx44.1 and Cx48.5, the expression of both connexins is required for normal lens development and homeostasis, because embryos injected with an antisense morpholino targeting both Cx44.1 and Cx48.5 developed more severe lens phenotype than the Cx48.5 specific knockdowns.

Then, what are the unique contributions of Cx44.1 and Cx48.5 to lens development and homeostasis? As has mentioned above, Cx44.1 is transcribed significantly earlier than Cx48.5, which might be crucial for the initiation of primary lens fiber differentiation. In addition, my preliminary data from Cx44.1 knockdown experiments revealed that Cx44.1 is also required for retinal development (appendix A). The role of Cx44.1 in retinal development is independent of lens development, since retinal specific antisense morpholinos generated small retinas with intact lenses. In addition to its role in the ocular lens Cx48.5 also has an essential role in the cardiovascular system in zebrafish. Cardiac conduction was severely impaired in the Cx48.5 knockdown embryos. These novel functions of Cx44.1 and Cx48.5 have not been reported for the knockout mice. In addition to the lens and heart, Cx48.5 is also expressed in the zebrafish testis and otic vesicles, and the function of Cx48.5 in these organs is still

unknown. A scheme of the function of Cx48.5 and Cx44.1 in the ocular lens is outline in Figure 5.1.

Figure 5.1

Functional roles of Cx44.1 and Cx48.5 in zebrafish lens development. Cx43, Cx44.1, and Cx48.5 are the three connexins expressed in the zebrafish lens. Cx43 is mainly expressed in the epithelial cells, while Cx44.1 and Cx48.5 are expressed in the lens fibers. Cx44.1 starts its expression when the primary fibers initiate differentiation at 21 hpf, while Cx48.5 is not transcribed until 36 hpf. Interference with the expression of either Cx44.1 or Cx48.5 resulted in disruption of lens fiber differentiation, lens growth, and lens transparency. These data suggest that Cx44.1 might has a unique role in the initiation of primary lens fiber differentiation, and both Cx44.1 and Cx48.5 contribute to primary and secondary lens fiber differentiation. Both Cx44.1 and Cx48.5 are required for lens growth and homeostasis. In addition to the lens, Cx44.1 has a role in retinal development, and Cx48.5 in the cardiacvascular system. (Figure adapted from Kral, 1998, website: http://aussie-health.westga.edu/research/cataracts/development.html)

Cx43: epithelial cells

Cx44.1:

- **Lens growth**
  - Proliferation ?
  - Initiation of 1° fiber differentiation
  - 1° & 2° fiber differentiation
- **Lens homeostasis**
- **Other organs**
  - Retina

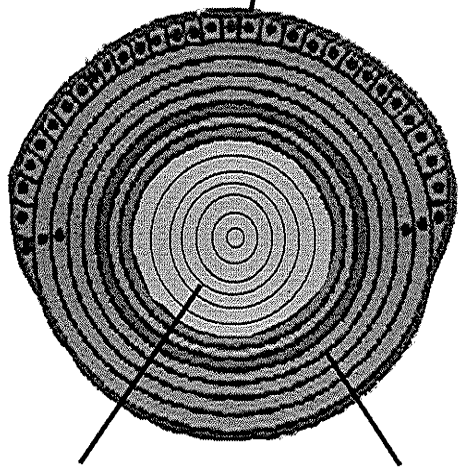

Primary (1°) lens fibers

Secondary (2°) lens fibers

Cx48.5:

- **Lens growth**
  - Proliferation ?
  - 1° & 2° fiber differentiation
- **Lens homeostasis**
- **Other organs**
  - Heart
  - Retina, testis, ear?

REFERENCES

Abraham V, Chou ML, George P, Pooler P, Zaman A, Savani RC, Koval M. 2001. Heterocellular gap junctional communication between alveolar epithelial cells. Am. J. Physiol. Lung Cell Mol. Physiol. 280:L1085-93.

Abrams CK, Oh S, Ri Y, Bargiello TA. 2000. Mutations in connexin 32: the molecular and biophysical bases for the X-linked form of Charcot-Marie-Tooth disease. Brain Res. Brain Res. Rev. 32:203-14.

Ahmad S, Evans WH. 2002. Post-translational integration and oligomerization of connexin 26 in plasma membranes and evidence of formation of membrane pores: implications for the assembly of gap junctions. Biochem. J. 365:693-9.

Alcolea S, Theveniau-Ruissy M, Jarry-Guichard T, Marics I, Tzouanacou E, Chauvin JP, Briand JP, Moorman AF, Lamers WH, Gros DB. 1999. Downregulation of connexin 45 gene products during mouse heart development. Circ. Res. 84:1365-79.

Alexander J, Stainier DY, Yelon D. 1998. Screening mosaic F1 females for mutations affecting zebrafish heart induction and patterning. Dev. Genet. 22:288-99.

Altevogt BM, Kleopa KA, Postma FR, Scherer SS, Paul DL. 2002. Connexin29 is uniquely distributed within myelinating glial cells of the central and peripheral nervous systems. J. Neurosci. 22:6458-70.

Amsterdam A, Burgess S, Golling G, Chen W, Sun Z, Townsend K, Farrington S, Haldi M, Hopkins N. 1999. A large-scale insertional mutagenesis screen in zebrafish. Genes Dev. 13:2713-24.

Bader D, Masaki T, Fischman DA. 1982. Immunochemical analysis of myosin heavy chain during avian myogenesis in vivo and in vitro. J. Cell Biol. 95:763-70.

Barrio LC, Suchyna T, Bargiello T, Xu LX, Roginski RS, Bennett MVL, Nicholson BJ. 1991. Gap junctions formed by connexins 26 and 32 alone and in combination are differently affected by applied voltage. Proc. Natl. Acad. Sci. USA 88:8410-8414.

Bassnett S, Mataic D. 1997. Chromatin degradation in differentiating fiber cells of the eye lens. J. Cell Biol. 137:37-49.

Belecky-Adams T, Tomarev S, Li HS, Ploder L, McInnes RR, Sundin O, Adler R. 1997. Pax-6, Prox 1, and Chx10 homeobox gene expression correlates with phenotypic fate of retinal precursor cells. Invest. Ophthalmol. Vis. Sci. 38:1293-303.

Bennett MV, Contreras JE, Bukauskas FF, Saez JC. 2003. New roles for astrocytes: Gap junction hemichannels have something to communicate. Trends Neurosci. 26:610-17.

Benedetti EL, Emmelot P. 1965. Electron microscopic observations on negatively stained plasma membranes isolated from rat liver. J. Cell Biol. 26:299-305

Berry V, Mackay D, Khaliq S, Francis PJ, Hameed A, Anwar K, Mehdi SQ, Newbold, RJ, Ionides A, Shiels A, Moore T, Bhattacharya SS. 1999. Connexin 50 mutation in a family with congenital "zonular nuclear" pulverulent cataract of Pakistani origin. Hum. Genet. 105:168-70.

Berthoud VM, Cook AJ, Beyer EC. 1994. Characterization of the gap junction protein connexin56 in the chicken lens by immunofluorescence and immunoblotting. Invest. Ophthalmol. Vis. Sci. 35:4109-17.

Bevans CG, Kordel M, Rhee SK, Harris AL. 1998. Isoform composition of connexin channels determines selectivity among second messengers and uncharged molecules. J. Biol. Chem. 273:2808-16.

Bevilacqua A, Loch-Caruso R, Erickson RP. 1989. Abnormal development and dye coupling produced by antisense RNA to gap junction protein in mouse preimplantation embryos. Proc. Natl. Acad. Sci. USA. 86:5444-8.

Beyer EC, Paul DL, Goodenough DA. 1987. Connexin43: a protein from rat heart homologous to a gap junction protein from liver. J. Cell Biol. 105:2621-9.

Beyer EC, Gemel J, Martinez A, Berthoud VM, Valiunas V, Moreno AP, Brink PR. 2001. Heteromeric mixing of connexins: compatibility of partners and functional consequences. Cell Commun. Adhes. 8:199-204.

Breitman ML, Clapoff S, Rossant J, Tsui LC, Glode LM, Maxwell LH, Bernstein A. 1987. Genetic ablation: targeted expression of a toxin gene causes microphthalmia in transgenic mice. Science. 238:1563-65.

Bruzzone R, White TW, Paul DL. 1996. Connections with connexins: the molecular basis of direct intercellular signaling. Eur. J. Biochem. 238: 1-27.

Cason N, White TW, Cheng S, Goodenough DA, Valdimarsson G. 2001. Molecular cloning, expression analysis, and functional characterization of connexin44.1: A zebrafish lens gap junction protein. Dev. Dyn. 221:238-47.

Chalcroft JP, Bullivant S. 1970. An interpretation of liver cell membrane and junction structure based on observation of freeze-fracture replicas of both sides of the fracture. J. Cell Biol. 47:49-60.

Chandross KJ, Kessler JA, Cohen RI, Simburger E, Spray DC, Bieri P, Dermietzel R. 1996. Altered connexin expression after peripheral nerve injury. Mol. Cell Neurosci 7:501-18.

Chen JN, Haffter P, Odenthal J, Vogelsang E, Brand M, van Eeden FJ, Furutani-Seiki M, Granato M, Hammerschmidt M, Heisenberg CP, Jiang YJ, Kane DA, Kelsh RN, Mullins MC, Nüsslein-Volhard C. 1996. Mutations affecting the cardiovascular system and other internal organs in zebrafish. Development. 123:293-302.

Chen JN, Fishman MC. 2000. Genetics of heart development. Trends Genet. 16:383-8.

Chen Q, Hung FC, Fromm L, Overbeek PA. 2000. Induction of cell cycle entry and cell death in postmitotic lens fiber cells by overexpression of E2F1 or E2F2. Invest. Ophthalmol. Vis. Sci. 41:4223-31.

Chen YH, DeHaan RL. 1996. Asymmetric voltage dependence of embryonic cardiac gap junction channels. Am. J. Physiol. 270:276-85.

Chen ZQ, Lefebvre D, Bai XH, Reaume A, Rossant J, Lye SJ. 1995. Identification of two regulatory elements within the promoter region of the mouse connexin 43 gene. J. Biol. Chem. 270:3863-8.

Cheng HL, Louis CF. 1999. Endogenous casein kinase I catalyzes the phosphorylation of the lens fiber cell connexin49. Eur. J. Biochem. 263:276-86.

Cheng S, Christie T, Valdimarsson G. 2003. Expression of connexin48.5, connexin44.1, and connexin43 during zebrafish (Danio rerio) lens development. Dev. Dyn. 228:709-15.

Chow RL, Roux GD, Roghani M, Palmer MA, Rifkin DB, Moscatelli DA, Lang RA. 1995. FGF suppresses apoptosis and induces differentiation of fibre cells in the mouse lens. Development. 121:4383-93.

Christie TL, Mui R, White TW, Valdimarsson G. 2004. Molecular Cloning, Functional Analysis, and RNA Expression Analysis of Connexin45.6: a Zebrafish Cardiovascular Connexin. Am. J. Physiol. Heart Circ. Physiol. Jan 2 [Epub ahead of print]

Cole LK, Ross LS. 2001. Apoptosis in the developing zebrafish embryo. Dev. Biol. 240:123-42.

Condorelli DF, Parenti R, Spinella F, Trovato Salinaro A, Belluardo N, Cardile V, Cicirata F. 1998. Cloning of a new gap junction gene (Cx36) highly expressed in mammalian brain neurons. Eur. J. Neurosci. 10:1202-8.

Coppen SR, Severs NJ, Gourdie RG. 1999. Connexin45 (alpha 6) expression delineates an extended conduction system in the embryonic and mature rodent heart. Dev. Genet. 24:82-90.

Coulombre AJ, Coulombre JL. 1964. Lens development. I. Role of the lens in eye growth. J. Exp. Zool. 156:39-47.

Counis MF, Chaudun E, Arruti C, Oliver L, Sanwal M, Courtois Y, Torriglia A. 1998. Analysis of nuclear degradation during lens cell differentiation. Cell Death Differ. 5:251-61.

Dahl G, Miller T, Paul D, Voellmy R, Werner R. 1987. Expression of functional cell-cell channels from cloned rat liver gap junction complementary DNA. Science. 236:1290-93.

Davis LM, Rodefeld ME, Green K, Beyer EC, Saffitz JE. 1995. Gap junction protein phenotypes of the human heart and conduction system. J. Cardiovasc. Electrophysiol. 6:Pt 1):813-22.

Delorme B, Dahl E, Jarry-Guichard T, Marics I, Briand JP, Willecke K, Gros D, Theveniau-Ruissy M. 1995. Developmental regulation of connexin 40 gene expression in mouse heart correlates with the differentiation of the conduction system. Dev. Dyn. 204:358-71.

Delorme B, Dahl E, Jarry-Guichard T, Briand JP, Willecke K, Gros D, Theveniau-Ruissy M. 1997. Expression pattern of connexin gene products at the early developmental stages of the mouse cardiovascular system. Circ. Res. 81:423-37.

Dermietzel R, Kremer M, Paputsoglu G, Stang A, Skerrett IM, Gomes D, Srinivas M, Janssen-Bienhold U, Weiler R, Nicholson BJ, Bruzzone R, Spray DC. 2000. Molecular and functional diversity of neural connexins in the retina. J. Neurosci. 20:8331-43.

De Sousa PA, Valdimarsson G, Nicholson BJ, Kidder GM. 1993. Connexin trafficking and the control of gap junction assembly in mouse preimplantation embryos. Development. 117:1355-67.

Diez JA, Ahmad S, Evans WH. 1999. Assembly of heteromeric connexons in guinea-pig liver en route to the Golgi apparatus, plasma membrane and gap junctions. Eur. J. Biochem. 262:142-8.

Driever W, Solnica-Krezel L, Schier AF, Neuhauss SC, Malicki J, Stemple DL, Stainier DY, Zwartkruis F, Abdelilah S, Rangini Z, Belak J, Boggs C. 1996. A genetic

screen for mutations affecting embryogenesis in zebrafish. Development. 123:37-46.

Easter SSJ and Nicola GN. 1996. The development of vision in the zebrafish (Danio rerio). Dev. Biol. 180:646-63.

Ebihara L. Steiner E. 1993. Properties of a nonjunctional current expressed from a rat connexin46 cDNA in Xenopus oocytes. J. Gen. Physiol. 102:59-74.

Ebihara L. 2003. New roles for connexons. News Physiol. Sci. 18:100-103.

Ekker SC. 2000. Morphants: a new systematic vertebrate functional genomics approach. Yeast 17:302-6.

Ekker SC, Larson JD. 2001. Morphant technology in model developmental systems. Genesis. 30:89-93.

Essner JJ, Laing JG, Beyer EC, Johnson RG, Hackett PBJ. 1996. Expression of zebrafish connexin43.4 in the notochord and tail bud of wild-type and mutant no tail embryos. Dev. Biol. 177:449-62.

Evans CW, Eastwood S, Rains J, Gruijters WT, Bullivant S, Kistler J. 1993. Gap junction formation during development of the mouse lens. Eur. J. Cell Biol. 60:243-49.

Feigenspan A, Teubner B, Willecke K, Weiler R. 2001. Expression of neuronal connexin36 in AII amacrine cells of the mammalian retina. J. Neurosci. 21:230-9.

Fini ME, Strissel KJ, West-Mays JA. 1997. Perspectives on eye development. Dev. Genet. 20:175-85.

Fishman MC, Stainier DY. 1994. Cardiovascular development. Prospects for a genetic approach. Circ. Res. 74:757-63.

Gao Y, Spray DC. 1998. Structural changes in lenses of mice lacking the gap junction protein connexin43. Invest. Ophthalmol. Vis. Sci. 39:1198-209.

Gavrieli Y, Sherman Y, Ben Sasson SA. 1992. Identification of programmed cell death in situ via specific labeling of nuclear DNA fragmentation. J. Cell Biol. 119:493-501.

Geimonen E, Jiang W, Ali M, Fishman GI, Garfield RE, Andersen J. 1996. Activation of protein kinase C in human uterine smooth muscle induces connexin-43 gene transcription through an AP-1 site in the promoter sequence. J. Biol. Chem. 271:23667-74.

Gong X, Li E, Klier G, Huang Q, Wu Y, Lei H, Kumar NM, Horwitz J, Gilula NB. 1997. Disruption of α_3 connexin gene leads to proteolysis and cataractogenesis in mice. Cell 91:833-43.

Goodenough DA, Gilula NB. 1974. The splitting of hepatocyte gap junctions and zonulae occludentes with hypertonic disaccharides. J. Cell Biol. 61:575-90.

Gourdie RG, Green CR, Severs NJ, Thompson RP. 1992. Immunolabelling patterns of gap junction connexins in the developing and mature rat heart. Anatomy & Embryology 185:363-78.

Gourdie RG, Severs NJ, Green CR, Rothery S, Germroth P, Thompson RP. 1993. The spatial distribution and relative abundance of gap-junctional connexin40 and connexin43 correlate to functional properties of components of the cardiac atrioventricular conduction system. J. Cell Sci. 105:985-91.

Gros DB, Jongsma HJ. 1996. Connexins in mammalian heart function. Bioessays. 18:719-30.

Gupta VK, Berthoud VM, Atal N, Jarillo JA, Barrio LC, Beyer EC. 1994. Bovine connexin44, a lens gap junction protein: molecular cloning, immunologic characterization, and functional expression. Invest. Ophthamol. Vis. Sci. 35:3747-58.

He DS, Jiang JX, Taffet SM, Burt JM. 1999. Formation of heteromeric gap junction channels by connexins 40 and 43 in vascular smooth muscle cells. Proc. Natl. Acad. Sci. USA. 96:6495-500.

Heasman J. 2002. Morpholino oligos: making sense of antisense? Dev. Biol. 243:209-14.

Heisenberg CP, Brand M, Jiang YJ, Warga RM, Beuchle D, van Eeden FJ, Furutani-Seiki M, Granato M, Haffter P, Hammerschmidt M, Kane DA, Kelsh RN, Mullins MC, Odenthal J, Nusslein-Volhard C. 1996. Genes involved in forebrain development in the zebrafish, Danio rerio. Development. 123:191-203.

Hennemann H, Suchyna T, Lichtenberg-Fraté H, Jungbluth S, Dahl E, Schwarz J, Nicholson BJ, Willecke K. 1992. Molecular cloning and functional expression of mouse connexin40, a second gap junction gene preferentially expressed in lung. J. Cell Biol. 117:1299-310.

Henry CA, Urban MK, Dill KK, Merlie JP, Page MF, Kimmel CB, Amacher SL. 2002. Two linked hairy/Enhancer of split-related zebrafish genes, her1 and her7, function together to refine alternating somite boundaries. Development. 129:3693-704.

Hopperstad MG, Srinivas M, and Spray DC. 2000. Properties of gap junction channels formed by Cx46 alone and in combination with Cx50. Biophys. J 79:1954-66.

Hove JR, Koster RW, Forouhar AS, Acevedo-Bolton G, Fraser SE, Gharib M. 2003. Intracardiac fluid forces are an essential epigenetic factor for embryonic cardiogenesis. Nature. 421:172-7.

Hu N, Sedmera D, Yost HJ, Clark EB. 2000. Structure and function of the developing zebrafish heart. Anat. Rec. 260:148-57.

Jacob A, Beyer EC. 2001. Mouse connexin 45: genomic cloning and exon usage. DNA Cell Biol. 20:11-9.

Jacobs MD, Soeller C, Sisley AM, Cannell MB, Donaldson PJ. 2004. Gap junction processing and redistribution revealed by quantitative optical measurements of connexin46 epitopes in the lens. Invest. Ophthalmol. Vis. Sci. 45:191-9.

Hu N, Yost HJ, Clark EB. 2001. Cardiac morphology and blood pressure in the adult zebrafish. Anat. Rec. 264:1-12.

Jeffery W, Strickler A, Guiney S, Heyser D, Tomarev S. 2000. Prox 1 in eye degeneration and sensory organ compensation during development and evolution of the cavefish Astyanax. Dev. Genes Evol. 210:223-30.

Jiang JX, White TW, Goodenough DA, Paul DL. 1994. Molecular cloning and functional characterization of chick lens fiber connexin 45.6. Mol. Biol. Cell 5:363-73.

Jiang JX, White TW, Goodenough DA. 1995. Changes in connexin expression and distribution during chick lens development. Dev. Biol. 168:649-61.

Jiang JX, Goodenough DA. 1996. Heteromeric connexons in lens gap junction channels. Proc. Natl. Acad. Sci. USA. 93:1287-91.

Jiang JX, Goodenough DA. 1998. Phosphorylation of lens fiber connexins in lens organ cultures. Eur. J. Biochem. 255:37-44.

John SA, Revel JP. 1991. Connexon integrity is maintained by non-covalent bonds: intramolecular disulfide bonds link the extracellular domains in rat connexin-43. Biochem. Biophys. Res. Commun. 178:1312-8.

Jowett T. 1999. Analysis of protein and gene expression. Methods Cell Biol. 59:63-85.

Kiang DT, Jin N, Tu ZJ, Lin HH. 1997, Upstream genomic sequence of the human connexin26 gene. Gene. 199:165-71.

Kajihara M, Kawauchi S, Kobayashi M, Ogino H, Takahashi S, Yasuda K. 2001. Isolation, characterization, and expression analysis of zebrafish large Mafs. J. Biochem. 129:139-46.

Kimmel CB, Ballard WW, Kimmel SR, Ullmann B, Schilling TF. 1995. Stages of embryonic development of the zebrafish. Dev. Dyn. 203:253-310.

Kirchhoff S, Nelles E, Hagendorff A, Kruger O, Traub O, Willecke K. 1998. Reduced cardiac conduction velocity and predisposition to arrhythmias in connexin40-deficient mice. Curr. Biol. 8:299-302.

Kistler J, Kirkland B, Bullivant S. 1985. Identification of a 70,000-D protein in lens membrane junctional domains. J. Cell Biol. 101:28-35.

Kistler J, Schaller J, Sigrist H. 1990. MP38 contains the membrane-embedded domain of the lens fiber gap junction protein MP70. J. Biol. Chem. 265:13357-61.

Konig N, Zampighi GA. 1995. Purification of bovine lens cell-to-cell channels composed of connexin44 and connexin50. J. Cell Sci. 108:3091-98.

Koval M, Harley JE, Hick E, Steinberg TH. 1997. Connexin46 is retained as monomers in a trans-Golgi compartment of osteoblastic cells. J. Cell Biol. 137:847-57.

Kruger O, Plum A, Kim JS, Winterhager E, Maxeiner S, Hallas G, Kirchhoff S, Traub O, Lamers WH, Willecke K. 2000. Defective vascular development in connexin 45-deficient mice. Development. 127:4179-93.

Kumai M, Nishii K, Nakamura K, Takeda N, Suzuki M, Shibata Y. 2000. Loss of connexin45 causes a cushion defect in early cardiogenesis. Development. 127:3501-12.

Lampe PD. 1994. Analyzing phorbol ester effects on gap junctional communication: a dramatic inhibition of assembly. J. Cell Biol. 127:1895-905.

Lampe PD, Lau AF. 2000. Regulation of gap junctions by phosphorylation of connexins. Arch. Biochem. Biophys. 384:205-15.

Lampe PD, TenBroek EM, Burt JM, Kurata WE, Johnson RG, Lau AF. 2000. Phosphorylation of connexin43 on serine368 by protein kinase C regulates gap junctional communication. J. Cell Biol. 149:1503-12.

Lang RA. 1999. Which factors stimulate lens fiber cell differentiation in vivo? Invest. Ophthalmol. Vis. Sci. 40:3075-8.

Lee S, Gilula NB, Warner AE. 1987. Gap junctional communication and compaction during preimplantation stages of mouse development. Cell. 51:851-60.

Li Z, Joseph NM, and Easter SS Jr. 2000. The morphogenesis of the zebrafish eye, including a fate map of the optic vesicle. Dev. Dyn. 218:175-88.

Lin JS, Fitzgerald S, Dong Y, Knight C, Donaldson P, Kistler J. 1997. Processing of the gap junction protein connexin50 in the ocular lens is accomplished by calpain. Eur. J. Cell Biol. 73:141-9.

Lin JS, Eckert R, Kistler J, Donaldson P. 1998. Spatial differences in gap junction gating in the lens are a consequence of connexin cleavage. Eur. J. Cell Biol. 76:246-50.

Lo WK, Shaw AP, Takemoto LJ, Grossniklaus HE, Tigges M. 1996. Gap junction structures and distribution patterns of immunoreactive connexins 46 and 50 in lens regrowths of Rhesus monkeys. Exp. Eye Res. 62:171-80.

Lohr JL, Yost HJ. 2000. Vertebrate model systems in the study of early heart development: Xenopus and zebrafish. Am. J. Med. Genet. 97:248-57.

Mackay D, Ionides A, Kibar Z, Rouleau G, Berry V, Moore A, Shiels A, Bhattacharya S. 1999. Connexin46 mutations in autosomal dominant congenital cataract. Am. J. Hum. Genet. 64:1357-64.

Makowski L, Caspar DL, Phillips WC, Goodenough DA. 1977. Gap junction structures. II. Analysis of the x-ray diffraction data. J. Cell Biol. 74:629-45.

Martinez-Wittinghan FJ, Sellitto C, Li L, Gong X, Brink PR, Mathias RT, White TW. 2003. Dominant cataracts result from incongruous mixing of wild-type lens connexins. J. Cell Biol. 161:969-78.

Mathias RT, Rae JL, Baldo GJ. 1997. Physiological properties of the normal lens. Physiol. Rev. 77:21-50.

McAvoy, J. W., Chamberlain, C. G., de Iongh, R. U., Hales, A. M., and Lovicu, F. J. 1999. Lens development. Eye. 13 (Pt 3b):425-37.

McGuirt WT, Smith RJ. 1999. Connexin 26 as a cause of hereditary hearing loss. Am. J. Audiol. 8:93-100.

McLachlin JR, Kidder GM. 1986. Intercellular junctional coupling in preimplantation mouse embryos: effect of blocking transcription or translation. Dev. Biol. 117:146-55.

McLachlan E, White TW, Ugonabo C, Olson C, Nagy JI, Valdimarsson G. 2003. Zebrafish Cx35: cloning and characterization of a gap junction gene highly expressed in the retina. J. Neurosci. Res. 73:753-64.

Menko SA. 2002. Lens epithelial cell differentiation. Exp. Eye Res. 75:485-90.

Monaghan P, Perusinghe N, Carlile G, Evans WH. 1994. Rapid modulation of gap junction expression in mouse mammary gland during pregnancy, lactation, and involution. J. Histochem. Cytochem. 42:931-8.

Morgenbesser SD, Williams BO, Jacks T, DePinho RA. 1994. p53-dependent apoptosis produced by Rb-deficiency in the developing mouse lens. Nature 371:72-74.

Mu H, Ohta K, Kuriyama S, Shimada N, Tanihara H, Yasuda K, Tanaka H. 2003. Equarin, a novel soluble molecule expressed with polarity at chick embryonic lens equator, is involved in eye formation. Mech. Dev. 120:143-55.

Mullins MC, Nusslein-Volhard C. 1993. Mutational approaches to studying embryonic pattern formation in the zebrafish. Curr. Opin. Genet. Dev. 3:648-54.

Mullins MC, Hammerschmidt M, Haffter P, Nusslein-Volhard C. 1994. Large-scale mutagenesis in the zebrafish: in search of genes controlling development in a vertebrate. Curr. Biol. 4:189-202.

Musil LS, Beyer EC, Goodenough DA. 1990. Expression of the gap junction protein connexin43 in embryonic chick lens: molecular cloning, ultrastructural localization, and post-translational phosphorylation. J. Membr. Biol. 116:163-75.

Nasevicius A, Ekker SC. 2000. Effective targeted gene 'knockdown' in zebrafish. Nat. Genet. 26:216-20.

Neuhaus IM, Bone L, Wang S, Ionasescu V, Werner R. 1995. Use of alternate promoters for tissue-specific expression of the gene coding for connexin32. Gene. 158:257-62.

Nicholson BJ, Weber PA, Cao F, Chang H, Lampe P, Goldberg G. 2000. The molecular basis of selective permeability of connexins is complex and includes both size and charge. Braz. J. Med. Biol. Res. 33:369-78.

Niessen H, Harz H, Bedner P, Kramer K, Willecke K. 2000. Selective permeability of different connexin channels to the second messenger inositol 1,4,5-trisphosphate. J. Cell Sci. 113:1365-72.

O'Brien J, al-Ubaidi MR, Ripps H. 1996. Connexin 35: a gap-junctional protein expressed preferentially in the skate retina. Mol. Biol. Cell. 7:233-43.

O'Brien J, Bruzzone R, White TW, Al-Ubaidi MR, Ripps H. 1998. Cloning and expression of two related connexins from the perch retina define a distinct subgroup of the connexin family. J. Neurosci. 18:7625-37.

Page RD. 1996. TreeView: an application to display phylogenetic trees on personal computers. Comput. Appl. Biosci 12:357-58.

Pal JD, Berthoud VM, Beyer EC, Mackay D, Shiels A, Ebihara L. 1999. Molecular mechanism underlying a Cx50-linked congenital cataract. Am. J. Physiol. 276:C1443-46.

Paul DL, Ebihara L, Takemoto LJ, Swenson KI, Goodenough DA. 1991. Connexin46, a novel lens gap junction protein, induces voltage-gated currents in nonjunctional plasma membrane of *Xenopus* oocytes. J. Cell Biol. 115:1077-89.

Pelster B, Burggren WW. 1996. Disruption of hemoglobin oxygen transport does not impact oxygen-dependent physiological processes in developing embryos of zebra fish (Danio rerio). Circ. Res. 79:358-62.

Reaume AG, de Sousa PA, Kulkarni S, Langille BL, Zhu D, Davies TC, Juneja SC, Kidder GM, Rossant J. 1995. Cardiac malformation in neonatal mice lacking connexin43. Science. 267:1831-34.

Reed KE, Westphale EM, Larson DM, Wang HZ, Veenstra RD, Beyer EC. 1993. Molecular cloning and functional expression of human connexin37, an endothelial cell gap junction protein. J. Clin. Invest. 91:997-1004.

Rees MI, Watts P, Fenton I, Clarke A, Snell RG, Owen MJ, Gray J. 2000. Further evidence of autosomal dominant congenital zonular pulverulent cataracts linked

to 13q11 (CZP3) and a novel mutation in connexin 46 (GJA3). Hum. Genet. 106:206-9

Reynhout JK, Lampe PD, Johnson RG. 1992. An activator of protein kinase C inhibits gap junction communication between cultured bovine lens cells. Exp. Cell Res. 198:337-42.

Robinson ML, MacMillan-Crow LA, Thompson JA, Overbeek PA. 1995. Expression of a truncated FGF receptor results in defective lens development in transgenic mice. Development. 121:3959-67.

Robinson SR, Hampson EC, Munro MN, Vaney DI. 1993. Unidirectional coupling of gap junctions between neuroglia. Science. 262:1072-4.

Rong P, Wang X, Niesman I, Wu Y, Benedetti LE, Dunia I, Levy E, Gong X. 2002. Disruption of Gja8 (alpha8 connexin) in mice leads to microphthalmia associated with retardation of lens growth and lens fiber maturation. Development. 129:167-74.

Rup DM, Veenstra RD, Wang HZ, Brink PR, Beyer EC. 1993. Chick connexin-56, a novel lens gap junction protein. Molecular cloning and functional expression. J. Biol. Chem. 268:706-12.

Saez JC, Berthoud VM, Branes MC, Martinez AD, Beyer EC. 2003. Plasma membrane channels formed by connexins: their regulation and functions. Physiol. Rev. 83:1359-400.

Saleh SM, Takemoto LJ, Zoukhri D, Takemoto DJ. 2001. PKC-gamma phosphorylation of connexin 46 in the lens cortex. Mol. Vis. 7:240-6.

Schmitt EA, Dowling JE. 1994. Early eye morphogenesis in the zebrafish, Brachydanio rerio. J. Comp. Neurol. 344:532-42.

Sedmera D, Reckova M, DeAlmeida A, Sedmerova M, Biermann M, Volejnik J, Sarre A, Raddatz E, McCarthy RA, Gourdie RG, Thompson RP. 2003. Functional and morphological evidence for a ventricular conduction system in zebrafish and Xenopus hearts. Am.. J. Physiol. Heart Circ. Physiol. 284:H1152-60.

Severs NJ, Rothery S, Dupont E, Coppen SR, Yeh HI, Ko YS, Matsushita T, Kaba R, Halliday D. 2001. Immunocytochemical analysis of connexin expression in the healthy and diseased cardiovascular system. Microsc. Res. Tech. 52:301-22.

Shiels A, Mackay D, Ionides A, Berry V, Moore A. 1998. A missense mutation in the human connexin50 gene (GJA8) underlies autosomal dominant "zonular pulverant" cataract, on chromosome 1q. Am. J. Hum. Genet. 62:526-32.

Silverstein DM, Thornhill BA, Leung JC, Vehaskari VM, Craver RD, Trachtman HA, Chevalier RL. 2003. Expression of connexins in the normal and obstructed developing kidney. Pediatr. Nephrol. 18:216-24.

Simon AM, Goodenough DA, Li E, Paul DL. 1997. Female infertility in mice lacking connexin 37. Nature. 385:525-29.

Simon AM, Goodenough DA, Paul DL. 1998. Mice lacking connexin40 have cardiac conduction abnormalities characteristic of atrioventricular block and bundle branch block. Curr. Biol. 8:295-98.

Sohl G, Willecke K. 2003. An update on connexin genes and their nomenclature in mouse and man. Cell Commun .Adhes. 10:173-80.

Spray DC, Harris AL, Bennett MV. 1981. Equilibrium properties of a voltage-dependent junctional conductance. J. Gen. Physiol 77:77-93.

Stainier DY, Fouquet B, Chen JN, Warren KS, Weinstein BM, Meiler SE, Mohideen MA, Neuhauss SC, Solnica-Krezel L, Schier AF, Zwartkruis F, Stemple DL, Malicki J, Driever W, Fishman MC. 1996. Mutations affecting the formation and function of the cardiovascular system in the zebrafish embryo. Development. 123:285-92.

Stolen CM, Griep AE. 2000. Disruption of lens fiber cell differentiation and survival at multiple stages by region-specific expression of truncated FGF receptors. Dev. Biol. 217:205-20.

Summerton J. 1999. Morpholino antisense oligomers: the case for an RNase H-independent structural type. Biochim. Biophys. Acta. 1489:141-58.

Tenbroek EM, Louis CF, Johnson R. 1997. The differential effects of 12-O-tetradecanoylphorbol-13-acetate on the gap junctions and connexins of the developing mammalian lens. Dev. Biol. 191:88-102.

Thisse C, Thisse B, Schilling TF, Postlethwait JH. 1993. Structure of the zebrafish snail1 gene and its expression in wild-type, spadetail and no tail mutant embryos. Development. 119:1203-15.

Thompson JD, Gibson TJ, Plewniak F, Jeanmougin F, Higgins DG. 1997. The CLUSTAL_X windows interface: flexible strategies for multiple sequence alignment aided by quality analysis tools. Nucleic. Acids. Res. 25:4876-82.

Tomarev SI, Sundin O, Banerjee-Basu S, Duncan MK, Yang JM, Piatigorsky J. 1996. Chicken homeobox gene Prox 1 related to Drosophila prospero is expressed in the developing lens and retina. Dev. Dyn. 206:354-67.

Trexler EB, Bennett MV, Bargiello TA, Verselis VK. 1996. Voltage gating and permeation in a gap junction hemichannel. Proc. Natl. Acad. Sci. U. S. A 93:5836-41.

Tu ZJ, Pan W, Gong Z, Kiang DT. 2001. Involving AP-2 transcription factor in connexin 26 up-regulation during pregnancy and lactation. Mol. Reprod. Dev. 59:17-24.

Turner DL, Weintraub H. 1994. Expression of achaete-scute homolog 3 in Xenopus embryos converts ectodermal cells to a neural fate. Genes Dev. 8:1434-47.

Unger VM, Kumar NM, Gilula NB, Yeager M. 1999a. Expression, two-dimensional crystallization, and electron cryo-crystallography of recombinant gap junction membrane channels. J. Struct. Biol. 128:98-105.

Unger VM, Kumar NM, Gilula NB, Yeager M. 1999b. Three-dimensional structure of a recombinant gap junction membrane channel. Science. 283:1176-80.

van Kempen MJ, Fromaget C, Gros D, Moorman AF, Lamers WH. 1991. Spatial distribution of connexin43, the major cardiac gap junction protein, in the developing and adult rat heart. Circ. Res. 68:1638-51.

Verheule S, van Kempen MJ, Postma S, Rook MB, Jongsma HJ. 2001. Gap junctions in the rabbit sinoatrial node. Am. J. Physiol. Heart Circ. Physiol. 280:H2103-15.

Vihtelic TS, Yamamoto Y, Sweeney MT, Jeffery WR, Hyde DR. 2001. Arrested differentiation and epithelial cell degeneration in zebrafish lens mutants. Dev. Dyn. 222:625-36.

Vihtelic TS, Hyde DR. 2002. Zebrafish mutagenesis yields eye morphological mutants with retinal and lens defects. Vision. Res. 42:535-40.

Wagner LM, Saleh SM, Boyle DJ, Takemoto DJ. 2002. Effect of protein kinase C gamma on gap junction disassembly in lens epithelial cells and retinal cells in culture. Mol. Vis. 8:59-66.

Warren KS, Fishman MC. 1998. Physiological genomics : mutant screens in zebrafish. Am. J. Physiol. 275:H1-7.

Westerfield M. 1995. The zebrafish book. University of Oregon Press, Eugene.

White TW, Bruzzone R, Goodenough DA, Paul DL. 1992. Mouse Cx50, a functional member of the connexin family of gap junction proteins, is the lens fiber protein MP70. Mol. Biol. Cell 3:711-20.

White TW, Bruzzone R, Wolfram S, Paul DL, Goodenough DA. 1994. Selective interactions among the multiple connexin proteins expressed in the vertebrate lens: the second extracellular domain is a determinant of compatibility between connexins. J. Cell Biol. 125:879-92.

White TW, Bruzzone R, Paul DL. 1995. The connexin family of intercellular channel forming proteins. Kidney Int. 48:1148-57.

White TW, Goodenough DA, Paul DL. 1998. Targeted ablation of connexin50 in mice results in microphthalmia and zonular pulverulent cataracts. J. Cell Biol. 143:815-25.

White TW, Paul DL. 1999. Genetic diseases and gene knockouts reveal diverse connexin functions. Annu. Rev. Physiol. 61:283-310.

White TW, Bruzzone R. 2000. Gap junctions: fates worse than death? Curr. Biol. 10:R685-8.

White TW, Sellitto C, Paul DL, Goodenough DA. 2001. Prenatal lens development in connexin43 and connexin50 double knockout mice. Invest. Ophthalmol. Vis. Sci. 42:2916-23.

White TW. 2002. Unique and redundant connexin contributions to lens development. Science. 295:319-20.

Wiens D, Jensen L, Jasper J, Becker J. 1995. Developmental expression of connexins in the chick embryo myocardium and other tissues. Anat. Rec. 241:541-53.

Wigle JT, Chowdhury K, Gruss P, Oliver G. 1999. Prox1 function is crucial for mouse lens-fibre elongation. Nat. Genet. 21:318-22.

Willecke K, Eiberger J, Degen J, Eckardt D, Romualdi A, Guldenagel M, Deutsch U, Sohl G. 2002. Structural and functional diversity of connexin genes in the mouse and human genome. Biol.Chem. 383:725-37.

Wride MA. 1996. Cellular and molecular features of lens differentiation: a review of recent advances. Differentiation. 61:77-93.

Wride MA, Sanders EJ. 1998. Nuclear degeneration in the developing lens and its regulation by TNFalpha. Exp. Eye. Res. 66:371-83.

Wride MA, Parker E, Sanders EJ. 1999. Members of the bcl-2 and caspase families regulate nuclear degeneration during chick lens fibre differentiation. Dev. Biol 213:142-56.

Wride MA. 2000. Minireview: apoptosis as seen through a lens. Apoptosis. 5:203-9.

Yamamoto Y, Jeffery WR. 2002. Probing teleost eye development by lens transplantation. Methods. 28:420-26.

Yancey SB, Biswal S, Revel JP. 1992. Spatial and temporal patterns of distribution of the gap junction protein connexin43 during mouse gastrulation and organogenesis. Development. 114:203-12.

Yeager M, Unger VM, Falk MM. 1998. Synthesis, assembly and structure of gap junction intercellular channels. Curr. Opin. Struct. Biol. 8:517-24.

Yelon D, Horne SA, Stainier DY. 1999. Restricted expression of cardiac myosin genes reveals regulated aspects of heart tube assembly in zebrafish. Dev. Biol. 214:23-37.

Yin X, Jedrzejewski PT, Jiang JX. 2000. Casein kinase II phosphorylates lens connexin 45.6 and is involved in its degradation. J. Biol. Chem. 275:6850-6.

Yin X, Gu S, Jiang JX. 2001. The development-associated cleavage of lens connexin 45.6 by caspase-3-like protease is regulated by casein kinase II-mediated phosphorylation. J. Biol. Chem. 276:34567-72.

Zhao HB, Santos-Sacchi J. 2000. Voltage Gating of Gap Junctions in Cochlear Supporting Cells: Evidence for Nonhomotypic Channels. J. Membr. Biol. 175:17-24.

Zimmer DB, Green CR, Evans WH, Gilula NB. 1987. Topological analysis of the major protein in isolated intact rat liver gap junctions and gap junction-derived single membrane structures. J. Biol. Chem. 262:7751-63.

APPENDIX A

To investigate the role of Cx44.1 during zebrafish lens development, Cx44.1 specific morpholinos were microinjected into 1-2 cell zebrafish embryos (ongoing project). Figure 1 shows the prelimilary analysis of the phenotype in the Cx44.1 morphants. The Cx44.1 morphants developed small lenses and eyes, suggesting a role of Cx44.1 in zebrafish lens and retinal development.

Figure 1

Lens and retinal development was abnormal in the Cx44.1 knockdown embryos. (A) Cx44.1 specific antisense morpholinos were microinjected into 1-2 cell zebrafish embryos. These embryos had reduced lens and retinal size. Abnormal lens morphology was observed by 3 dpf. (B) Control eye. Panels show DIC images taken at 3 dpf. Scale bar = 50μm.

A

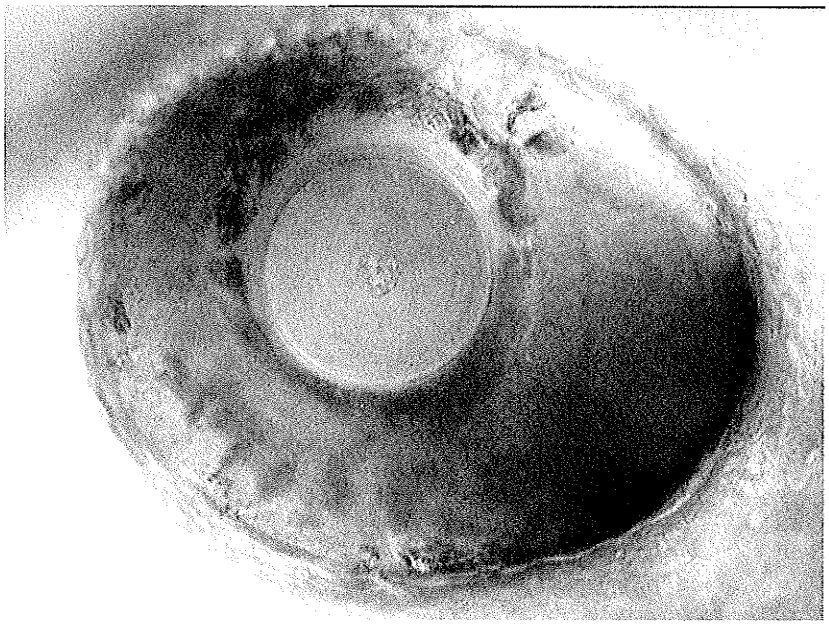

B

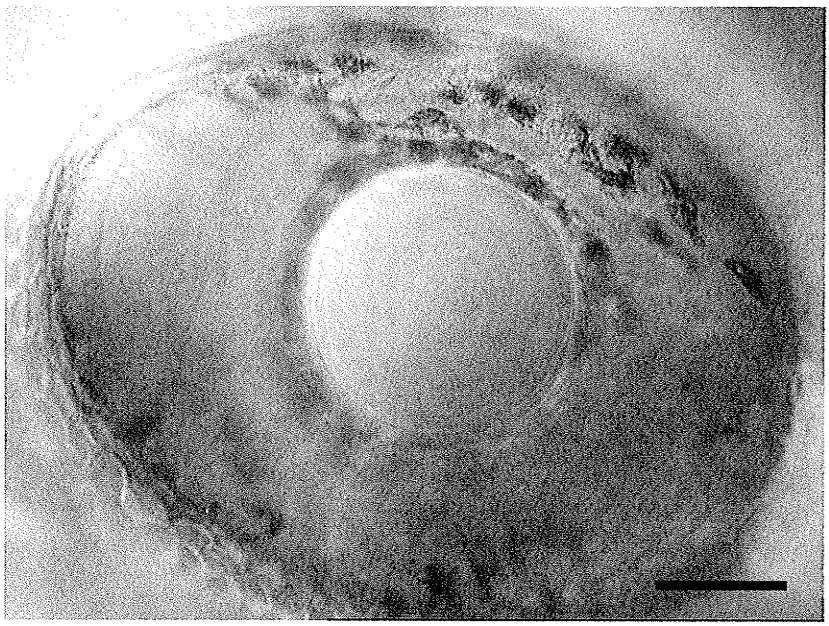

APPENDIX B

This work was performed to determine the physiological properties of the gap junction channels composed of Cx48.5 using the *Xenopus* oocytes expression system. This work was done in collaboration with Dr. Thomas W. White (Department of Physiology and Biophysics, SUNY, Stony Brook). The results show that Cx48.5 formed functional channels (Fig. 2), and the voltage gating behavior of these channels was similar to the Cx46 group (Fig. 3 & 4). Connexin48.5 also formed hemichannels in the single *Xenopus* oocytes (Fig. 5 & 6). This feature is conserved in the Cx46 group, but not the Cx50 group. These studies suggest that Cx48.5 belongs to the Cx46 subfamily of connexins.

Figure 2

Cx48.5 forms functional channels between pairs of *Xenopus* oocytes. Junctional conductance (G_j) developed between pairs of *Xenopus* oocytes as measured by dual voltage clamp. Oocytes were co-injected with the Cx48.5 cRNA and an oligonucleotide antisense to mRNA for Xenopus Cx38 to eliminate the possible contribution of endogenous coupling to the recorded conductances. Antisense treated water-injected cells were used as negative controls. Cells were then stripped of the vitelline envelope in hypertonic medium and paired with the vegetal poles facing each other 24-48 hr prior to electrophysiological measurements. Bars show the mean ± SD of the number of pairs indicated, symbols show the clustering of all data points.

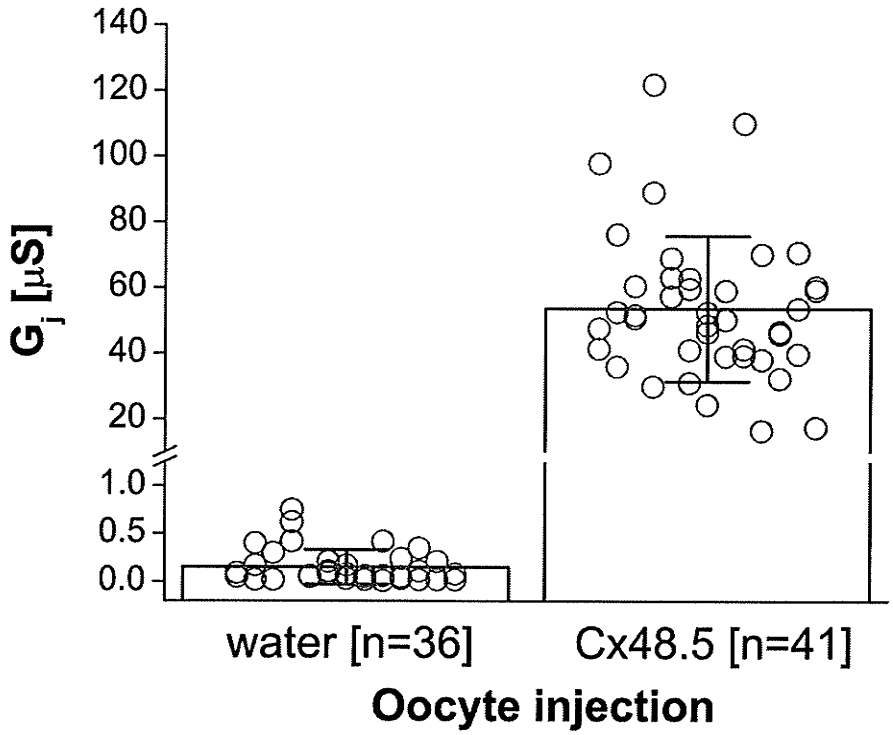
140
120
100
80
60
40
20
1.0
0.5
0.0
G_j [μS]
water [n=36]
Cx48.5 [n=41]
Oocyte injection

Figure 3

Voltage gating behavior of gap junction channels formed by Cx48.5. A time dependent decay of junctional currents (I_j) was induced by transjunctional voltage (V_j) steps. At V_j steps > ±40 mV, I_j decayed symmetrically over the time course of the voltage step. The voltage gating of intercellular channels composed of zebrafish Cx48.5 displayed a high degree of conservation to other GJA3 orthologs such as chicken Cx56 and rat Cx46.

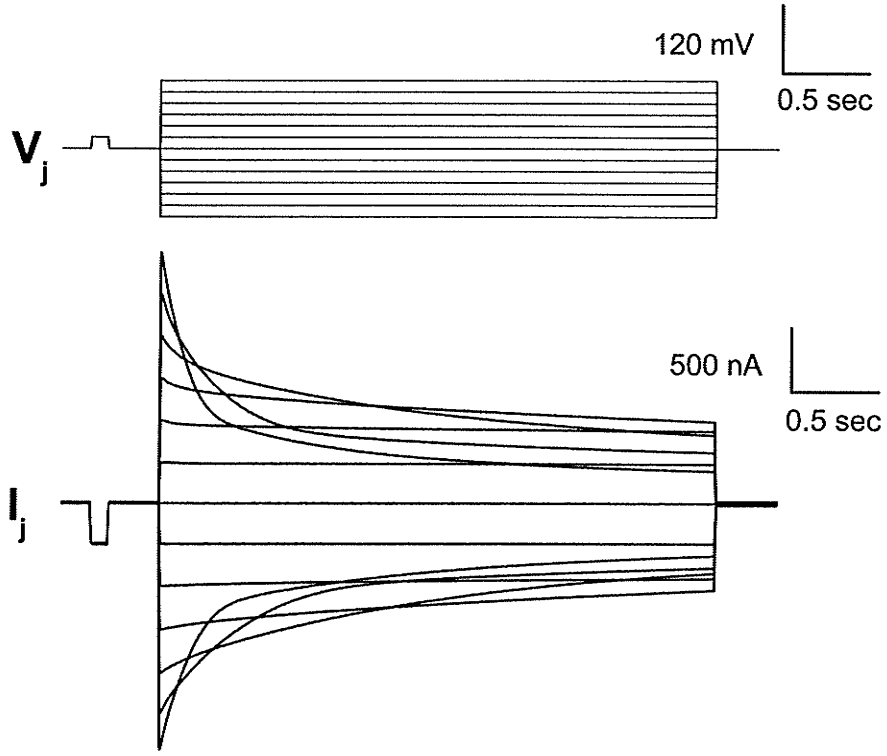
120 mV
0.5 sec
V_j
500 nA
0.5 sec
I_j

Figure 4

Quantitation of Cx48.5 voltage gating. The relationship of V_j to steady-state junctional conductance (G_{jss}) normalized to the values obtained at ±20 mV for Cx48.5. Solid lines represent the best fits to Boltzmann equations, whose parameters are given in Table Y. The voltage gating of intercellular channels composed of zebrafish Cx48.5 displayed a higher degree of conservation to the Cx46 orthologs than the Cx50 orthologs.

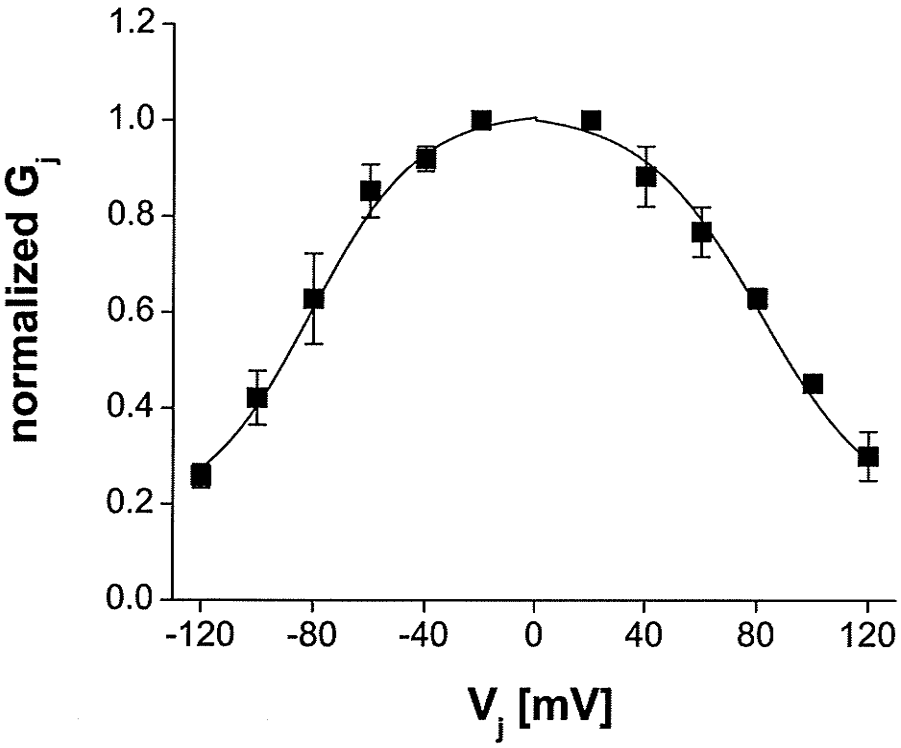
normalized G_j
1.2
1.0
0.8
0.6
0.4
0.2
0.0
-120
-80
-40
0
40
80
120
V_j [mV]

Figure 5

Single *Xenopus* oocytes injected with Cx48.5 cRNA or water were studied by voltage clamp. Cells were initially clamped at -40 mV. Depolarizing voltage steps of 10, 20, 30, 40, 50, 60, 70, 80, 90 and 100 mV were imposed, and the whole-cell currents were recorded. Cx48.5 induced rapidly activating outward currents that exhibited a slower partial inactivation at higher membrane potentials (≥ 10 mV). In contrast, oligo-injected control cells showed negligible membrane currents.

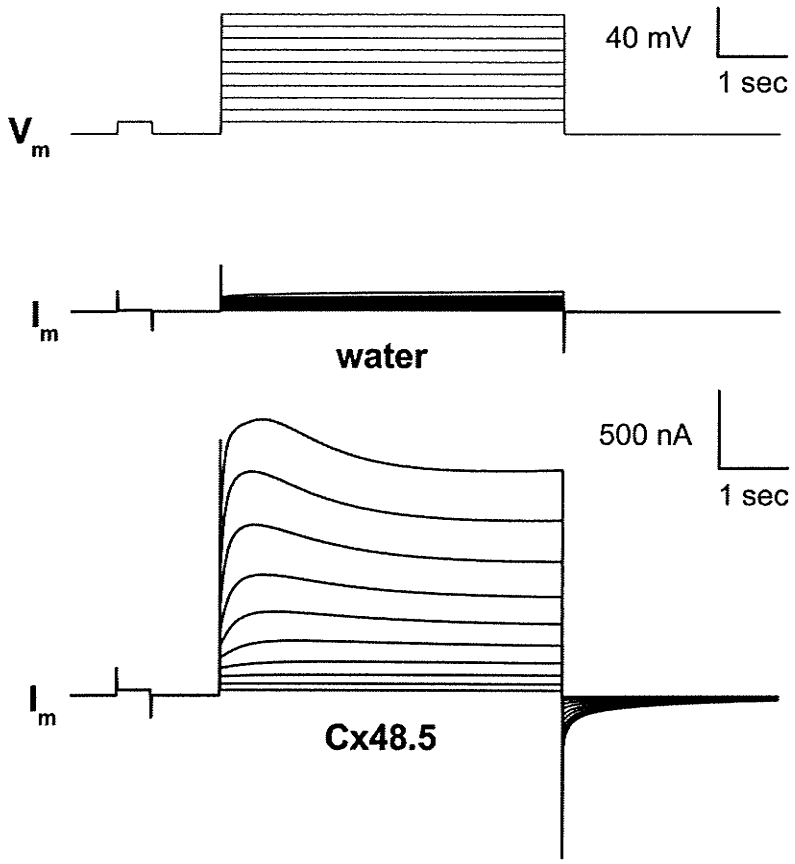
40 mV
1 sec
V_m
I_m
water
500 nA
1 sec
I_m
Cx48.5

Figure 6

Current-voltage relationships in Cx48.5 and water injected oocytes. Whole cell membrane currents (Im) were measured at the end of a voltage step. At membrane potentials (Vm) > -10 mV, Cx48.5 injected cells displayed whole cell currents not seen in oligo-injected controls. Results are shown as the mean ± SD of the indicated number of cells.

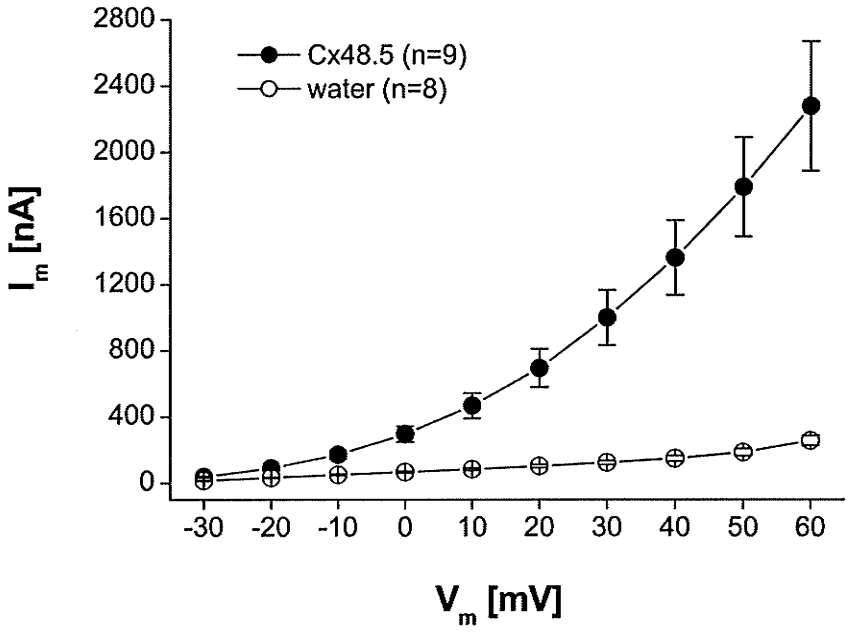
Cx48.5 (n=9)
water (n=8)
2800
2400
2000
1600
1200
800
400
0
I_m [nA]
-30
-20
-10
0
10
20
30
40
50
60
V_m [mV]